REMOVAL OF ORGANIC FOULANTS FROM MEMBRANES BY USE OF ULTRASOUND

Report to the
WATER RESEARCH COMMISSION

by

C Aldrich and BC Qi
University of Stellenbosch

WRC Report No 1229/1/05
ISBN No 1-77005-313-1

JULY 2005

Disclaimer

This report emanates from a project financed by the Water Research Commission (WRC) and is approved for publication. Approval does not signify that the contents necessarily reflect the views and policies of the WRC or the members of the project steering committee, nor does mention of trade names or commercial products constitute endorsement or recommendation for use.

EXECUTIVE SUMMARY

In filtration where porous membranes are used, the most important disadvantage is the reduced permeate flux owing to fouling of the membranes. Fouling is caused by pore plugging and adsorption of rejected macromolecules or other solutes in the membrane system. This requires periodic cleaning of membranes, which can add considerably to the overall cost of plant operation owing to lost productivity related to down-time, the cost of the chemicals used in cleaning, higher pressures and associated pumping costs to maintain membrane productivity, as well as reduced lifetime of the membranes.

Rationale of Study

Ultrasound has been identified as a promising approach to combating fouling in membranes. In principle it can be used on-line and may even eliminate the use of chemical cleaning or alternative measures completely, which could lead to major advances in the development and implementation of membrane technology. However, these conclusions have been based on small-scale laboratory studies, which have not taken the economic feasibility of the approach into account. The objective of this investigation was therefore to assess the techno-economic feasibility of using ultrasound on a large-scale to alleviate fouling in membrane filtration plants.

Aims

The focus was on the application of ultrasound on (capillary ultrafiltration systems) and the following aims were pursued.

- A literature review of the use of ultrasound to reduce or prevent fouling in membranes, or to otherwise enhance membrane performance.
- Experimental investigation of different operating strategies in the application of ultrasound to reduce the fouling if membranes, including continuous or intermittent sonication, sonication with or without backwashing, etc.
- Experimental assessment of possible damage to membranes by sustained use of ultrasound in membrane systems, as some conflicting results are reported in the literature.
- Measurement of the propagation and distribution of ultrasonic energy in capillary membranes, as these are commonly used and this information could be important in the assessment of the economic feasibility of defouling with ultrasound.
- Estimation of the cost and feasibility of using ultrasound in large-scale capillary membrane systems.

Methodology

Three ultrasonication systems were used, viz. two horn transducers or probes and an ultrasonic bath. One probe operated at fixed frequency of approximately 30 kHz, generating a maximum acoustic power density of 130 W/cm^2 with a nominal power output of 50 W (IKA Labortechnik Staufen, United Kingdom, U50). The other probe (Model W-375, Heat Systems Ultrasonics, Inc., Plainview, NY, USA) with a frequency of 20 kHz and a power density of 83 W/cm^2. This probe was not available for all the experiments. The ultrasonic bath (30 × 24 × 20 cm^3) operated at a fixed frequency of approximately 20 kHz, generating 2.8 W/cm^2 with a nominal power output of 240 W (Ultrasonic cleaner, Denmark, 3A). Unless otherwise stated, power densities associated

with ultrasonic equipment refer to the ratios of the nominal power output to the facial areas of the transducers involved in the generation of the ultrasound.

The ultrasonic devices were used in various configurations with small membrane cells of three different sizes. In the first cell designed to contain flat sheet membranes, experiments were done on flat sheet polyamide reverse osmosis membranes in the ultrasonic bath, where effluent containing $CaSO_4$, $FeCl_3$ and CMC were filtrated. In addition, experiments were done on flat sheet poly(ether sulphone) ultrafiltration membranes, used to filter lignocellulose decomposition leachate, where sonication was done with both the ultrasonic probe and bath.

In the 2nd membrane cell designed to hold capillary tubes, experiments were done with tubular poly(ether sulphone) membranes with pure water and Congo Red dye to assess possible membrane damage that could arise from ultrasonication with the 30 kHz ultrasonic probe. In addition, experiments were done on aqueous effluent containing natural organic matter and sonication with both the 20 kHz and 30 kHz probes.

In the large cylindrical membrane cell (1200 mm in length and 90 mm in diameter) work was done on capillary poly(ether sulphone) ultrafiltration membranes, sonicated with the 30 kHz probe.

Apart from the filtration done in the above three membrane cell configurations, the distribution of the acoustic energy generated by the 30 kHz probe was investigated in the large cylindrical membrane cell, as well as in a rectangular vessel, both of which contained capillary membranes.

The experimental results obtained with the filtration of aqueous effluent containing natural organic matter (water from the Steenbras dam near Gordon's Bay), as well data reported in the literature were used to develop cost models that could be used to estimate the large-scale economics of using ultrasound in the defouling of ultrafiltration membranes. A cost model for conventional filtration with ultrafiltration membranes was developed, using backflushing as antifouling measure, which could be compared with a model where ultrasonication was used as an antifouling measure. These models took into account the membrane and non-membrane capital costs, as well as the following operating costs: pumping feed, recycle and backwashing, membrane replacement and labour and maintenance.

Summary of Results

Although based on limited experiments, practically no difference could be observed between defouling with the 20 kHz and 30 kHz probes, which were operated at 130 W/cm^2 and 89 W/cm^2 respectively.

The literature review clearly indicated that foulants can be removed by ultrasound over a wide range of frequencies (from 20–100 kHz) and specific power inputs (ranging from 0.5-83 W/cm^2). In theory, and according to some limited experimental results reported in the literature, low frequency high power sonication gives the best results, as it maximizes cavitation in the fluid.

In addition, it was found that continuous on-line ultrasonication is not necessary. For all practical purposes, similar results could be obtained by means of intermittent sonication. Experiments have also shown that even better results can be obtained by using ultrasound in conjunction with chemical cleaning of the membranes. This was confirmed by several other studies described in the literature.

No membrane damage could be observed as a result of ultrasonication. The literature is divided on this issue, but it appears as if membrane damage is unlikely to occur, as long as sufficient flow conditions are maintained during sonication.

In addition, experiments have confirmed that the ultrasonic energy decreases rapidly with distance from the source, suggesting that depending on the configuration of the plant, membrane modules would each probably require multiple ultrasonic transducers. In a rectangular vessel, the attenuation was approximately 20% higher in the presence of the membrane capillaries (with capillaries, α = 0.049 cm^{-1} versus without capillaries, α = 0.041 dB/cm^{-1}). In the large-scale cylindrical membrane filter, the attenuation was less (α = 0.013 dB/cm^{-1}). These data give some indication of the influence of the filter geometry on the attenuation of the ultrasound, but cannot be used quantitatively in the scale-up or design of large-scale membrane filters, as the relationship between ultrasound intensity levels and acoustic cavitation in the fluid cannot be quantified.

The data related to the large-scale capillary filtration unit was used to develop models of the cost of the treatment of effluent containing natural organic matter. Simulation studies with the cost models were conducted with a high (0.222 m^3/s) and a lower capacity (0.0222 m^3/s) plant designed to treat water containing natural organic substances.

The results for 0.222 m^3/s at a permeate flux of 2000 L/m^2h are given below. As can be seen from these cost breakdowns, the use of ultrasound to combat fouling is not cost effective in the high capacity plant, where it accounts 64.4% of the total cost of the overall treatment cost per unit volume of water. However, simulation with the lower capacity plant (0.0222 m^3/s) suggested that ultrasound may be a viable alternative to conventional means of treating effluent containing natural organic matter, and by implication possible other effluents as well.

	Without US	With US
Total cost of treatment ($/m^3$)	0.062	0.144
Capital Costs	**42.4**%	**76.8**%
Membrane costs	42.0%	12.0%
Non-membrane costs	0.4%	0.2%
Ultrasonic transducers	0%	64.6%
Operational Costs	**57.6**%	**23.2**%
Pumping feed	18.5%	8.0%
Pumping recycle	2.2%	2.0%
Pumping backwashing	0.7%	0.3%
Membrane replacement	36.1%	10.3%
Labour and maintenance	0.1%	2.5%
Ultrasonic power	0%	0.1%

The results for 0.0222 m^3/s at a permeate flux of 2000 L/m^2h were as follows.

	Without US	With US
Total cost of treatment ($/$m^3$)	0.065	0.063
Capital Costs	**43.6**%	**45.8**%
Membrane costs	40.2%	27.5%
Non-membrane costs	3.4%	3.5%
Ultrasonic transducers	0%	14.8%
Operational Costs	**56.4**%	**54.2%**
Pumping feed	17.7%	18.2%
Pumping recycle	2.1%	4.5%
Pumping backwashing	0.7%	0.7%
Membrane replacement	34.5%	23.7%
Labour and maintenance	1.4%	5.7%
Ultrasonic power	0%	1.4%

Second, in both cases the power requirements to drive the ultrasonic equipment is not particularly important, therefore optimization in terms of intermittent operation appears to be relatively unimportant.

Recommendations

On the basis of the results and analyses discussed above, the following recommendations can be made.

- Since the sonicators used in the experiments were laboratory scale systems, further experiments need to be conducted with industrial scale systems. More specifically, the integration of these systems with existing membrane modules should be considered in line with some of the latest advances in sonochemical reaction systems, where multi-transducer multi-frequency systems are proposed. This would give a better indication of some of the important issues surrounding the capital and operating cost associated with ultrasonication.

- Moreover, the economic feasibility of using ultrasound to combat membrane fouling should be verified experimentally by running a filtration unit in a closed circuit, using both conventional means and ultrasound to clean the membranes in order to experimentally verify the cost, also in terms of the disposal the chemicals, where used for cleaning.

- In additional, the cost models used in this investigation need to be refined, either by use of existing cost estimation software or by more detailed modeling in order to compare different designs and operating strategies more accurately.

ACKNOWLEDGEMENTS

The guidance of the WRC steering committee is highly appreciated, i.e. by name Profs EP Jacobs (University of Stellenbosch), PP Coetzee (RAU), JH Knoetze (University of Stellenbosch), RD Sanderson (University of Stellenbosch), Drs G Offringa (WRC), P Cilliers (HMO) and Messrs CJ Brouckaert (University of Natal), FJ du Toit (Sasol Technology), GW Lok (Eskom), G Steenveld (WRC) and TBF Stenden (Eskom).

TABLE OF CONTENTS

LIST OF TABLES

LIST OF FIGURES

ACRONYMS

BSA	Bovine Serum Albumin
CMC	Carboxy Methyl Cellulose
FBB	Fast Blue B salt (Tetrazotized O-Dianisidine)
LDL	Lignocellulose Decomposition Leachate
NOM	Natural Organic Matter
NUS	Non-ultrasonic
PSE	Poly(sulphone ether)
PSU	Polysulphone
RO	Reverse Osmosis
TMP	Transmembrane Pressure
TOC	Total Organic Carbon
UF	Ultrafiltration
US	Ultrasonic(s)/Ultrasound

1. INTRODUCTION

Membrane fouling limits the widespread use of ultrafiltration membranes in the processing of industrial wastewaters, as it can lead to reduced performance, higher energy consumption and even failure to meet product specifications. Various pretreatment techniques and processes including prefiltration are employed to prevent or reduce the rate of membrane fouling, such as chemicals that are added to prevent mineral scaling, alteration of membrane surfaces (Meier-Haack et al., 2003) and the addition of biocides to combat biofouling. Unfortunately all these techniques are inefficient in one way or another, so that periodic membrane cleaning is still unavoidable.

For example, for membrane cleaning to take place, the unit needs to be shut down for chemical or mechanical cleaning, or both. The downtime is significant and the cleaning process is labour intensive. The chemicals used for cleaning may also reduce the lifetime and efficiency of the membrane modules.

For this reason, more effective methods for alleviating or preventing fouling in membranes is seen as an important issue in the overall development of cost-effective membrane systems. One of the methods that have recently emerged as a potentially more effective means of dealing with fouling of membranes is the use of ultrasound. Ultrasonication can be introduced into a membrane module on-line, so that the unit does not have to be shut down or opened up. In principle, no additional labour is required and no chemicals need to be involved.

Although several laboratory studies have confirmed the potential of the technique, few studies if any, has been undertaken to assess the feasibility and cost implications of using ultrasound as an anti-fouling measure on an industrial scale. Therefore, the objective of this project was to investigate the feasibility of using ultrasonic cleaning of membranes on large scale systems. As no experiments could be conducted on a large scale, the assessment had to be based on the scale-up of laboratory data.

The specific objectives of this investigation can be summarized as follows

- A literature review of the use of ultrasound to reduce or prevent fouling in membranes, or to otherwise enhance membrane performance.
- Experimental assessment of possible damage to membranes by sustained use of ultrasound in membrane systems, as some conflicting results are reported in the literature.
- Measurement of the propagation and distribution of ultrasonic energy in capillary membranes, as these are commonly used and this information could be important in the assessment of the economic feasibility of defouling with ultrasound.
- Estimation of the cost and feasibility of using ultrasound in large-scale capillary membrane systems.

The report is organized as follows. In the following section, the literature related to the use of ultrasound to mitigate fouling in membrane filters is reviewed. Thereafter, experiments conducted at the University of Stellenbosch are described. The first of these describe the measurement of the ultrasound intensity in vessels with and without membrane fibres. This is followed by the experimental assessment of a number of strategies to reduce the fouling of membranes by use of ultrasonication, as well as the assessment of possible damage caused to membrane capillaries by ultrasound. The last sections of the report consist of a techno-economic consideration of ultrasound systems in membrane filters, a summary and conclusions, and recommendations.

2. LITERATURE REVIEW OF ULTRASONIC DEFOULING OF ULTRAFILTRATION MEMBRANES

2.1. BACKGROUND

Membrane fouling occurs by the irreversible deposition of retained particles, colloids, macromolecules, salts, etc., on the membrane surface and/or inside the membrane. This fouling is ubiquitous and is one of the most challenging problems to be solved before the full potential of industrial membrane filtration can be realized (Dekker and Boom, 1995), as results in a significant decline of the permeate flux in ultrafiltration and microfiltration (Williams and Wakeman, 2000). Although considerable progress has been made to overcome fouling, most of the proposed solutions cannot be implemented satisfactorily in practical membranes (Cui and Wright, 1994; Nosov, 1965).

Typical methods of membrane cleaning which are used in practice are backwashing and backflushing, although backflushing is only possible for some tubular membranes. Moreover, chemicals such as detergents and acids or alkalis are often used to clean fouled membranes (Harvey, 1965; Peterson, 1967; Howkins, 1969; Liu et al., 2004; Madaeni and Mansourpanah, 2004). Unfortunately, these chemicals sometimes damage the membrane materials and cause secondary pollution. Thus, chemical cleaning should be minimized or avoided (Semmelink, 1970). Accordingly, cleaning methods without the use of chemicals have been developed, such as periodic reversals in the flow direction and periodic reductions in the feed pressure along with continuous flow. In addition to these methods, a pulsed electric field was applied to the cleaning of cellulose nitrate microfiltration membranes (Semmelink, 1973). It was found that cleaning by the pulsed electroosmotic technique is moderately effective when the particles of the membrane and the solute have the same sign of ?-potential. This cleaning method has the advantage of cleaning the membrane without interrupting the filtration operation.

Ultrasound has been widely used as a method of cleaning materials, since the cavitation that it produces in fluids generates high local pressures and temperatures that can assist in the removal of recalcitrant contaminants (Tarleton, 1988). Likewise, ultrasonic enhancement technology has been successfully applied to some membrane separation processes such as microfiltration, dialysis (Li et al., 1996) and membrane distillation (Tarleton and Wakeman, 1990; Wakeman and Tarleton, 1991, 1993; Wakeman and Smythe, 2000). It is widely believed that ultrasonic cavitation, acoustic streaming, ultrasonically induced vibration of membranes and ultrasonic heating (Muraldidhara, 1986) are the main causes of the enhancement. Zhu et al. (1999) developed a model of ultrasonic enhancement on membrane distillation based on the mechanisms of ultrasonic cavitation and acoustic streaming, allowing the effects of ultrasonic intensity, ultrasonic frequency, solution temperature and excited membrane area on permeate flux of membrane distillation to be analyzed theoretically. From this they have observed that the enhancement ratio can be improved by increasing ultrasonic intensity, decreasing ultrasonic frequency or decreasing the solution temperature.

This has led to an increasing interest in the application of ultrasound treatment to membrane fouling systems and the use of ultrasound to enhance the solute permeate flux (Chai et al., 1999, Kobayashi et al., 1999, Masselin et al., 2001).

2.2. MEMBRANE FOULING IN ULTRAFILTRATION

Different membrane fouling phenomena can be categorized as follows:

- Crystalline fouling, also called mineral scaling, where minerals are deposited on membrane surfaces owing to their high concentration in the feed stream.
- Particle and colloid fouling.
- Biofouling, owing to adhesion and accumulation of microorganisms forming biofilms.

Membrane fouling has the effect of limiting the flux, either owing to an increased hydrodynamic boundary layer (the polarization boundary layer) or an increased hydrodynamic barrier (the gel layer polarization model). The interaction between solute macromolecules and the membrane surface, as well as between the macromolecules within the polarization layer also affects membrane fouling.

There are several reasons why the transmembrane flux of a solution or suspension is usually much lower than the flux observed with pure water. They are changes in membrane properties, changes in properties of feed solution, concentration polarisation (67-95% flux reduction) and membrane fouling (5-30% flux reduction) (Maartens, 1998).

At least three steps are involved in the fouling of UF membrane (Nilsson, 1990). The first step is the transfer of solute to the membrane surface. This step is seldom the rate-limiting step, as concentration polarization fouling reach near equilibrium within a few minutes of operation. The second step is the transfer of solute towards the membrane, to be adsorbed onto the membrane or to pass through it after a set of reversible adsorption/desorption steps in the membrane pores. The third stage is associated with the kinetics of adsorption which, according to Van Dulm et al. (1983), is a relatively fast diffusion controlled process.

The overall resistance to liquid transmission through a membrane is caused by a combination of separate, but interactive processes such as concentration polarization, gel layer or cake layer formation, adsorption of solutes onto the external surface of the membrane, solute-solute adsorption and blockage of the membrane pores (Kobayashi et al., 1999). In practice, it is difficult to distinguish the individual effects of ultrasonication on each of these processes.

Using a non-invasive ultrasonic monitoring technique, Li et al. (2002) found that the thickness of the fouling layer on the polysulphone (PSU) UF membranes used to filter a Kraft Mill effluent increased rapidly at the beginning, because of concentration polarization and fouling layer formation, followed by a slow increase owing to gradual growth of the fouling layer. Moreover, the thickness of the fouling layer increased faster at the beginning of 2h during dead-end filtration than during crossflow (12.5 cm/s) filtration. Although their thicknesses became the same after 2h of fouling operation in dead-end and crossflow filtrations, the compressibility of the fouling layer was still different under the different operation conditions. Complete membrane coverage with a fouling layer was found under dead-end and crossflow (12.5 cm/s) filtration conditions after 8 hours. In dead-end filtration, a number of particles arrived simultaneously at the deposited layer so that a disordering arrangement of particles was seen on the membrane surface. This is because the particles deposited approach the membrane directly at right angles, giving a compact cake that could resist deformation under pressure (Yazen et al., 1995).

In crossflow filtration, the particles ending up in the cake approach the membrane at acute angles. The surfaces of these cakes are also subject to shear forces by the crossflow of the suspension, which tends to remove the larger particles from the surface, leading to preferential capture of finer particles (Lu and Ju, 1989; Yazen et al., 1995). At the same time, there are more large particles reaching the membrane in crossflow filtration than in dead-end mode. A simple force balance shows that if the drag forces are smaller than the adhesive forces, the larger particles will be retained on the membrane surface (Lu and Yu, 1989; Vyas et al., 2001). Note that the flow rate of 12.5 cm/s is much lower than flow rates commonly used in UF. The result shows coverage of the membrane surface with fine particles, with larger particles interspersed in between on the surface of the fouling layer. As growth of the fouling layer progresses, more fouling layers are formed, until the entire membrane is covered with a uniform fouling layer, tightly absorbed onto the membrane surface.

In addition, (Lu and Yu, 1989; Vyas et al., 2001) observed a linear relationship between the absolute value of the amplitude of differential ultrasonic signals and the fouling resistance during the fouling of tubular poly(ether sulphone) (PES) UF membranes by bovine serum albumin (BSA). The fouling resistance appeared to increase with time as a result of protein adsorption, aggregation and gelation on the membrane surface, leading to a 65% decline in the flux. The aggregation and deposition of BSA formed a dense layer as a second barrier on the membrane surface, while the thickness of the gel layer increased slowly as fouling continued. A very thin layer with high gel concentration resulted in a continuous flux decline (Li and Sanderson, 2003).

In summary, membrane fouling is complicated in that it includes physical, chemical and biological effects, involving adsorption of feed components, clogging of pores, deposition of solids on membrane surfaces accompanied by crystallization and compaction of membrane structures, chemical interaction between membrane materials and components of the feed solution, gel conservation and bacterial growth (Li and Sanderson, 2003). For this reason, the results of studies in membrane fouling cannot be generalized and in this project the emphasis was on therefore on the defouling of ultrafiltration membranes contaminated with organic foulants, although the experimental results also covered other systems.

2.3. PREVENTING AND REDUCING MEMBRANE FOULING WITH ULTRASOUND

2.3.1. Generation of ultrasound

The main types of transducers used to generate ultrasound can be classified as electro- and magnetostrictive. The former (piezo-electric crystals, such as lead zirconate) are most widely used and can generate a wide range of ultrasonic frequencies, but are limited in their power output to 20-50 W. Magnetostrictive transducers are generally more expensive and exploit the property of certain materials, such as nickel, to contract when placed in a magnetic field (magnetostriction), returning to their original size when the field is removed. These materials have an upper limit of frequency response of approximately 70 kHz (Mason, 2000).

2.3.2. Factors affecting acoustic cavitation

As was mentioned before, ultrasonic cleaning is based on the complex phenomenon of acoustic cavitation, where microbubbles in the fluid implode or collapse to produce shock waves. These high intensity ultrasonic fields are sufficiently powerful to erode even the hardest surfaces and can be used to remove extremely tenacious foulants or deposits from membrane surfaces, among other. The disadvantage is that acoustic cavitation can also be damage delicate equipment, but this will be considered in more detail later.

Although ultrasound has been used for various purposes for more than 50 years, cavitation cannot be measured reliably as yet. Indirect methods, such as erosion tests on metal surfaces, accelerated chemical reactions, etc., have all proved to be ineffective beyond the simple detection of cavitation as such.

Effective application of the ultrasonic cleaning process requires consideration of a number of parameters. While time, temperature and chemicals remain important in ultrasonic cleaning as they are in other cleaning technologies, there are other factors which must be considered to maximize the effectiveness of the process. Especially important are those variables which affect the intensity of ultrasonic cavitation in the liquid.

Maximizing cavitation of the cleaning liquid is obviously very important to the success of the ultrasonic cleaning process. Several variables affect cavitation intensity. Temperature is the single most important variable to be considered in maximizing cavitation intensity. This is because so many liquid properties affecting cavitation intensity are related to temperature. Changes in temperature result in changes in viscosity, the solubility of gas in the liquid, the diffusion rate of dissolved gases in the liquid, and vapor pressure, all of which affect cavitation intensity.

The viscosity of a liquid must be minimized for maximum cavitation. Viscous liquids are sluggish and cannot respond rapidly enough to form cavitation bubbles and violent implosion. The viscosity of most liquids is reduced as temperature is increased.

For most effective cavitation, the cleaning liquid must contain as little dissolved gas as possible. Gases dissolved in the liquid are released during the bubble growth phase of cavitation and prevents the forceful implosion required for the desired ultrasonic effect. The amount of dissolved gases in a liquid is likewise reduced as the liquid temperature is increased.

Moreover, the diffusion rate of dissolved gases in a liquid is increased at higher temperatures. This means that liquids at higher temperatures give up dissolved gases more readily than those at lower temperatures, which aids in minimizing the amount of dissolved gas in the liquid.

A moderate increase in the temperature of a liquid brings it closer to its vapour pressure, meaning that vaporous cavitation is more easily achieved. Vaporous cavitation, in which the cavitation bubbles are filled with the vapour of the cavitating liquid, is the most effective form of cavitation. As the boiling temperature is approached, however, the cavitation intensity is reduced as the liquid starts to boil at the cavitation sites.

Cavitation intensity is directly related to ultrasonic power at the power levels generally used in ultrasonic cleaning systems. As power is increased substantially above the cavitation threshold, cavitation intensity levels off and can only be further increased through the use of focusing techniques.

In contrast, cavitation intensity is inversely related to ultrasonic frequency. As the ultrasonic frequency is increased, cavitation intensity is reduced because of the smaller size of the cavitation bubbles and their resultant less violent implosion. The reduction in cavitation effect at higher frequencies may be overcome by increasing the ultrasonic power.

2.3.3. Ideal parameters to adjust ultrasonic power output for cleaning (Piazza and Puskas, 2002)

There are various ultrasonic variables available to the user to define what the achievable levels of cleanliness and damage minimization are. The most important variables involved in an ultrasonic system's performance are *sweep*, *power control* and *centre frequency control*.

Most modern day ultrasonic systems eliminate possible damage to structures subjected to ultrasound by continually changing the frequency generated within 1 to 2 kHz. This is called *sweeping* the frequency and is successfully employed to prevent the standing waves that may cause damage. Modulation of the frequency through sweep affects ultrasonic performance via three mechanisms. First, sweeping ensures that all of the transducers emit ultrasound evenly and uniformly. Second, by introducing more frequencies into a tank, sweep excites, at resonance, a larger bubble population. This pumps more energy into bubble pulsation and implosion. The third important aspect of sweep is the minimization of damage mechanisms. Smoothly or otherwise varying the sweep frequency, such as dual sweep, eliminates potentially damaging power impulses with equal time intervals. The equal intervals of these impulsive excitations, especially in transducers characterized by a sharp resonance, threaten to excite delicate parts of the equipment into damaging sympathetic vibration. With an understanding of the effects of a sweeping frequency, the ideal sweep is a fast sweep with a constantly varying rate, over as large a bandwidth as the transducers would allow.

Modulation of power into a tank through *duty cycle* and *amplitude control* affects ultrasonic activity in different ways. Changing of the peak pressures in a tank through amplitude control changes the average implosion energy about which a bubble population is centred, but smoothly and slowly. Duty cycle serves to quickly modify a bubble population through degassing. Duty cycle also changes the number of cavitation implosions a part is exposed to, thus reducing the opportunity for damage. The ideal power control is strongly related to the part being cleaned, as well as the type of contaminant, and must be addressed on an ad hoc basis.

The ability to discretely change the ultrasonic *frequency* in a tank from a transducer's primary frequency to any of its overtones, called *centre frequency control*, is perhaps the most versatile and important of the various modifiable ultrasonic parameters available to the engineer. Cavitation implosion energy changes with the inverse of the square of the frequency. As such the only method by which to affect large-scale changes in implosion energy is through large discontinuous jumps in frequency, say 72 kHz to 104 kHz. Again the efficacy of cleaning is strongly a function of implosion energy and is different for each application. The ideal ultrasonic device allows centre frequency control in a single process for maximal particle removal efficiency across a wide spectrum of particle sizes.

For a given ultrasonic instrument, the power output and power supplying mode can be adjusted via *amplitude control* and *duty cycle* control, while the mode of frequency sweep and the centre frequency are normally pre-adjusted.

In addition to a sound knowledge of the fundamentals of ultrasonic cleaning and the ideal operating parameters of the instruments to achieve maximal ultrasonic cleaning of fouled membranes, it is necessary to know the actual ultrasound energy supplied to the membrane system at different power control levels, as was measured in this case by means of hydrophones.

2.3.4. Application of ultrasound to prevent or remove fouling in membrane systems

According to Chai et al. (1998), the enhancement of the permeate flux by ultrasonication can be attributed to the enhancement of bulk mass transfer in concentration polarization layer near membrane. As mentioned previously, one of the physical phenomena associated with ultrasound is cavitation. Cavitation can be defined as the formation, growth, and implosive collapse of bubbles. When a cavitating bubble is oscillating near a solid surface, it does so asymmetrically and generates microjets (microcurrents) of high velocity. The high velocities generated can bring vigorous streaming turbulence along the membrane surface, which efficiently decreases the thickness of boundary layers and diffusion resistances of the fouled membrane, thereby enhancing the rates of mass transfer through the membrane. It is believed that diffusion in membranes can be enhanced by the ultrasonically produced microcurrents in the liquid. Owing to acoustic streaming, turbulent flow at the boundary layer increases, the resistance of mass transfer decreases and the rate of mass transfer increases (Band et al., 1997).

Chai et al. (1999) applied an ultrasound cleaning technique to remove fouling of flat-sheet ultrafiltration and microfiltration membranes with peptone solution in crossflow filtration. They found that the cleaning of fouled membranes by ultrasound in conjunction with flushing to be more effective than using flushing alone. The same results were also noticed in our previous work on the laboratory scale system and were confirmed by Li et al. (1995), who have successfully applied ultrasound to remove fouling of flat sheet microfiltration membranes with Kraft paper effluent.

When the membrane is fouled, some foulants (contaminants) are comprised of insoluble particles loosely attached and held in place by ionic or cohesive forces on the membrane surface. Cavitation as a result of ultrasonic activity displaces and removes these loosely held foulants, including large molecular organic components or precipitates of the inorganic components that were previously deposited on the membrane surface. For effective removal, the particles to be removed should be wettable by the coupling medium (e.g. flushing water).

In a pressure driven membrane system the flux declines owing to membrane fouling resulting directly from concentration polarization at the membrane surface. The conventional approach to improve the performance of such a membrane system is careful selection of membrane materials and the use of relatively high crossflow velocities. Flows of up to 4 m/s have been used to limit polarization. The high velocity increases the shear rate and subsequently transfers material away from the membrane surface. High crossflow velocities have two significant disadvantages: High energy consumption and a large pressure drop over the length of the membrane module.

Feed pretreatment can also reduce fouling effects. Pretreatment can be physical, such as prefiltration and centrifugation or chemical, such as precipitation, coagulation, flocculation, addition of antiscalants or disinfectants.

Many alternative methods to limit polarization have been suggested (Williams and Wakeman, 2000). One way to reduce fouling is by enhancing the local shear near the membrane surface. This increases the mass transfer of accumulated materials back into the bulk feed (Dekker and Boom, 1995; Williams and Wakeman, 2000). The local shear rate near the membrane surface can be increased by inducement of Dean or Taylor vortices, rotating membranes, vibrating membrane modules, use of corrugated (or grooved) membranes, as well as use of scouring particles. Dean or Taylor vortices shorten the path length along the membrane surface for a particle that might be retained. By shortening the path, the chance that the particle will attach to the membrane is reduced.

Another method is to remove the materials accumulated at the membrane surface by a periodic flow reversal, such as backflushing, pulsing and shocking (Dekker and Boom, 1995; Williams and Wakeman, 2000). For example, with high frequency backpulsing (0.1–1 Hz) with short pulses (0.1 s or less), it seems that the fouling layer remains loose and does not get the opportunity to compact. Pulsating flow can also improve the flux. Oscillations and unsteady flows can be obtained by introducing pulsations into feed or filtrate channels (Williams and Wakeman, 2000).

Likewise, gas sparging has been found to enhance ultrafiltration in the downwards crossflow operation (Cui et al., 1994). Addition of gas to the process stream seems to disrupt the concentration polarization layer. However, it does not appear to be as effective as vortex promoter and handling the gas injected into the membrane system poses a problem.

2.4. FLUX ENHANCEMENT VIA ULTRASONICATION

Since ultrasonically assisted flux enhancement is closely related to ultrasonic defouling, some of the developments in this field are also considered here in more detail.

2.4.1. Early Developments

In an early Russian monograph (Nosov, 1965), ultrasound assisted filtration is mentioned, that is a filter for liquid slurries is described where the ultrasonic transducer is connected to the filter element. In a patent by Harvey, (1965), the use of an acoustic liquid whistle or ultrasound was proposed to prevent clogging of the membrane and to remove concentration-polarization.

Similarly, a US patent of 1967 (Peterson, 1967) describes a process where a suspension of solids in a liquid is sieved and clogging of the sieve is prevented by vibration induced by an ultrasonic probe placed in the fluid. The meshed sieve sizes were given to be 100 μm down to 5 μm. A Russian publication about ultrasound in hydrometallurgy (Howkins, 1969), describes experiments using ultrasound to assist filtering. The authors also found an increase in flow rate with ultrasonic agitation and attributed this to the inhibition of the formation of deposits or the continuously removal of deposits from the filter element. The authors gave various reasons why ultrasonically enhanced filters could not go beyond laboratory stage at the time. The same author (Howkins, 1969) also studied haemodialysis in artificial kidney machines and found that ultrasonic agitation of fluid layers near the membrane could produce a major increase in the rates of dialysis.

Semmelink (1970) observed that the application of ultrasonic vibrations to the filtering of liquids leads to an increase in the flow rate. The main reason for the increase in flow rate with ultrasonic agitation was found to be the fact that a deposit of solid particles was continuously removed from the filter element. Without the ultrasonic agitation a

filter deposit is formed and this deposit was found to be responsible for the rapid decline in flow rate. Semmelink also found that a uniform removal of the deposit could be achieved by placing the radiating face of the transducer close to the filter element, but not connecting it to the element. The transducer was placed 1 cm above the filter disk. The filter element was metal wire cloth with a nominal pore size of 8 μm. The electrical input to the transducer was 20 W at 20 kHz and the static pressure was 13 kPa, with Chicago tap water being the filtrant.

In another paper presented by Semmelink (1973), the application of ultrasonic vibrations to the filtering of liquids and specifically by the reverse osmosis (RO) process was described. The project was done by the Central Acoustics Laboratory of the University of Cape Town in South Africa and was aimed at determining the economics of ultrasound enhanced water purification processes, focusing on RO. A commercial transducer-generator combination was used. The operating frequency was fixed at 20 kHz; the maximum power output was 500 W. The radiating face was set just above the filter element. A Nuclepore plastic membrane and stainless steel wire cloth, both with nominal pore size of 5 μm was used. The static pressure was 5 kPa and Cape Town tap water was the filtrant. It was found that without ultrasonic irradiation, the flow rate rapidly decreased. With ultrasonic irradiation the decrease was found to be much smaller and it approached a constant value after a few hours.

2.4.2. More Recent Developments

A paper by Tarleton (1988) describes how electric an ultrasound fields can be used to reduce fouling in microfiltration. The experiments were carried out in dead-end filtration mode at constant pressure. A stainless steel filter cell consisting of a conventional leaf filter, electrodes and ultrasound transducers were used. The maximum power to the ultrasonic transducer was 600 W. Two ultrasound frequencies were used: 23 and 40 kHz. The authors found that the pH of the suspension affected the efficiency of the ultrasound. Ultrasound appeared to have a minimum effect when pH-levels corresponded to the points of zero and maximum zeta potential. It was also suggested that the influence of ultrasound in filtration might be dependent on the surface properties of the particulates in suspension and also on particle shape and orientation.

Tarleton and Wakeman studied the effects of electrical and ultrasonic fields and the combined fields on crossflow microfiltration (MF), (Tarleton and Wakeman, 1990; Wakeman and Tarleton, 1991; Tarleton and Wakeman, 1992). Experiments were carried out at ultrasound frequencies of 23 and 40 kHz with maximum power output of 600 W. Different types of membranes were used. Crossflow velocities of 0 to 0.2 $m.s^{-1}$ were used. They found that both fields can reduce membrane fouling by an amount dependent on applied field strength, acoustic frequency, suspension concentration, liquid viscosity, particle size and particle surface charge. The combined fields had a synergistic effect. The authors also found that when the force fields are used in MF, lower crossflow velocities can be used, implying lowered energy consumption and reduced degradation of shear sensitive streams. The lower ultrasonic frequency gave a greater flux improvement. When the ultrasound source was brought closer to the membrane, the effect of ultrasound on improving filtration rates increased. It was found that at higher solids concentrations, the filtration rate enhancements possible with an ultrasonic field were reduced. It was observed that the application of ultrasound leads to a flux increase for smaller particles, but for larger particles it could lead to a reduced flux rate. The authors also examined the power consumption of their setup, but did not optimize it.

Wakeman and Smythe, (2000a, 2000b), studied the effects of electric and acoustic fields on constant pressure filtration. The ultrasonic frequency was fixed at 23 kHz and the power input to the transducers was 275-300 W. Unless otherwise stated, references to

power inputs mean nominal electrical power input to the ultrasonic device. Specific power output refers to the ratio of the nominal power input to the surface area of the sonotrode (probe) of the ultrasonic equipment. The ultrasonic transducer was attached to one side of the filter cell and the ultrasonic energy was applied tangentially to the filter surface. Sartorious cellulose nitrate membranes with a pore size rating of 0.2 μm were used. Experiments were carried out at constant vacuum. In their experiments they observed a decrease in the filtration rate when the ultrasonic field was applied. They also found that acoustic fields have little effect on filtration rates close to the suspension isoelectric point (IEP). It produces a slight improvement in filtration rate at high pH, but have a deleterious effect at intermediate pHs. The combined fields exhibited a synergy closer to the IEP and high pH values. It was found that ultrasound enhances the effect of an applied electric field close to the IEP of the suspension by reducing the effective particle size and increasing electrophoretic velocities.

Muralidhara et al., (1986), developed an electro-acoustic process for the dewatering of a slurry. The process combines electrical and acoustic fields. The two applied fields have a synergistic effect and leads to higher dewatering rates and energy savings. An ultrasound frequency of 20 kHz was used.

Chai et al., (1998), studied the ultrasound effect on crossflow filtration of polyacrylonitrile (PAN) ultrafiltration (UF) membranes. The ultrasound effects on permeate flux and rejection of solids were investigated. Two types of PAN UF membranes reinforced with woven cloth were used. A 1 wt% dextran solution was used in the experiments and the applied pressure was fixed at 30 kPa throughout the UF experiments. The ultrasonic frequency was 45 kHz with input power of 248 W. The ultrasonic transducers were placed 50 mm from the membrane and the dense skin layer of the membrane faced the transmission direction of the ultrasound. Experiments were conducted with ultrasound on and off for alternating periods and also with continuous ultrasound irradiation. They found that the sonication treatment increases permeate flux for dextran solute, which is highly rejected by the PAN membrane. They observed no ultrasound effect for water and small effect for dextran with low rejection by the membrane. The authors found evidence that the increase in permeate flux can be attributed to the enhancement of bulk mass transfer in the concentration polarization layer near the membrane.

In a different set of experiments Chai et al. (1999), studied ultrasound-associated cleaning of various polymeric membranes for water treatment. Experiments were conducted with aqueous peptone solutions of 1, 2, 4 and 6 wt%. An ultrasound cleaning technique was applied to remove fouling of UF and MF membranes. Polysulphone (PS), polyacrylonitrile (PAN) and polyvinylidene fluoride (PVDF) membranes were used. The ultrasonic frequency was 45 kHz and the power output 2.73 $W.cm^{-2}$. The feed flow rate and operating pressure was fixed at 325 $ml.min^{-1}$ and 30 kPa, respectively, throughout the experiments. The authors found that water cleaning under sonication is effective in cleaning polymeric membranes fouled by peptone solution. It was also found that a PS membrane fouled by high concentrations of peptone could be cleaned completely by this method and that an increase in the operating temperature showed a high cleaning efficiency by water cleaning under sonication.

In another set of experiments Kobayashi et al. (1999) studied ultrasound enhanced crossflow membrane filtration. The ultrasound effects on a permeate flux of dextran solutions through PAN UF membranes were examined. Dextran solutions of 0.5, 1, 2, 3 and 5 wt.% were used. The ultrasonic frequencies were 28, 45 and 100 kHz and the power output 150 to 300 W. The effect of the ultrasound propagation direction was also examined. It was found that ultrasound with a frequency of 28 and 45 kHz enhanced the permeate flux of PAN UF membranes in crossflow filtration. It was also found that the enhancement of the permeate flux depended on ultrasound intensity and the irradiation

direction relative to the membrane. Evidence was found that the ultrasound irradiation enhanced permeation by increasing mass transfer across the concentrated dextran layer close to the membrane surface.

Band et al. (1999) investigated the enhancing effect of specially modulated ultrasound signals in water desalination by ion-exchange hollow fibres, (Band et al., 1997). The ultrasonic frequency was 45-49 kHz and the power output 23-61 W. It was found that, depending on the concentration of the solutions and hydrodynamic conditions, ultrasound enhanced different steps of the overall ion-exchange process. The effect also increased with temperature (in the range of 20-50 ºC). It was found that the flux increase was proportional to the applied ultrasound power. The authors also found that acoustic cavitation may be controlled via appropriate amplitude modulation of the driving ultrasound.

Simon et al., (2000), studied the enhancement of dead-end ultrafiltration by ultrasound. The ultrasonic frequency was fixed at 20 kHz and the maximum power output was 40 W. The emitter was placed 14 mm from the membrane. Experiments were also done with a conventional mechanical stirrer. The authors concluded that low-frequency ultrasound could improve dead-end UF performance. The improvement is the due to the removal of part of the boundary layer from the membrane surface. The removal of the boundary layer is effected by stirring – mechanical or ultrasonic. Higher permeate fluxes were achieved by either increasing stirrer speed or ultrasonic power – a virtual ultrasonic stirrer speed, depending on the ultrasonic power, was defined.

Masselin et al. (2001), studied the effect of ultrasound on polymeric membranes immersed in a water bath. The ultrasonic frequency they used was 47 kHz. Three different polymeric membranes were studied, namely poly(ether sulphone) (PES), poly(vinylidene fluoride) (PVDF) and polyacrylonitrile (PAN). The effect of ultrasonic irradiation on the polymeric structure was determined by the measurement of the water permeability and the ratio of surface porosity to thickness. The authors showed that only the PES membrane was affected over its entire surface, the PVDF and PAN membranes were more resistant – only the PAN50a and PVDF40 membranes were affected significantly and mainly at the edges of the membranes. The degradation of membrane surfaces under ultrasonic stress led to an increase in the pore radius for large pores, an overall increase in pore density and porosity and to the formation of large cracks, mainly at the edges of the membranes. The conclusion was that ultrasound should be used with care with membranes – the nature of the polymeric material, the ultrasonic frequency and intensity should be taken into account.

2.4.3. Related work

Lenart and Auslander, (1980), examined the effect of ultrasound on the diffusion of certain electrolytes through cellophane membranes. They used ultrasound with an intensity of 1.2-6 $W.cm^{-2}$ and a frequency of 1 MHz. They found accelerated diffusion with ultrasonic irradiation.

The patent by Kost and Langer, (1988), uses ultrasound to enhance the permeability of molecules of small and large molecular weight in a membrane system irradiated with ultrasound of an intensity of 0.05-30 $W.cm^{-2}$ and a frequency between 10 kHz and 20 MHz for polymeric membranes and an intensity of 0.05-3 $W.cm^{-2}$ and a frequency of 1-3 MHz for biological membranes.

Li et al. (1995, 1996) investigated the influence of ultrasound on the diffusion of electrolytes through a cellophane membrane. They found that diffusion through the membrane with ultrasonic irradiation is faster than without ultrasound.

A summary of the most important studies on the use of ultrasound to reduce or prevent fouling in membrane filtration reported in the literature is given in Table **1**.

Table 1. Summary of the most important studies on ultrasonic defouling of membranes.

Author(s)	Membrane (Area, m^2)	Effluent	Filter Vol (L)	Freq (kHz)	Power[a] (W/cm^2)	Press (kPa)	Comments
Harvey (1965)	(RO)	-		-	-	-	US patent, use of acoustic whistles and ultrasonication to reduce clogging
Lenart and Auslander (1980)	cellophane	-		-	1.2-6	-	Studied effect on diffusion of electrolytes
Kost and Langer (1988)	polymer	-		10-20000	0.5-30	-	US patent, sonication for control of permeability of membrane
Band et al. (1997)	Ion exchange hollow fibres	salt water		25-49	23-61 W	-	Effect depended on salt concentration and power
Takata et al. (1998)	regenerated cellulose (RO, 0.045, 540), MWCO $1x10^4$ Da	NOM (river water) with PAC and H_2SO_4		0.06	-	60	Sustained vibration led to 50% higher flux than without, only commercial application
Chai et al. (1998)	PAN (UF, 0.0096)	1 wt% aq. dextran	Bath (11.52)	45	2.59	30	No effect for pure water, but strong effect for highly rejected dextran
Kobayashi et al. (1999)	PAN (UF, MF)	0.5, 1, 2, 3 5 wt% aq. dextran solutions	Bath (11.52)	28, 45, 100	150-300 W		Ultrasound intensity and direction of radiation important, 28-45 kHz worked best

[a] Power densities refer to the ratios of the nominal power output to the facial areas of the transducers involved in the generation of the ultrasound. However, values indicated by a W indicate the nominal power output only.

Chai et al. (1999)	PES, PVDF, PAN (UF, MF)	1, 2, 4 and 6 wt% aq. peptone solutions	Bath (11.52)	45	2.73	30	Cleaning of especially the PES membrane highly effective
Simon et al. (2000)	-	-		20	40 W	-	Dead-end filtration, both ultrasonic and mechanical stirring increased permeate flux
Masselin et al. (2001)	PES, PVDF, PAN	water		47	-	-	Reported membrane damage in dead-end filtration
Li et al. (2002)	Nylon (MF, 0.00315)	Kraft paper mill		20	82.9	50	Ultrasound with flushing most effective
Chai et al. (2003)	-	-		-	-	-	
Kobayashi et al. (2003)	PS (UF)	0.5 wt% aq. peptone solution		28, 45, 100	23	60	28 kHz gave better results than higher frequencies
Kobayashi et al. (2003)	cellulose	1 wt% aq. milk solution		28, 45, 100	23	60	28 kHz better than 47 kHz and 100 kHz
Muthukum-aran et al. (2004)	PS (0.0165)	6 wt% aq. whey solutions		50	10	55	Defouling independent of sonication time, higher power better

2.5. SUMMARY

In summary, the literature shows that the use of ultrasound to remove foulants from membrane filters works. Nonetheless, the fact that no commercial system has been reported yet demands closer scrutiny of the efficiency of ultrasonication as a means to clean membranes. In fact, few commercial systems are presently used in the wider field of sonochemical processing, owing to restricted reactor volumes, difficulty in controlling the reactors and relatively high operating costs (Mason, 1992). First of all, although the literature documents a number of studies (
Table **1**) where ultrasound has been used successfully to clean or prevent fouling on membranes, it has to be emphasized that all these experiments had been based on small laboratory-scale systems.

This is a crucial point, because the effect of the ultrasound is directly linked to the *acoustic cavitation* arising from the propagation of the sound waves in the fluid media. These studies therefore show that ultrasound can be used to defoul membranes (at least in the case studies considered), but do not necessarily indicate that the approach would be *cost-effective* on a large-scale, despite suggestions to the effect by several authors.

The reason for this is that acoustic cavitation is highly localized in the region of the transducer or sonicator. This is a fundamental limitation that cannot be surmounted by simply increasing the power input to the sonotrode. As a result, large-scale ultrasonic equipment tend to contain multiple transducers in conjunction with suitable reactor geometries (with large surface area to volume ratios, for example, if the transducers are attached to the surfaces of the reactor).

In most instances, the power required by the ultrasonic equipment is stated in nominal terms only, i.e. the mechanical power input to the devices, and then mostly stated as specific power input with regard to the area of the sonotrode tip. This is not useful as far

as scale-up is concerned, because it gives little indication of the energy distribution within the fluid (or more importantly, the distribution of cavitational bubbles in the fluid). Part of the reason for this is probably that the accurate measurement of cavitational fields in fluids remains a major challenge.

From the perspective of the design of membrane systems equipped with ultrasonicators, it would perhaps be more convenient to consider the power per unit volume of membrane filter (as cavitation can only be sustained in liquid media). In most instances 50-80 W/L seems to be the requirement for maintaining cavitation. More power is wasted and less power may lead to less or lack of cavitation.

With regard to the optimal frequency to be used, it is clear qualitatively that lower ultrasonic frequencies give rise to larger, but fewer cavitation bubbles, which implode with higher intensity than the more numerous, but smaller bubbles generated at higher ultrasonic frequencies. The optimal frequency would therefore depend on the details of the filtration system, but appears not be a major factor in the feasibility of the large-scale application of ultrasound in the first place.

3. MEASUREMENT OF ULTRASOUND IN CAPILLARY FILTRATION SYSTEMS

Experiments were conducted with distilled water to assess the distribution of the ultrasound intensity within membrane units. Two geometries were investigated, viz. a rectangular and a tubular unit, each of which contained a bundle of capillary membrane fibres, i.e. a total of 660 fibres (approximately 12692/m^2 cross-sectional area) in the rectangular unit and 220 fibres in the tubular unit (approximately 34582 fibres/m^2 cross-sectional area). Ultrasound pressure measurements were performed using a hydrophone, calibrated as described in Appendix B.

For the rectangular vessel, the ultrasound probe was placed at three locations, as indicated by the solid circle (top row, 2nd column of markers), triangle (top row, 5th column of markers) and square (5th row, 5th column of markers) in Figure 1, which shows a view of the tank with dimensions 600 x 130 x 400 mm. All the measurement locations were separated by a distance of 70 mm, both horizontally and vertically. Above the level of the top horizontal row of markers (30 mm depth), the tank was free of membrane fibres. Figure 2 shows a similar view of the measuring points, as viewed from the side of the tank.

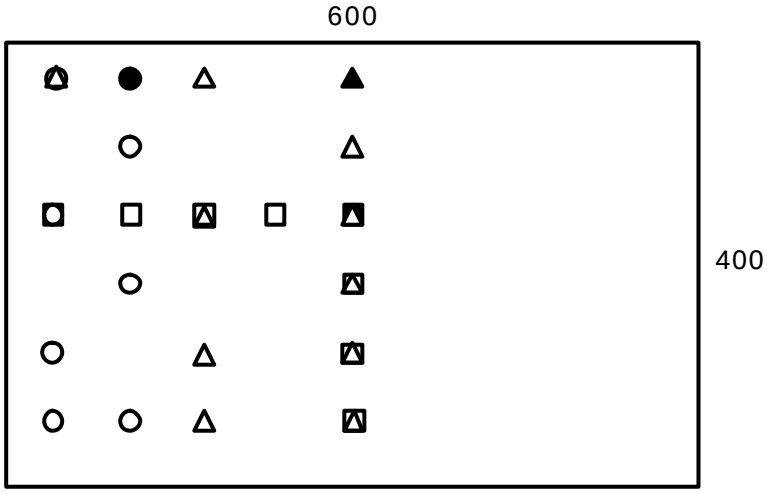

Figure 1. Diagram showing a view of the approximate locations of measurement points in the 600 x 400 x 130 mm^3 rectangular membrane filtration system. Solid markers indicate source or ultrasonic probe positions and open markers indicate the corresponding hydrophone positions.

For the tubular vessel, the ultrasound probe was placed at positions C1 and B2, as indicated in Figure 3. Above the level of A1-B1-C1-D1-E1, the tube was free of membrane fibres. When the probe was placed at C1, the sound intensity levels at positions A1, A3, B1, B3 were measured. When the probe was placed at position B2, positions A2, C2, D2 and E2 were monitored. These measurements were done both with and without flow.

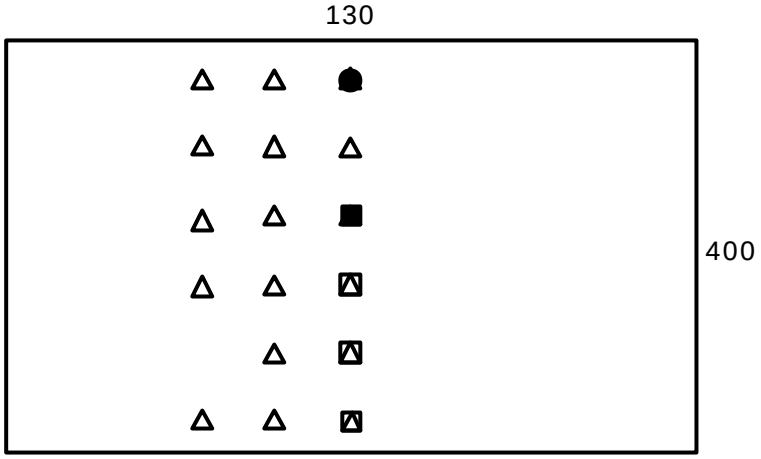

Figure 2. Diagram showing a lateral view of the approximate locations of measurement points in the 600 x 400 x 130 mm^3 rectangular membrane filtration system. Solid markers indicate source or ultrasonic probe positions and open markers indicate the corresponding hydrophone positions.

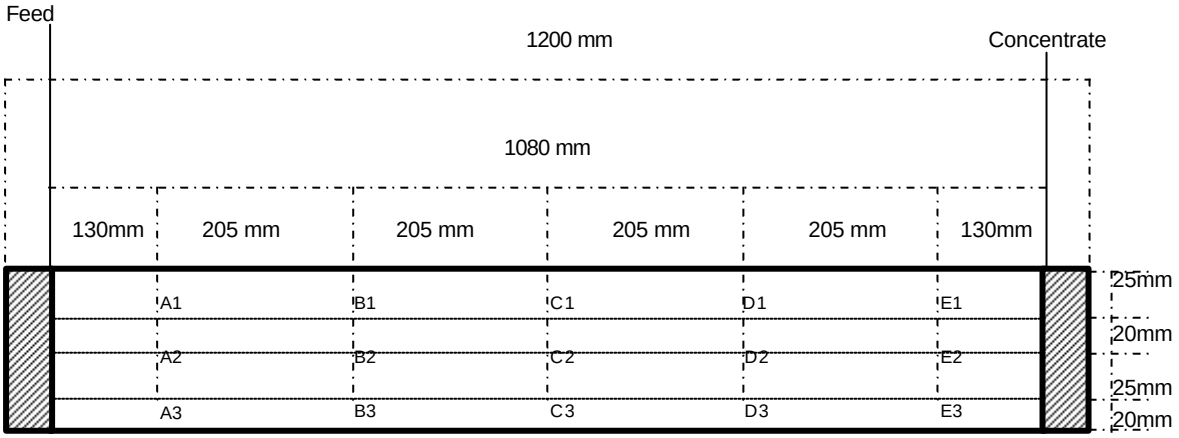

Figure 3. Diagram of the ultrasound energy measurement locations in the tubular (cylinder) membrane system.

3.1. ULTRASOUND ENERGY OUTPUT AT DIFFERENT AMPLITUDE SETTINGS OF THE ULTRASONICATOR

The intensity of the ultrasound measured in the free water medium at a radial distance of 10 mm at different amplitude settings is shown in Figure 4. The amplitude settings of the instrument is a measure of the nominal power output of the ultrasonicator, where an amplitude setting of 10 was equivalent to 130 W/cm^2, i.e. the ratio of nominal power output to facial area of horn or transducer. (According to the operating instructions supplied with the ultrasonicator, the instrument had an efficiency of approximately 85%, which means that a relatively high percentage of the power would actually be imparted

to the fluid.) The results show a curvilinear relationship between the ultrasound intensity level[b] and amplitude setting over the range of amplitude settings considered.

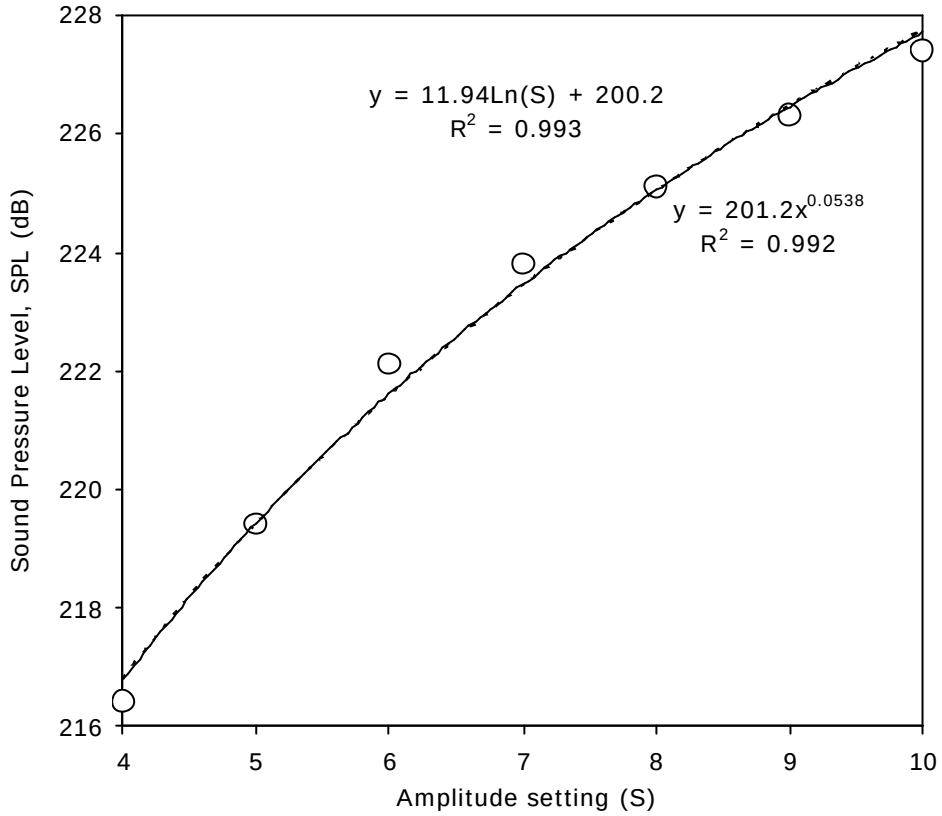

Figure 4. Sound pressure level, SPL (dB) in the free water medium at different amplitude settings (S) of the instrument, measured 10 mm from the sonic source with a reference pressure value of 1 μPa. The relationship is described equally well by an exponential or a power function.

The ultrasound waves produced by the sonicator generally did not show constant amplitudes. In the radial direction of the ultrasound, the amplitude of the sound wave decreased with increased distance from the ultrasound source. In the axial direction of the ultrasound, the ultrasound waves with stronger and more constant amplitudes were observed at the location where the higher sound pressures were detected.

[b]The relationship between sound intensity level L_I (dB) and specific power in SI units (W/m^2) is given by L_I (dB) = $10*\log(I/I_{ref})$, where I and I_{ref} are measured in W/m^2. Equivalently, the relationship between sound pressure level L_p (dB) and pressure in SI units (Pa) is given by L_p (dB) = $20*\log(p/p_{ref})$, where p and p_{ref} are measured in Pa. Note that the decibel values have to be interpreted relative to the reference sound pressure or intensity, I_{ref} or p_{ref}. The reference sound pressure in this case is 1 μPa and $I_{ref} = p^2_{ref}/\rho c$ is therefore $I_{ref} = 6.7 \times 10^{-19}$ W/m^2 (with the density of water, ρ = 1000 kg/m^3 and the velocity of sound in water, c = 1500 m/s).

3.2. ULTRASOUND PRESSURE (ENERGY) DISTRIBUTION IN THE RECTANGULAR FILTRATION VESSEL

The results from the measurements made on the rectangular filtration vessel shown in Figures 5-9 indicate that

- In the presence of membrane fibres the sound pressure levels were up to approximately 5 dB less than in the absence of the fibres at various distances up to 280 mm from the probe (Figure 8). This is equivalent to a reduction of approximately 70% in the ultrasound intensity at these various measuring points.

- The energy distribution of the ultrasound in the membrane system varies both along the axial and radial directions. For example, in Figure 8 the decrease in the sound intensity level is approximately 23 dB over a distance of 250 mm. This is equivalent to a decrease in intensity (W/cm^2) of approximately 99.5% over that distance.

- The ultrasonic intensity was up to approximately 30-40% lower (up to 2.5 dB less) when flow of 513 mL/min was introduced in the membrane module, compared to when the intensity of the energy in stationary fluid (water), as indicated in Figure 5.

- Coverage of the probe with a steel cap led to an approximate decrease of up to 8 dB in the ultrasonic energy inside the vessel (see Figures 6, at a distance of 140 mm). This is equivalent to a loss in intensity of approximately 84%.

- Generally, the ultrasonic intensity level (or equivalently, the sound pressure level, dB) showed a maximum on the ultrasonic beam and decreased immediately with an increase in the radial distance from the ultrasonic beam. However, this decrease became less at the further distance from the ultrasonic beam.

- The ultrasonic intensity exhibited periodic variation along the axis of the ultrasonic beam. At the vicinity of the ultrasonic horn, a cloud of cavitation bubbles was observed. The ultrasound intensity was at a minimum near the radiation surface of the ultrasound horn (±10 mm). This was probably owing to the absorption of the ultrasound in this bubble medium.

- The further the distance from the ultrasonic beam, the weaker the periodic variation of the ultrasonic intensity became.

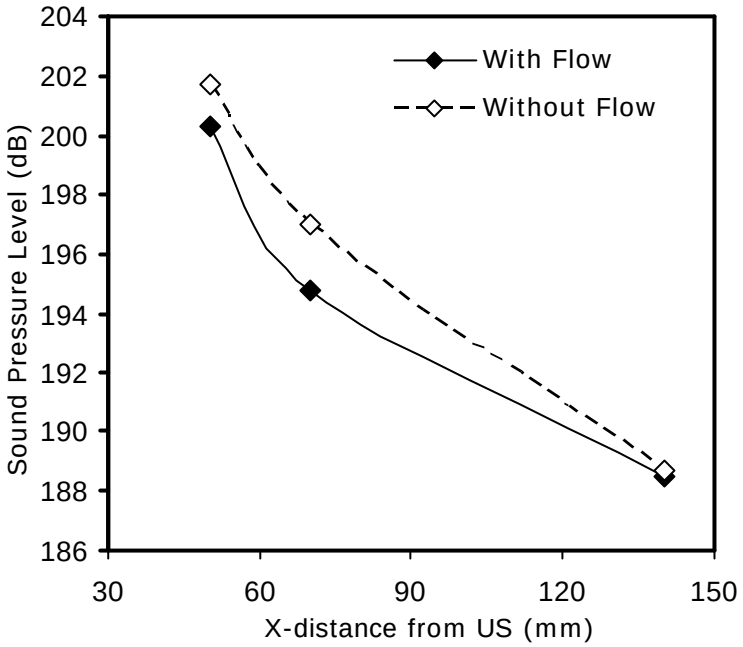

Figure 5. Influence of the flow through the module on the energy distribution of the ultrasound in the radial direction (X-distance) of the sound beam in the rectangular membrane filtration system.

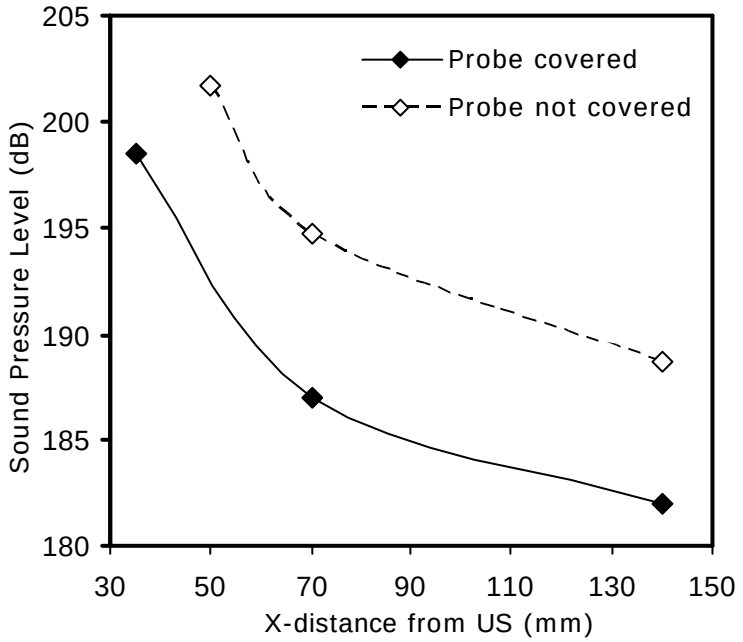

Figure 6. Influence of probe coverage on the energy distribution of the ultrasound in the radial direction (X-distance) of the sound beam in the rectangular membrane filtration system without flow.

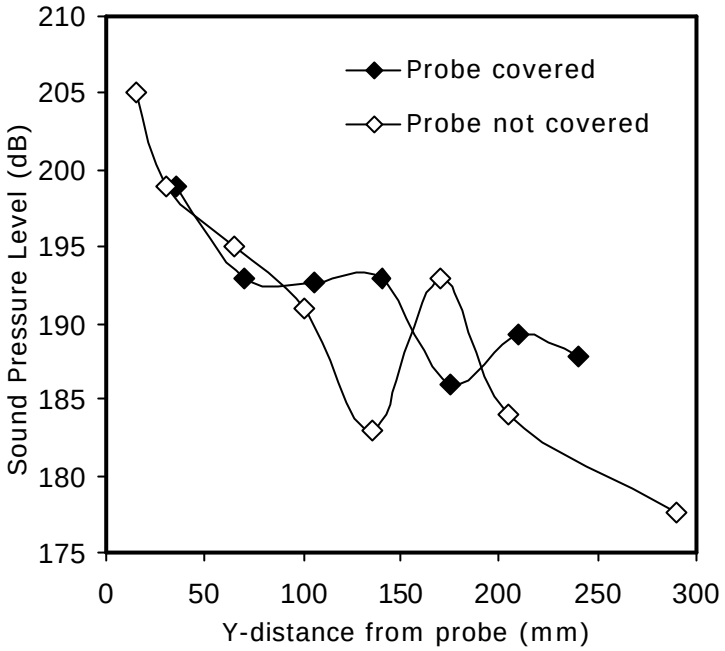

Figure 7. Influence of probe coverage on the energy distribution of the ultrasound in the axial direction (Y-distance) of the sound beam in the rectangular membrane filtration system without flow.

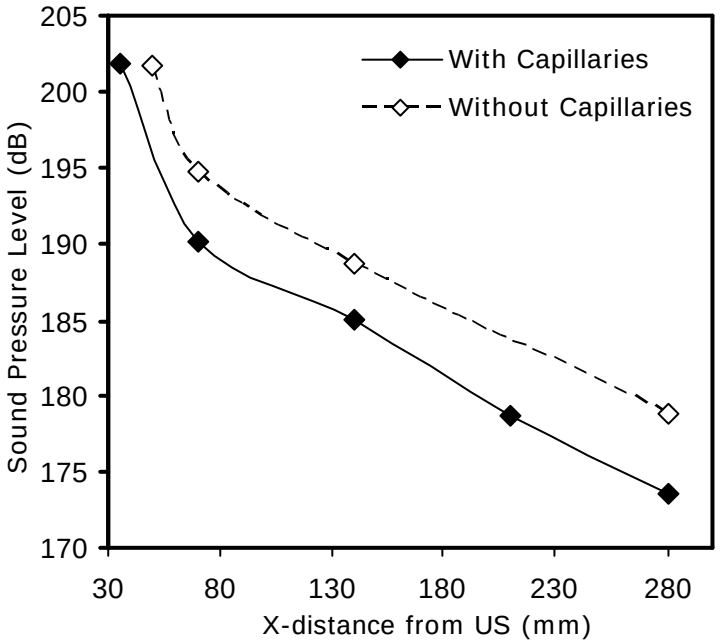

Figure 8. Influence of the presence of membrane capillaries on the ultrasound energy distribution in the radial direction (X-distance) of the sound beam in the rectangular membrane filtration system.

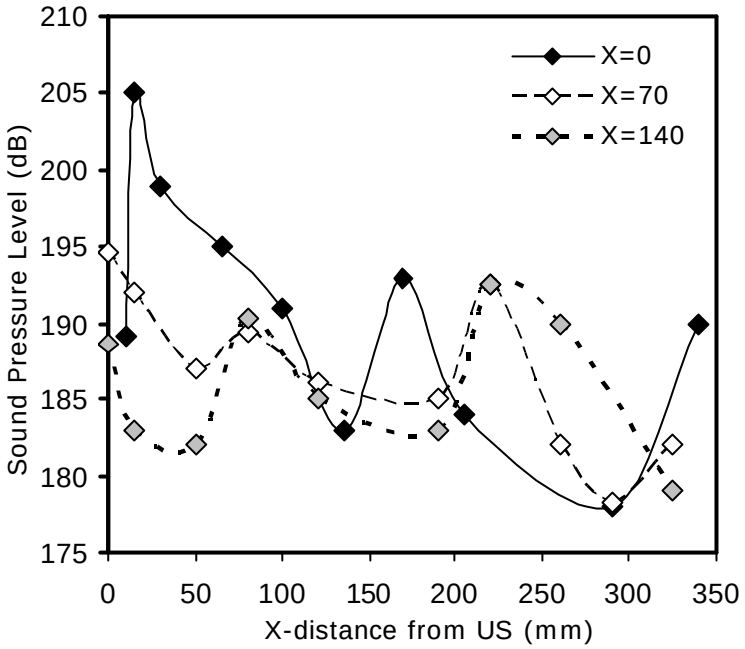

Figure 9. Energy distribution of the ultrasound in the axial direction (Y-distance) of the sound beam at different radial distance (X-distance) levels in the rectangular membrane filtration system.

3.3. ULTRASOUND PRESSURE (INTENSITY) LEVEL DISTRIBUTION IN THE TUBULAR FILTRATION SYSTEM

When the ultrasonic probe was placed at position C1 in tubular filtration system, the energy levels at the measuring points were too low to enable a signal to be captured, although a strong ultrasound signal was detected in the vicinity of the probe. This implied that when the ultrasonic source was positioned near the top wall of the tube, away from the membrane fibres, which were positioned towards the bottom wall of the tube, the distribution of the sonic energy was highly localized rather than evenly distributed inside the tubular space. When the ultrasonic probe was placed in the central space of the tube, among the membrane fibres, the sound pressure signals at the positions to be measured were easily captured by the hydrophone. The measurements indicated that the ultrasound energy was better transmitted along the tube, with the sonic intensity decreasing with the distance from the sonic emitter along the axial direction of the tube.

As indicated in Figure 10, a decrease of approximately 16 dB was observed over 600 mm of the axial distance of the tube in the presence of flow and a decrease of approximately 14 dB in the absence of flow. This is equivalent to a loss of 97.5% along the tube in the tubular membrane filtration system when the sonic source was placed in the centre of the tube, among the membrane fibres with flow. The flow itself led to a decrease of approximately 75% in the intensity of the ultrasound.

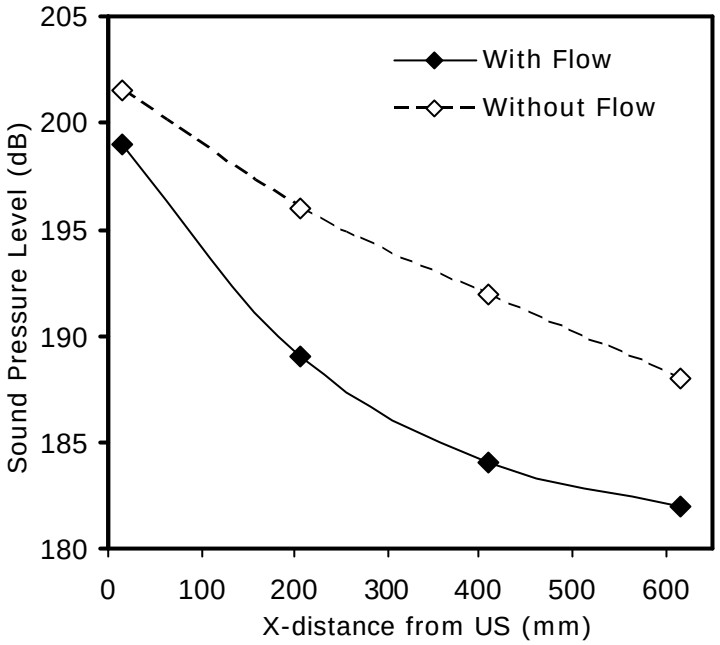

Figure 10. Influence of the flow through the module on the energy distribution of the ultrasound in the radial direction (X-distance) of the sound beam in the tubular membrane filtration system.

3.4. THE ULTRASOUND WAVE ATTENUATION IN CAPILLARY MEMBRANE FILTRATION SYSTEM

Ultrafiltration membranes, which are made from poly(ether sulphone) can be viewed homogeneous, because the pore size of the membrane fibre is normally far smaller than the wave length of the applied ultrasound. Under ultrafiltration and ultrasonication conditions, all the pores of the membranes and the gaps among the capillary membrane fibres are filled with fluid. The attenuation of the ultrasound wave in the membrane filtration system is caused by absorption in the fluid (water), reflection by the membrane fibre surface and absorption in the membrane fibres themselves.

The attenuation in the fluid, membrane solid/water interface and membrane solid phase can be calculated theoretically when the density of the membrane fibre and the sound velocity in the membrane fibres can be measured accurately. Some of these calculations are discussed in more detail in Appendix A.

Using the sound pressure P measured by hydrophone, the relationship between the relative ultrasound pressure, $y = \log(P_0/P)$, and the distance x travelled by the sound are shown in Figures 11 and 12.* The results show that either in rectangular or tubular membrane filtration systems, the changes of $\log(P_0/P)$ with the distance travelled (x) in the radial direction of the ultrasound generally exhibit a linear relationship, although this is not strictly true at the vicinity of the sound beam.

The slopes of the curves in Figures 11 and 12 represent the attenuation coefficients of the ultrasound in the two vessels, expressed in dB/mm. These values are similar to the approximate values reported for the propagation of ultrasound in water by Krautkrämer and Krautkrämer (1969), that is α = 1 to 4 m^{-1}. In the rectangular vessel, the attenuation was approximately 20% higher in the presence of the fibres (with fibres, α = 0.049 cm^{-1} versus without fibres, α = 0.041 cm^{-1}).

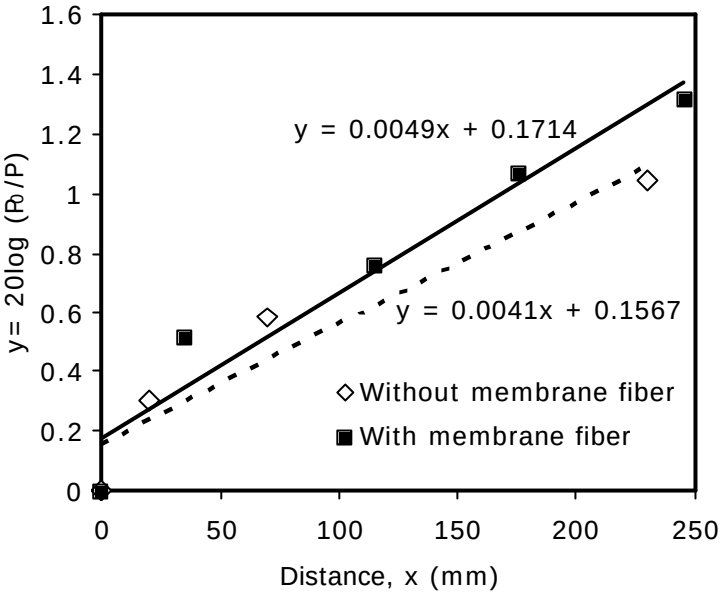

Figure 11. Plot of 20*log(P_0/P) to the radial travel distance (X-distance) of the ultrasound in the rectangular membrane filtration system.

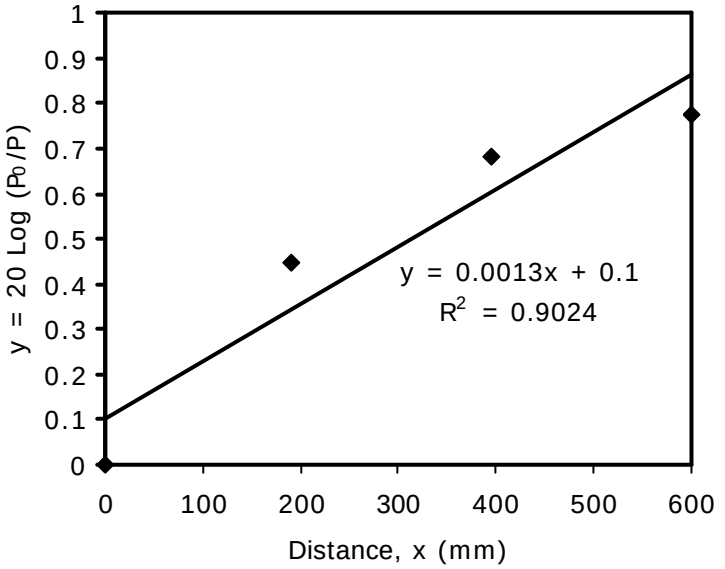

Figure 12. Plot of 20*log(P_0/P) to the radial travel distance (X-distance) of the ultrasound in the rectangular membrane filtration system.

3.5. CONSIDERATIONS IN THE SCALE-UP OF ULTRASONIC CLEANING OF THE MEMBRANE FILTERS

Generally, industrial ultrasonic devices or reactors are not simply larger versions of laboratory-scale systems. For example, probe systems operating at typical face intensities of 5 x 10^4 to 1 x 10^6 W/m^2 at frequencies of 20-60 kHz suffer from the serious drawback that the cavitational fields they generate cannot be transmitted more than several centimetres beyond the tips of the probes (McCausland et al., 2001). Even banks of probes are reported to be incapable of transmitting cavitation through more than 10 to 70 cm. Moreover, single transducers are also limited in the amount of power that they can transmit. The highly localized distribution of cavitational fields around transducer

faces or tips is a fundamental limitation, which means that scale-up is almost always based on the use of *multiple transducers* appropriately placed in reactor or cleaning vessels (Gogate et al., 2003). In this way, power densities of 70-80 W/L could be achievable in large volumes (McCausland et al., 2001).

Therefore to be effective, the ultrasonic power delivered to the membrane filtration system must be sufficient to cavitate the entire volume of liquid with the workload in place, amounting to approximately 50-100 W/gallon or 13020 W/m^3, if the current design of most cleaning systems is taken as a measure. In addition, ultrasonic transducers can treat limited volumes of reactor or filter space only, regardless of their power output and these two factors have to be taken into account in scale-up.

Although other factors have also to be taken into account, such as the physical properties of the effluent, these factors are relatively invariant for aqueous effluent systems (e.g. the density, viscosity and sound velocity of the effluent) and therefore the most important issue in terms of scale-up is the geometry of the membrane filtration unit.

4. ASSESSMENT OF VARIOUS APPROACHES BASED ON THE USE OF ULTRASOUND TO REMOVE FOULANTS FROM MEMBRANES

In general, the experimental setup used in this investigation consisted of a membrane unit, an ultrasonicator used to generate the ultrasound, as well as ancillary apparatus, such as a (peristaltic) pumping system, gauges and feed and product tanks. A summary of all the experiments that were done are given in Table 2.

Table 2. Summary of experiments conducted on ultrasonic defouling of membranes.

NO	SCALE	MEM CONFIG	MEM MATERIAL	TYPE	EFFLUENT	SONIC
A	Small	Flat sheet	Polyamide	RO	$CaSO_4$	B
B	Small	Flat sheet	Polyamide	RO	$FeCl_3$	B
C	Small	Flat sheet	Polyamide	RO	CMC	B
D	Small	Flat sheet	Poly(ether sulphone)	UF	LDL	B, P1
E	Small	Capillary	Poly(ether sulphone)	UF	Milli-Q H_2O	P1
F	Small	Capillary	Poly(ether sulphone)	UF	Congo Red	P1
G	Large	Capillary	Poly(ether sulphone)	UF	NOM	P1
H	Small	Capillary	Poly(ether sulphone)	UF	NOM	P1, P2, V

B = 20 kHz bath, P1 = 30 kHz probe, P2 = 20 kHz probe, V = mechanical vibrator (20 Hz)

Three ultrasonication systems were used in the experiments described below, viz. two horn transducers or probes and an ultrasonic bath. One probe (P1) operated at fixed frequency of approximately 30 kHz, generating a maximum acoustic power density of 130 W/cm^2 with a nominal power output of 50 W (IKA Labortechnik Staufen, United Kingdom, U50). The other probe (P2) (Model W-375, Heat Systems, Ultrasonics, Inc., USA) operated with a frequency of 20 kHz and a power density of 83 W/cm^2. This probe was not available for all the experiments. The 30 × 24 × 20 cm^3 ultrasonic bath (B) operated at a fixed frequency of approximately 20 kHz, generating 2.8 W/cm^2 with a nominal power output of 240 W (Ultrasonic cleaner, Denmark, 3A). Unless otherwise stated, the power densities refer to the ratios of the nominal power output to the facial areas of the transducers involved in the generation of the ultrasound.

4.1. FILTRATION OF $CaSO_4$, $FeCl_3$ AND CMC WITH A REVERSE OSMOSIS POLYAMIDE MEMBRANE WITH THE BATH SYSTEM (A, B and C in Table 2)

A commercial polyamide-based reverse osmosis membrane suitable for low-pressure operation was obtained from Fluid Systems Company, USA. The $CaSO_4$ solution was prepared by the reaction of certain amounts of $Ca(OH)_2$ and H_2SO_4 (analytically pure reagents obtained from Sigma Aldrich, South Africa). Desired concentrations of Fe^{3+} were prepared by dissolving certain amounts of $FeCl_3.6H_2O$ (analytical grade from Merck, USA) into distilled water, and adjusting the pH of the solution by use of HCl (analytical grade from Merck). The sample of carboxymethyl cellulose (CMC) with a molecular weight of 250,000 was obtained from Sigma-Aldrich, South Africa. The CMC solutions were prepared by dispersing a known weight of CMC in cold distilled water and then dissolving it with boiling distilled water. The solutions were prepared fresh each day. Distilled water was used in all tests.

The experimental setup is shown in Figure 13. Tubular poly(ether sulphone) ultrafiltration membranes, supplied by Weir-Envig (Pty) Ltd, Paarl, South Africa, were used in flat-sheet form by slitting tubes and folding them open, to provide membrane sheets

with dimensions of 2.5 x 14 cm. All membrane sheets were cut from a single tubular ultrafiltration membrane. The molecular mass cut-off of the membrane was around 30 kDa. The membrane sheets were saturated overnight with distilled water before use. The membrane unit was comprised of a flat-sheet UF cell, which could either be immersed in the ultrasonic bath or be equipped with the ultrasonic probe placed at the permeate discharge side. No probes were used in these experiments.

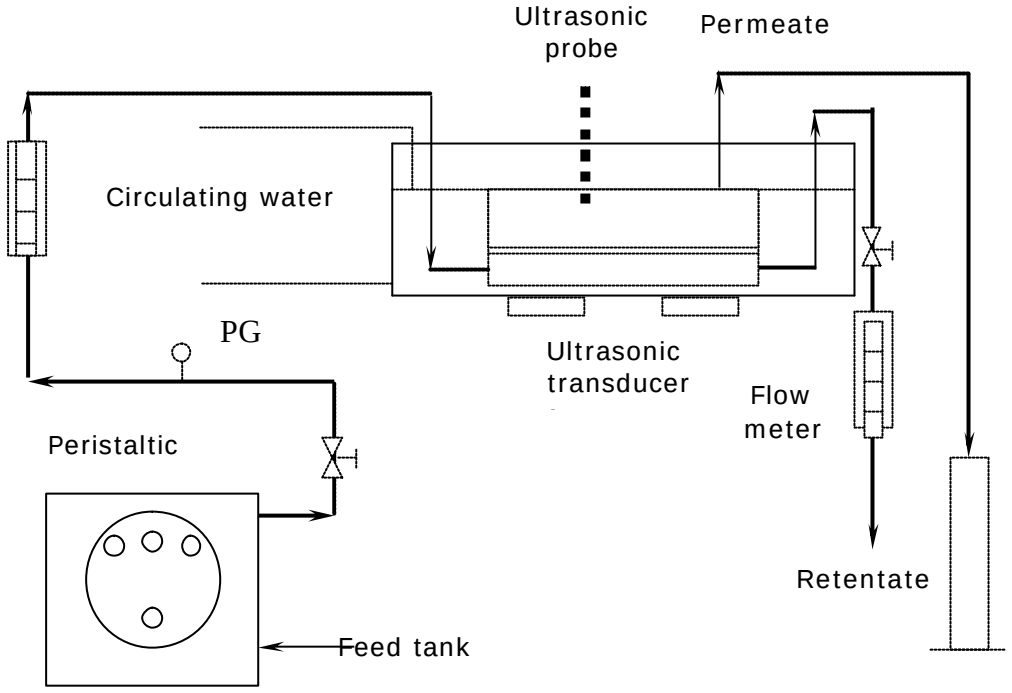

Figure 13. Experimental setup with reverse osmosis (RO) membranes.

The membrane was placed in the crossflow filtration unit, which was immersed in the water bath of the bath sonicator (Ultrasonic cleaner, Denmark). Two of the four ultrasonic transducers in the ultrasonic bath were used to act on the membrane cell, which had an effective filtration area of 14 × 4 cm^2. The temperature of the solutions in the feed tank was maintained at 20 °C to within ±1 °C. During the experiments, the flow rate of the feed solutions and operating pressure were maintained at about 5 mL/min and 100 kPa, respectively. The permeate flux ($L.m^{-2}.h^{-1}$) of the membrane was determined by measuring the volume of the permeated solution at certain intervals.

The calcium and iron concentrations in the feed, retentate and permeate solutions were analyzed with an atomic absorption spectrometer (Varian, AA20, Australia). The CMC concentrations in the feed, retentate and permeate solutions were determined by the total organic carbon (TOC) using a TOC analyzer (Dhorman). Experiments were replicated at least once and only the mean values are reported.

Fresh sheet of the flat polyamide reverse osmosis membrane was cut into rectangular sections of approximately 18 × 6 cm^2. All membranes were cut from a single sheet of membrane for all the filtration experiments on the same types of solutions. All the membranes were immersed in distilled water for 24 hours prior to the filtration experiments. The morphological changes of the membrane with and without ultrasonic treatment were investigated by using a scanning electron microscope (SEM) images.

The rejection values reported in this study are based on the definition: $R = 1 - C_P/C_R$, where C_P is the concentration of the permeate and C_R is the concentration of the retentate. C_P and C_R thus represents the steady state bulk concentration of Ca, Fe and TOC in the permeate and retentate streams leaving the membrane cell in the reverse osmosis filtration tests for $CaSO_4$, $FeCl_3$ and CMC solutions, respectively.

4.1.1. Filtration of $CaSO_4$ solutions

Two different concentrations (500 mg/L and 1000 mg/L) of $CaSO_4$ solutions were tested for filtration in the presence and absence of ultrasound. In each case the total filtration time was 3 hours. Figures 14 and 15 show the effect of ultrasound treatment on the permeate flux and rejection of the membrane filtration for $CaSO_4$ solutions, respectively. The permeate flux for the membrane filtration of $CaSO_4$ solutions increased markedly in the presence of ultrasonication as indicated in Figure 17, while the rejection values decrease only marginally at both solution concentrations, as shown in Figure 18. On average, the permeate flux increased by about 50.8% for the 500 mg/L $CaSO_4$ solution and by approximately 69.7% for the 1000 mg/L $CaSO_4$ solution during 3 hours of filtration in the presence of ultrasound. As can be seen from Figures 14 and 15, the higher feed concentration resulted in both a lower permeate flux and lower rejection. It is known that fouling occurs easily in a polymeric membrane system when the concentration of the feed solution increases (Reihanian et al., 1983). $CaSO_4$ concentrations used in the experiments were much lower than their saturated concentration of 2060 mg/L at 22°C (Mairal, 1998). However, $CaSO_4$ crystals were still deposited on the membrane surface, owing to seeding of the membrane during filtration. Ultrasound treatment could enhance the permeate flux without much loss in rejection. This could be attributed to the enhancement of ion diffusion and ultrasonic cleaning of the membrane surface.

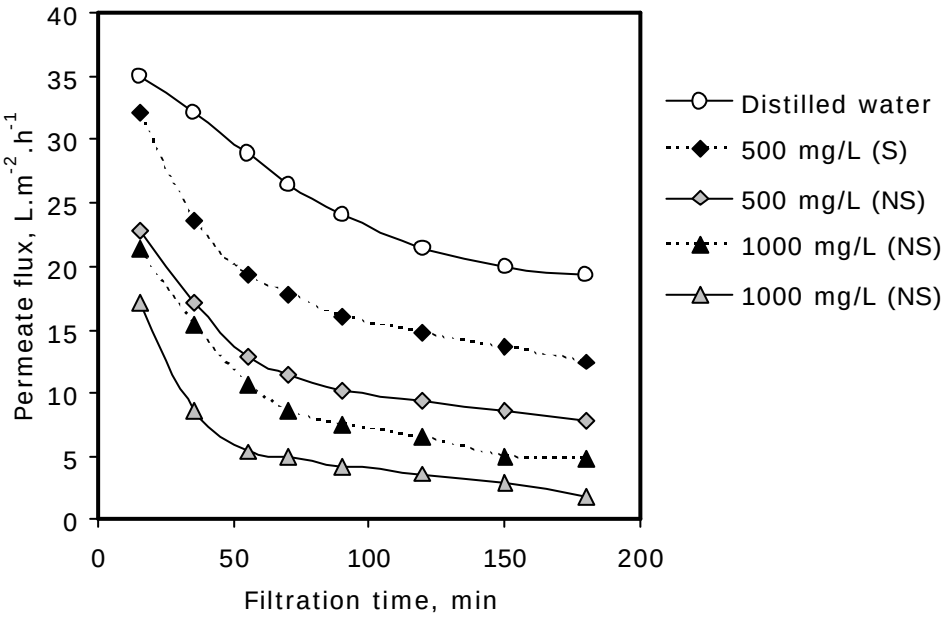

Figure 14. Effect of ultrasound treatment on the permeate flux of membrane filtration for $CaSO_4$ solutions. S and NS indicate sonication and no sonication respectively. The

maximum standard deviation of the observations of the permeate flux did not exceed 3.4% of the averages indicated in the figure.

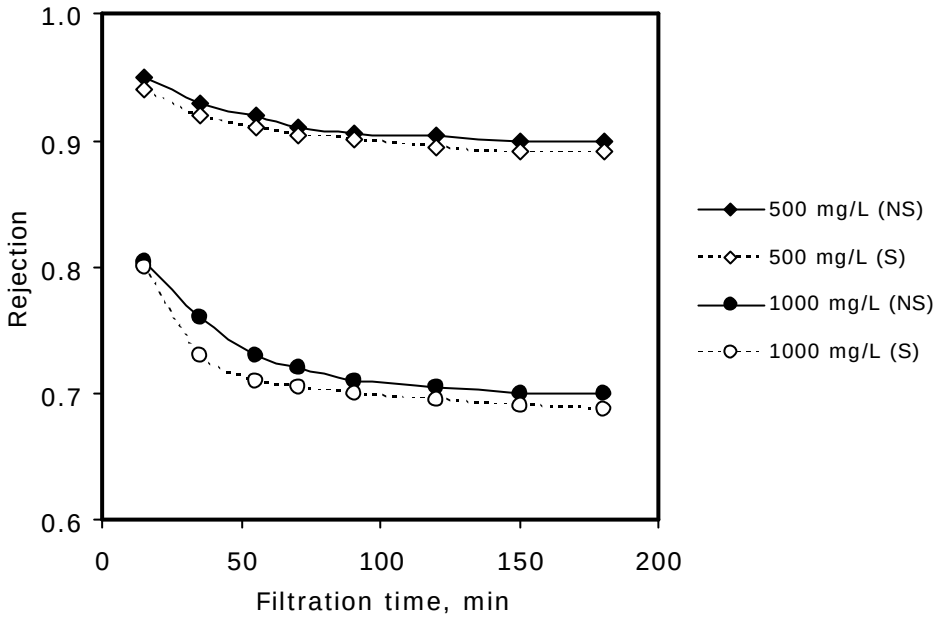

Figure 15. Effect of ultrasound treatment on the rejection of membrane filtration for $CaSO_4$ solutions. S and NS indicate sonication and no sonication respectively. The maximum standard deviation of the observations of the rejection values did not exceed 0.37% of the averages indicated in the figure.

The ultrasonic defouling of the reverse osmosis membrane during the filtration of the $CaSO_4$ solutions can also be observed from images of the morphology of the membrane surfaces. The differences in the surface morphologies of the fresh membrane, membrane fouled with 1000 mg/L $CaSO_4$ in the absence of ultrasound and membrane fouled with 1000 mg/L $CaSO_4$ in the presence of ultrasound after 3 hours of filtration is shown in Figures 16-18, respectively.

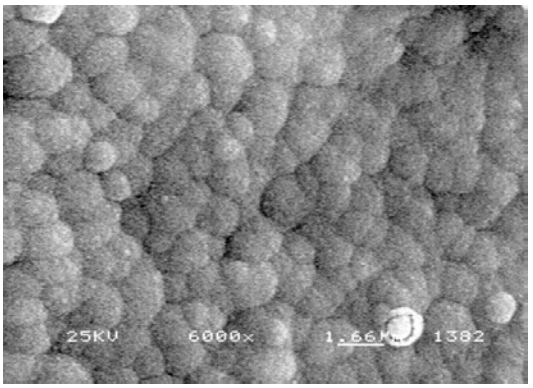

Figure 16. Morphological image of the fresh reverse osmosis membrane showing the microstructure the membrane surface (25 kV, magnification 6000, scale bar 1.66 μm).

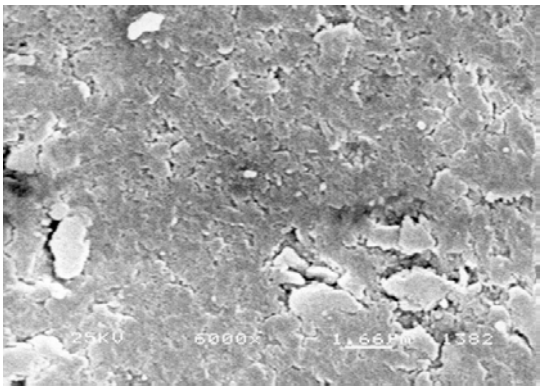

Figure 17. Morphological image of the fouled reverse osmosis membrane with $CaSO_4$ in the absence of ultrasound (25 kV, magnification 6000, scale bar 1.66 µm).

The network structure of the membrane is evident in Figure 16. Figure 17 shows the microstructure of the reverse osmosis membrane fouled with $CaSO_4$ in the absence of ultrasound. As can be seen from Figure 17, most of the membrane surface was covered with a layer of $CaSO_4$, which was the reason for the sharp decrease in the permeate flux observed during the filtration of the 1000 mg/L $CaSO_4$ solution in the absence of ultrasound. Ultrasonication removed most, but not all of the foulant deposited by the $CaSO_4$ during filtration, as indicated in Figure 18. It can also be seen from Figure 18 that the microstructure of the membrane surface remained undamaged during the sonication process. Acoustic vortex microstreaming within the pores of the membrane, as well as at the solid-liquid interface probably contributed to the cleaning of the membrane surface. On the other hand, some deposition of $CaSO_4$ could have occurred as a result of hot spots created within the liquid during sonication, as the solubility of $CaSO_4$ is lowered with an increase in temperature (Mairal, 1998).

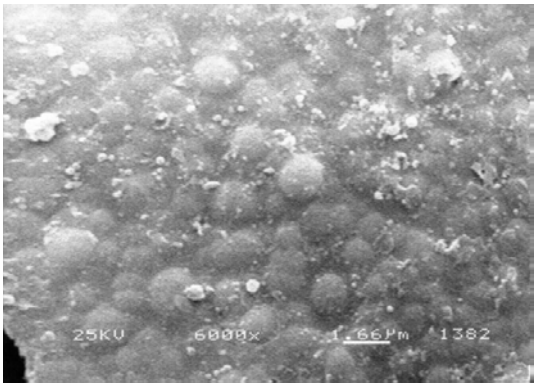

Figure 18. Morphological image of the fouled reverse osmosis membrane with $CaSO_4$ in the presence of ultrasound (25 kV, magnification 6000, scale bar 1.66 µm).

4.1.2. Filtration of $FeCl_3$ solution

The $FeCl_3$ solution with 20 mg/L Fe^{3+} was tested for filtration in the presence and absence of ultrasound. The $FeCl_3$ was hydrolysed to a floc shape $Fe(OH)_3$ suspension at pH 4.5. The total filtration time was 3 hours. Figures 19 and 20 show the respective effects of ultrasound treatment on the permeate flux and rejection of filtration for the $FeCl_3$ solution.

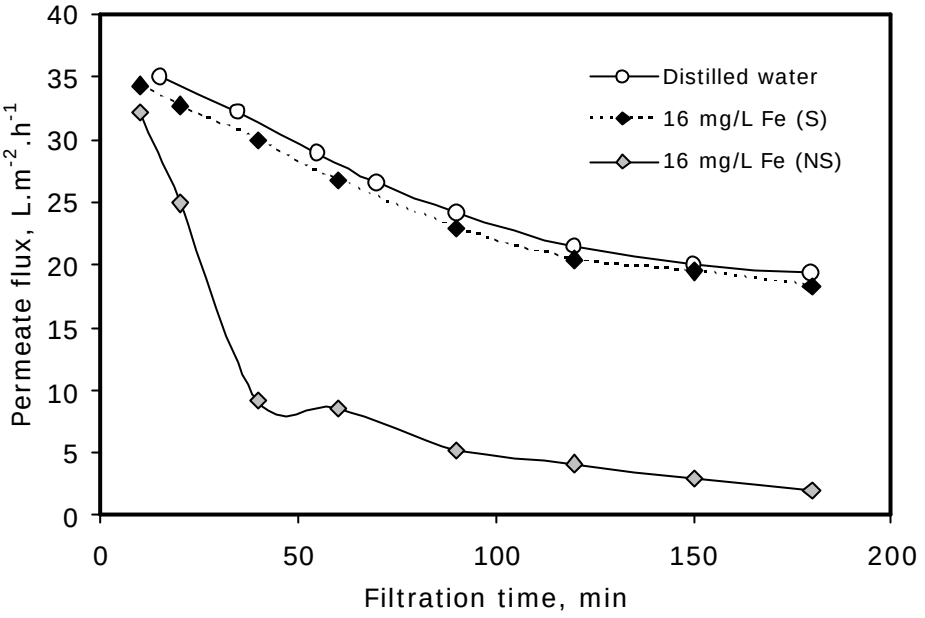

Figure 19. Effect of ultrasound treatment on the permeate flux of membrane filtration for $FeCl_3$ solution. S and NS indicate sonication and no sonication respectively.

The permeate flux for the membrane filtration of the $FeCl_3$ solution increased significantly in the presence of ultrasonication, as indicated in Figure 19, while the rejection values showed negligible decrease, as shown in Figure 20. On average, the permeate flux increased by about 215% for $FeCl_3$ solution with 20 mg/L Fe^{3+} during 3 hours of filtration in the presence of ultrasound. In the absence of ultrasound, the permeate flux sharply decreased, owing to the rapid deposition of $Fe(OH)_3$ flocs on the membrane surface. In the presence of ultrasound, the permeate flux of the $FeCl_3$ solution very closely resembled distilled water, suggesting that no $Fe(OH)_3$ flocs were deposited on the membrane surface during filtration in the presence of ultrasound. The maximum standard deviation of the observations of the permeate flux did not exceed 3.8% of the averages indicated in the figure. This conclusion is supported by an analysis of the morphologies of the membrane surfaces, as indicated in Figures 21 and 22. These figures show the differences in the surface morphologies of the membrane fouled with 20 mg/L Fe^{3+} solution in absence of ultrasound (Figure 21**Figure 21**) and the membrane fouled with 20 mg/L Fe^{3+} solution in the presence of ultrasound after 3 hours of filtration (Figure 22).

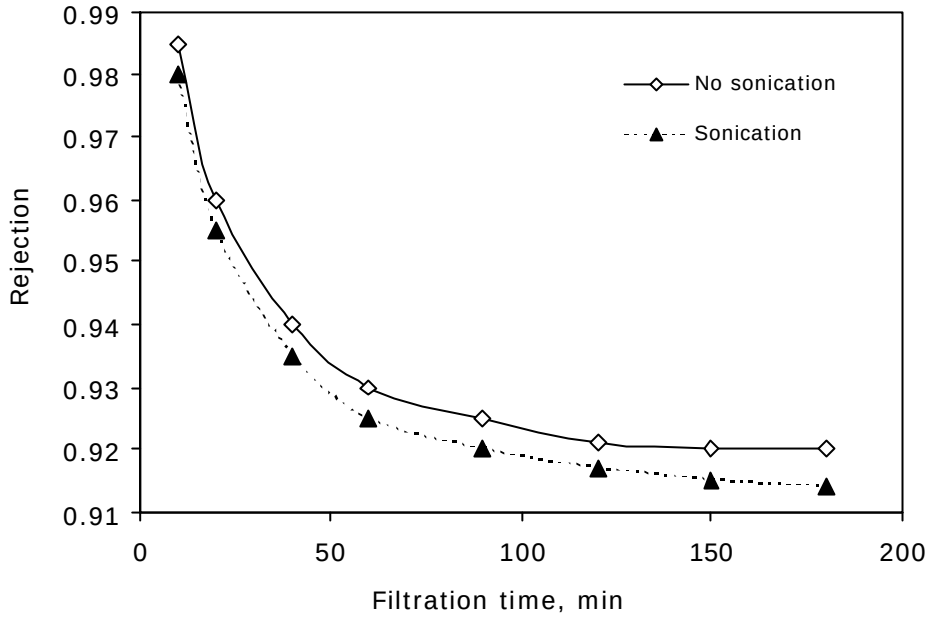

Figure 20. Effect of ultrasound treatment on the rejection of membrane filtration for $FeCl_3$ solution. S and NS indicate sonication and no sonication respectively. The maximum standard deviation of the observations of the permeate flux did not exceed 0.71% of the averages indicated in the figure.

As be seen from Figure 21, the membrane surface was completely covered with a layer of $Fe(OH)_3$ flocs, which was the reason for the sharp decrease in the permeate flux observed during the filtration of the 20 mg/L Fe^{3+} solution in the absence of ultrasound. Apart from some small loose particles on the membrane surface (Figure 22), the membrane surface was clear and the microstructure of the membrane surface remained undamaged during the sonication process.

The defouling effect of the membrane during $Fe(OH)_3$ filtration can be attributed to mechanical cleaning associated with the high-speed microstreams and enhanced dispersion of $Fe(OH)_3$ flocs in the ultrasonic cavitation process.

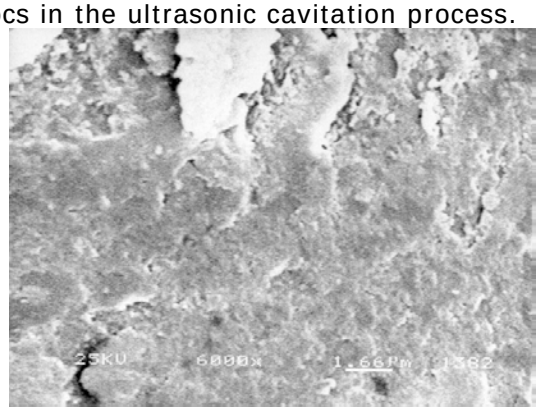

Figure 21. Morphological image of the fouled reverse osmosis membrane with $Fe(OH)_3$ flocs in the absence of ultrasound (25 kV, magnification 6000, scale bar 1.66 μm).

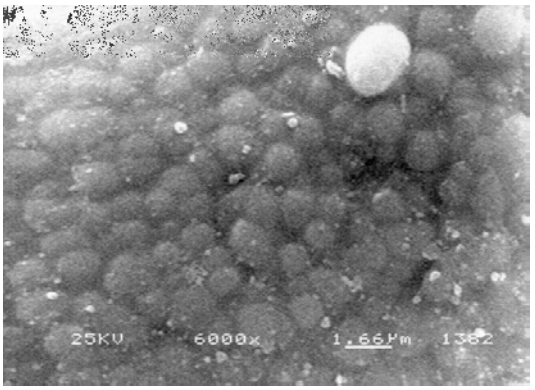

Figure 22. Morphological image of the fouled reverse osmosis membrane with $Fe(OH)_3$ flocs in the presence of ultrasound (25 kV, magnification 6000, scale bar 1.66 µm).

4.1.3. Filtration of CMC solutions

500 mg/L and 1000 mg/L concentrations of CMC solutions were tested for filtration in the presence and absence of ultrasound. As before, the total filtration time was 3 hours. Figures 23 and 24 show the respective effects of ultrasound treatment on the permeate flux and rejection during filtration.

The permeate flux for the membrane filtration of CMC solutions increased considerably in the presence of ultrasonication, as indicated in Figure 23. In contrast, the rejection values showed a negligible decrease at both CMC concentrations, as shown in Figure 24. On average, the permeate flux increased by approximately 164% and 113% for the 500 mg/L and 1000 mg/L CMC solutions respectively during 3 hours of filtration in the presence of ultrasound. As can be seen from Figures 23 and 24, the higher feed concentration resulted in a lower permeate flux, as well as lower rejection. The enhanced permeate flux and concomitant lower loss in rejection could be attributed to the increase in the solubility of the CMC, the decrease of the viscosity of the solution and the high-speed microstream cleaning of the membrane surface during the ultrasonic cavitation.

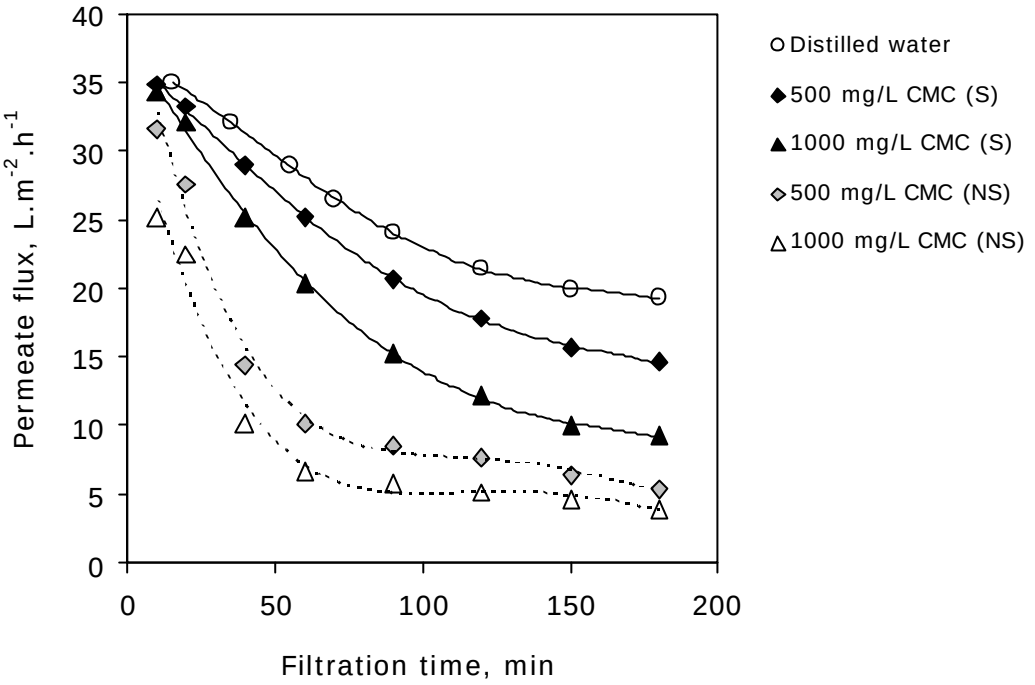

Figure 23. Effect of ultrasound treatment on the permeate flux of membrane filtration for CMC solutions. S and NS indicate sonication and no sonication respectively. The maximum standard deviation of the observations of the permeate flux did not exceed 1.7% of the averages indicated in the figure.

The ultrasonic defouling of the reverse osmosis membrane in the CMC solution can also be observed from images of the morphologies of the membrane surfaces. The difference in the surface morphology of the membrane fouled with 1000 mg/L CMC in the absence of ultrasound and the membrane fouled with 1000 mg/L CMC in presence of ultrasound after 3 hours of filtration is obvious from a comparison of Figures 25 and 26.

As can be seen from Figure 25, the CMC flocs were evenly distributed on the membrane surface. This is likely to have caused a sharp decrease in the permeate flux observed in 1000 mg/L CMC filtration in the absence of ultrasound. In the presence of ultrasound, the membrane surface was kept clear, as indicated in Figure 26. In addition, it can also be seen from Figure 26 that the microstructure of the membrane surface remained undamaged during the sonication process.

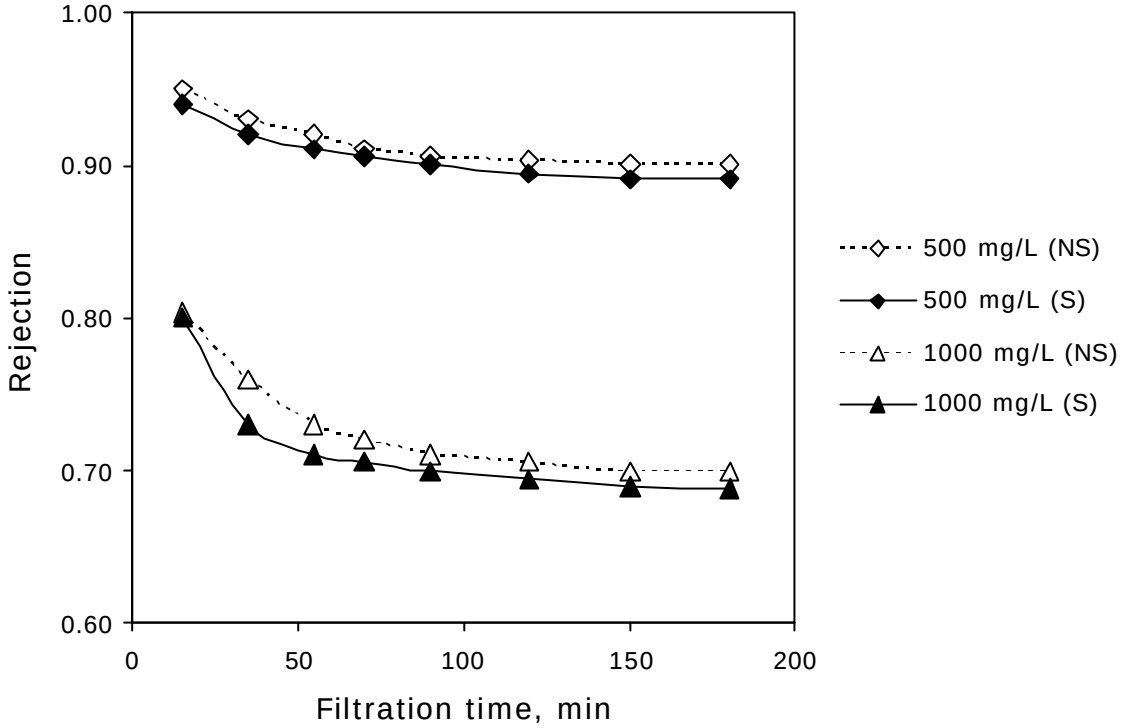

Figure 24. Effect of ultrasound treatment on the rejection of membrane filtration for CMC solutions. S and NS indicate sonication and no sonication respectively. The maximum standard deviation of the observations of the rejection did not exceed 0.34% of the averages indicated in the figure.

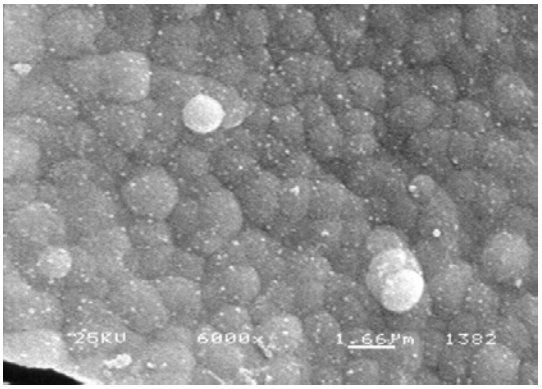

Figure 25. Morphological image of the fouled reverse osmosis membrane with 1000 mg/L CMC solution in the absence of ultrasound (25 kV; magnification 6000; bar 1.66 µm).

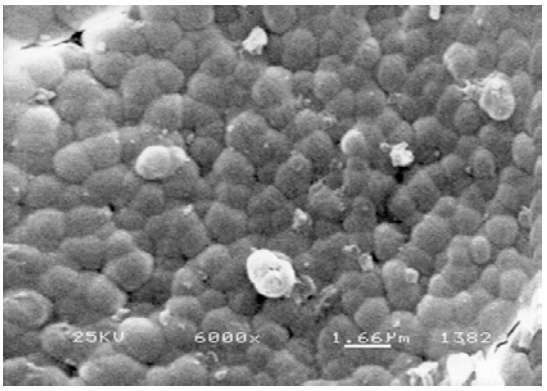

Figure 26. Morphological image of the fouled reverse osmosis membrane with 1000 mg/L CMC solution in the presence of ultrasound (25 kV; magnification 6000; bar 1.66 μm).

4.1.4. Off-line ultrasonic cleaning

In the above experiments, ultrasound was used for online defouling of the reverse osmosis membrane during filtration. In order to assess the off-line defouling of membranes, water cleaning combined with sonication was investigated for the reverse osmosis membrane fouled with different concentrations of the CMC solutions. After two hours of membrane filtration with CMC solutions without sonication, distilled water was fed to the membrane cell at a flow rate of 90 mL/min in the presence of ultrasound. The pressure in the membrane cell was maintained at approximately 10 kPa during ultrasonic cleaning, which lasted for 30 minutes.

As can be seen from Figures 27 and 28, sonically assisted washing of the fouled membranes was highly effective at a power to volume ratio of approximately 17 kW/m^3. After 3 cycles of fouling and defouling, the permeate flux of the defouled membrane remained at almost the same level as that for fresh membranes (Figure 23), while the rejection was also virtually unchanged (Figure 24). The foulant layer on the membrane surface was removed by the microstreams generated by cavitation during ultrasonic cleaning. In addition, the CMC solubility was increased during sonication, and the dissolved CMC was discharged along with the distilled water effluent.

Clearly, off-line ultrasonically assisted water washing is a promising method for cleaning of fouled membranes that needs to be investigated further, as it may offer a more economic way for membrane cleaning than continuous on-line sonication.

4.1.5. Conclusions regarding the poly-amide reverse osmosis membranes

On-line ultrasonic defouling of the polyamide-based reverse osmosis membranes used in this investigation resulted in a significant increase in the permeate flux, with virtually no loss in rejection. On average, the permeate flux increased by approximately 50.8% for a 500 mg/L $CaSO_4$ solution and approximately 69.7% for a 1000 mg/L $CaSO_4$ solution during 3 hours of filtration in the presence of ultrasound. Likewise, the permeate flux increased by about 215% for a $FeCl_3$ solution with 20 mg/L Fe^{3+} during 3 hours of filtration in the presence of ultrasound. The permeate flux increased by approximately 264% and 113% respectively for a 500 mg/L and a 1000 mg/L CMC solution during 3 hours of filtration in the presence of ultrasound. Morphological studies of the membrane surfaces done by the authors indicated that ultrasound could effectively remove both the inorganic foulants of $CaSO_4$ and $Fe(OH)_3$ and the organic foulant carboxymethyl cellulose on the membrane surface. Off-line ultrasonically assisted cleaning of the membranes

with water was highly effective and could restore the permeate flux with almost no change in rejection.

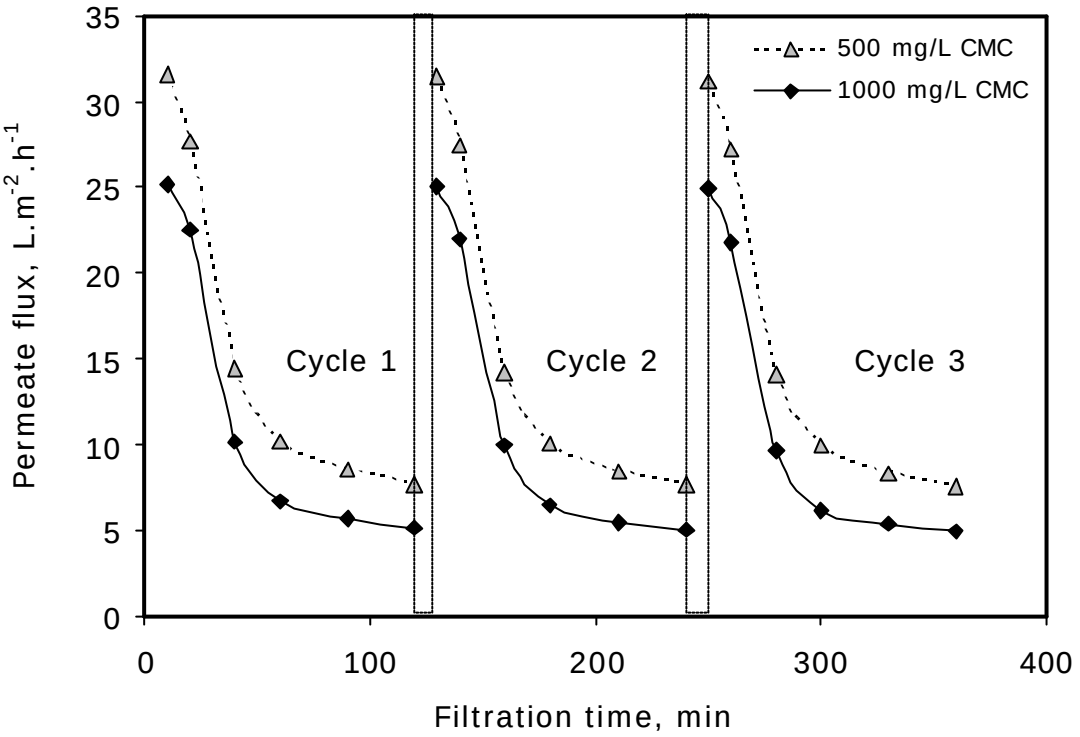

Figure 27. Effect of off-line ultrasonic washing on the change of the permeate flux of membrane filtration for CMC solutions. The maximum standard deviation of the observations of the permeate flux did not exceed 2.1 % of the averages indicated in the figure. The shaded areas indicate 10-minute periods of sonication following 2 hours of filtration without sonication.

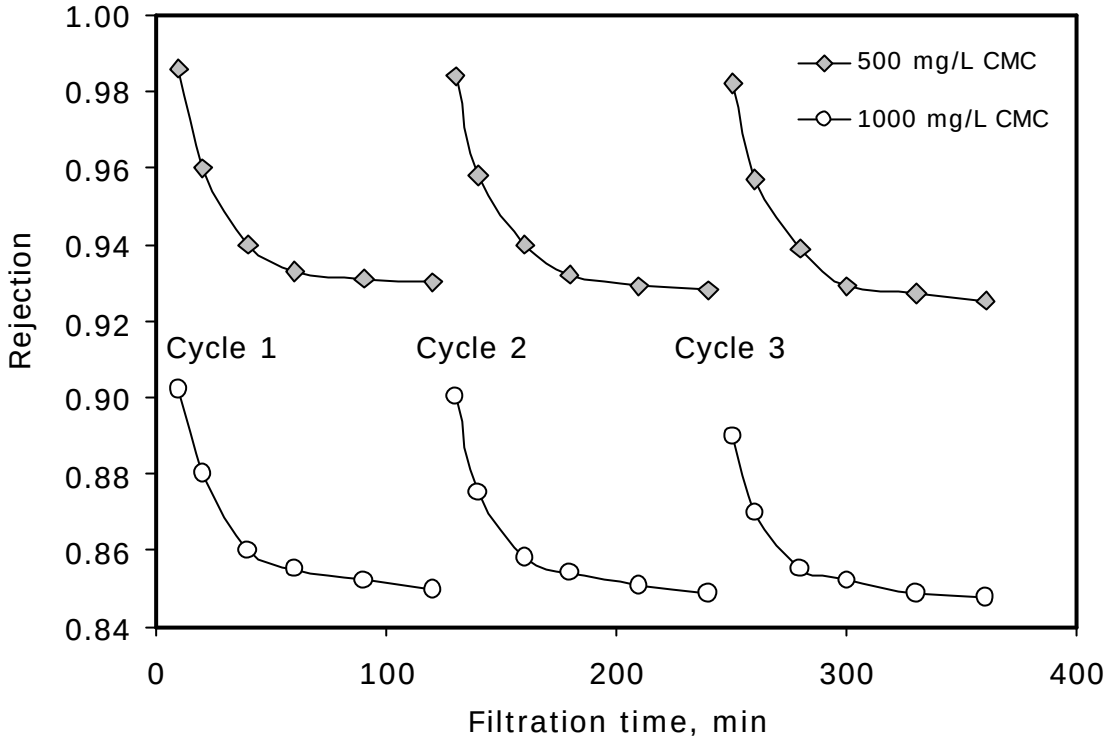

Figure 28. Effect of off-line ultrasonic washing on the rejection of membrane filtration for CMC solutions. The maximum standard deviation of the observations of the rejection did not exceed 0.6% of the averages indicated in the figure.

4.2. ULTRAFILTRATION OF LIGNOCELLULOSE DECOMPOSITION LEACHATE (D in Table 2).

Raw lignocellulose decomposition leachate (LDL) is a liquid by-product of the anaerobic digestion of lignocellulose substances (sun-dried tobacco dust, from the British American Tobacco Company in Paarl, South Africa). To prevent precipitation of the humic compounds in the LDL, the pH of the LDL solution was adjusted to 7.9 with NaOH, and the solution stored at 4 °C in the dark.

Organic substances in LDL are heterogeneous and complicated in chemical structure and reactivity. UV-visible absorbency was used to measure the humic organic content of the LDL in order to quantify these humic-like substances. Fast Blue B salt (FBB) (tetrazotized O-dianisidine, Sigma-Aldrich, South Africa) reactivity and the E_4/E_6-ratio were also analyzed to monitor the characteristics of the feed and the permeate water quality of the UF membrane.

After performing a routine scan on the LDL sample in the wavelength range of 200 to 600 nm with a CARY 1E UV-Visible Spectrophotometer (Varian, Starna GmbH, Germany), using quartz cuvets with a path length of 10 mm, the UV-absorbencies at wavelengths of 230 nm (UV_{230}), 254 nm (UV_{254}) and 340 nm (UV_{340}) were used to monitor the concentration of the humic-like compounds in the samples.

FBB reactivity was assayed by mixing 1.0 mL of the permeate or feed with 0.1 mL FBB (4.21 mM) to determine the concentration of 1-naphthol and other hydroxylated aromatic compounds present in the permeate or feed. The increase in absorbency was

recorded for 30 sec. at 530 nm. The reactivity was measured as the increase in absorbency per second.

The E_4/E_6-ratio of samples was determined by calculating the ratio of the UV-absorbency at 465 nm and 665 nm (UV_{465}/UV_{665}) to determine changes in molecular conformations of the humic-like compounds in the permeate or feed.

Electrospray mass spectroscopy (ES-MS) of the LDL was analyzed to characterize the polymer-like structure of the humic compounds in the LDL. This was performed on a Quattro triple quandropole mass spectrograph with electrospray ionization (Column: Phenomenex Luna C18, 3µm, 2x150 mm; mobile phase: acetonitrile/water; detector: mass detector, Macromass UK).

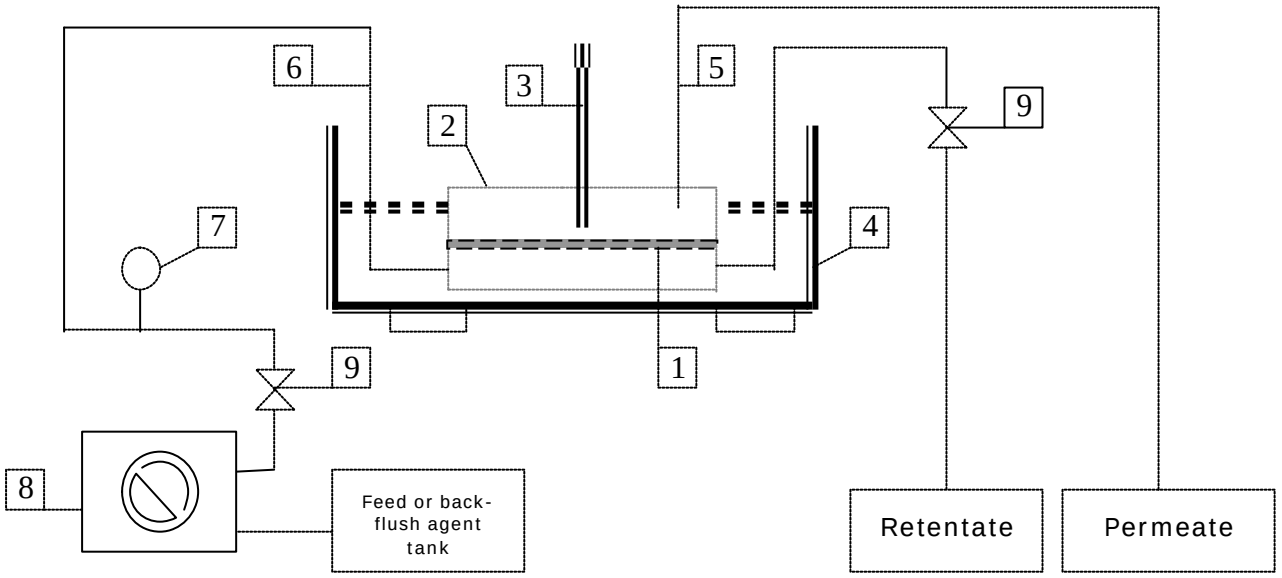

1. UF membrane sheet
2. Membrane cell, made of Plexiglas, with effective filtration area of 2.5 x 14 cm^2
3. Ultrasonic probe
4. Ultrasonic bath
5. Permeate
6. Lignocellulose decomposition leachate (LDL) feed
7. Pressure gauge
8. Peristaltic pump
9. Flow meter

Figure 29. Schematic representation of the experimental setup used for the ultrafiltration of lignocellulose decomposition leachate with ultrasound.

The LDL was fed into the membrane cell using a peristaltic pump (101 U/R model, Watson Marlow, Watson-Marlow Limited, Cornwall, UK, 4.8/1.6 mm Tygon tubing) at a maximum speed of 32 rpm and a constant feed pressure of 95±5 kPa, at ambient temperature of approximately 26-28 °C. The experimental setup is shown diagrammatically in Figure 29.

Ultrasound was introduced when a steady filtration state in terms of the permeate volume flux was reached (about 180 min after the start of UF), or at an early stage of UF operation (around 45 min after the start of UF). The 30 kHz ultrasonic probe (P1) was immersed approximately 10 mm above the membrane surface in each experiment.

The permeate volume flux was recorded every 30 min. To avoid any potential variable influence from membrane sheets and feed water, a relative permeate volume flux was

used to evaluate the UF performance under various experimental conditions. The relative permeate volume flux is

$$F_r = 100J_{j30}/J_{i30}\ (\%)$$

- F_r = relative permeate flux (%)
- J_{i30} = accumulated volume of permeate flux during the first 30 min of filtration (ml).
- J_{j30} = accumulated volume of permeate flux during the second, third, fourth, etc., 30 min period of filtration (ml).

4.2.1. Experimental Setup

- Feed:
  The LDL was diluted 1:4 and was pumped into the membrane cell at the speed of 99 rpm, the filtration was carried out at the pressure of 90-100 kPa, under room temperature over the filtration time if nothing else is stated.

- Analysis and Process Monitoring:
  The volumes of permeate were recorded over the filtration time and the samples were collected for UV-absorbency, FBB reactivity and E4/E6 analysis to assess the filtration process.

- Sonication in the ultrafiltration process:
  To obtain a reproducible filtration and fouling process of the membrane for investigating the effects of sonication on the filtration process, a dead-end module was used. After stable filtration conditions were achieved (with variation in permeate flux rate having reached a minimum), ultrasonication was introduced in the ultrafiltration process.

- Sonication in the membrane cleaning process with back-flush:
  a) The membrane was fouled for a period of 150 minute. The back-flush was performed by turning the fouled membrane up-side down and was carried out under the crossflow module at the filtration pressure of 80-95 kPa with the sonication on or off for 30 minutes. The pure distilled water and 0.2 N NaOH-0.02 N HCl were used as the cleaning agents.

  b) The filtration side of the membrane was turned back, pure distilled water was gently pumped through the membrane, if the NaOH-HCl back-flush was used, till the pH of permeate was detected to be neutral.

  c) The pure distilled water was replaced with the 1:4 LDL which was pumped through the back-flushed membrane to compare the UF membrane performance after different back-flush under the same crossflow filtration conditions.

- GPC analysis:
  The molecular size of the humic compounds in the feed LDL and the foulants which were retained on the UF membrane were analyzed with GPC instrument (Waters HPLC with U6K injector and Model 991 diode array detector, ultrahydrogel DP 500 column, with molecular range of 500 to 50,000 dalton).

4.2.2. Filtration of LDL

Analysis of the LDL solution (Figure 30) revealed a strong linear relationship between UV-absorbency (UV_{230}, UV_{254} or UV_{340}) and concentration of the LDL (the range of 1:4 to 1:10 dilution with distilled water). For a routine analysis, the UV_{254} and UV_{340} were used to monitor the humic organic compound content in the feed and the permeate. Since raw LDL is too concentrated for dead-end filtration, the LDL diluted by distilled water to a ratio of 1:4 was used as the UF feed throughout the experiments.

ES-MS analysis of the LDL compounds (the solid residues of the LDL after evaporation in

air, followed by washing with 35% formic acid and 1% NH_3) is shown in Figure 31

Figure 31. The ES-MS spectrum indicates that the organic compounds in the LDL consist mostly of heterogeneous polymer-like structures, with low molecular mass.

Changes in relative permeate volume flux (F_r) with filtration time and without sonication, are shown in Figure 32. The F_r declined sharply within the first 60 min of filtration, followed by a more gradual decline thereafter. After 420 min of filtration, the F_r stabilized at around 15% to 16%. The total decline in F_r from 30 min to 800 min of filtration was 86.6%. This indicated that a polarized layer formed rapidly at the commencement of filtration, then stabilized as filtration proceeded.

The COD and UV-absorbency of the permeate, compared to the feed (filtration time 0 min), were noticeably reduced (see Figure 33). Both the COD and the UV-absorbency of the permeate showed no evident changes with filtration time. This confirmed that most of humic organic compounds in LDL was retained by the UF membranes.

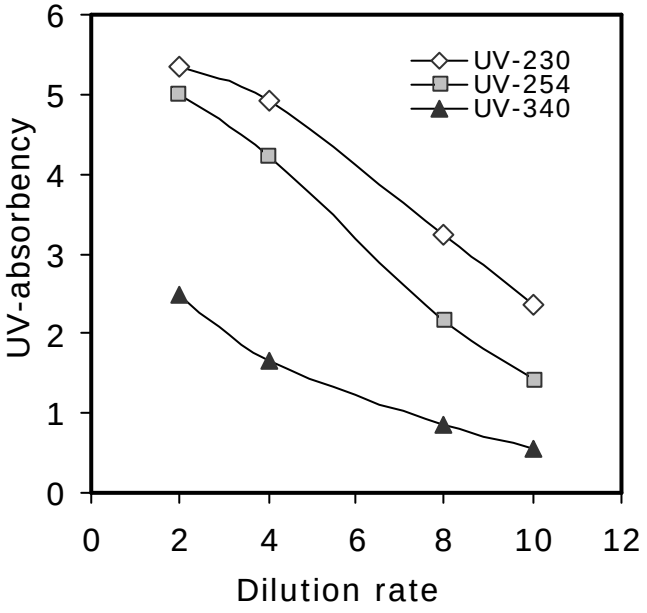

Figure 30. UV-absorption curves of the feed LDL.

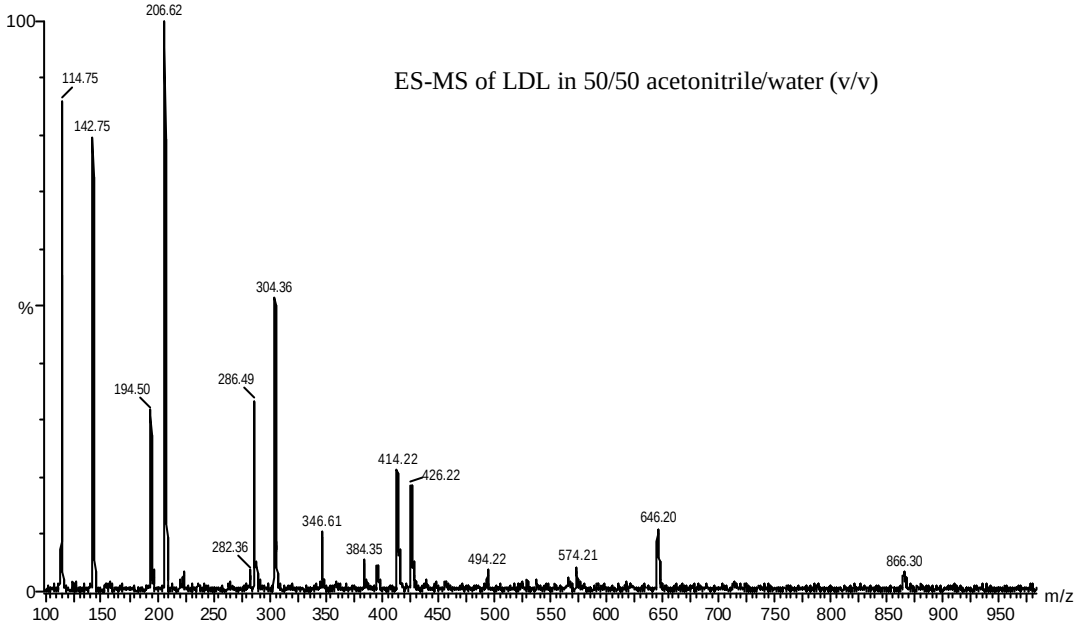

Figure 31. ES-MS spectrum of the LDL.

A lower E_4/E_6 ratio indicates a higher degree of condensation of aromatic compounds, and/or the presence of larger molecules in solution (Chen et al., 1977). Figure 34 shows that, compared to the feed (filtration time 0 min), the E_4/E_6 ratio of the permeate increased, indicating that the larger molecules in the feed were retained by the membrane.

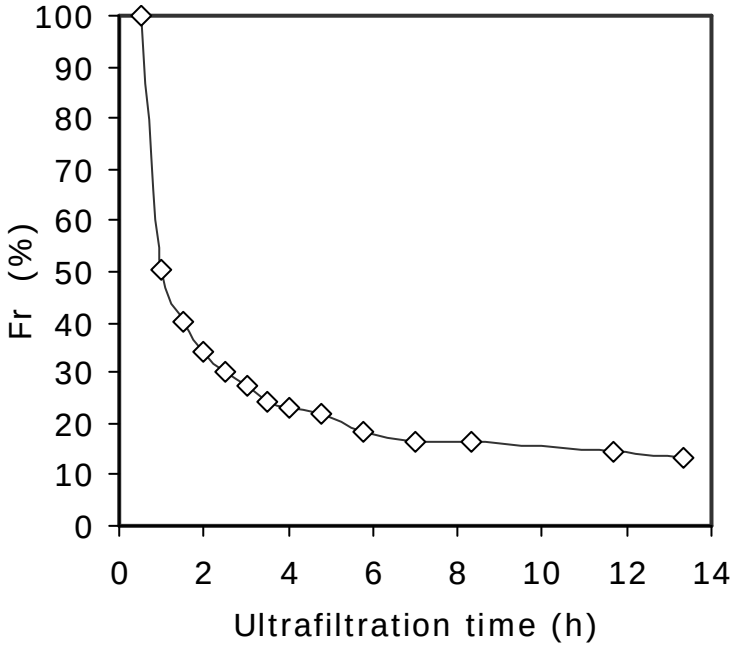

Figure 32. Changes in relative permeate flux (F_r) of the UF membrane with filtration time.

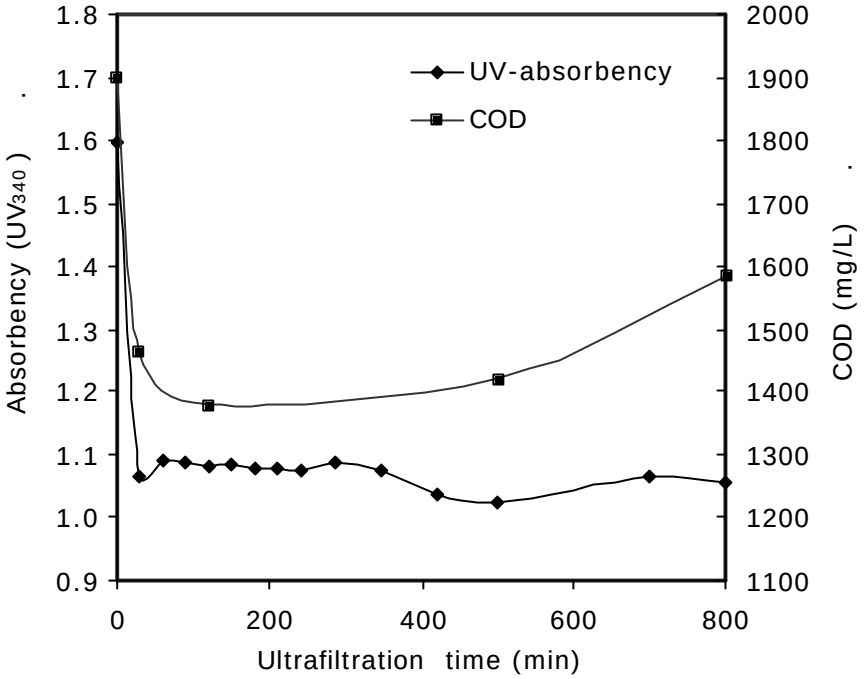

Figure 33. Changes in COD and UV-absorbency of the permeate with UF time.

However, compared to the feed (filtration time 0 min), the FBB reactivity of the permeate varied early in filtration, and then became more consistent at values similar to those of the feed at longer filtration times. This suggests that, overall, most of the FBB-reactive compounds in the LDL, such as hydroxylated aromatic compounds, was rejected by the UF membranes.

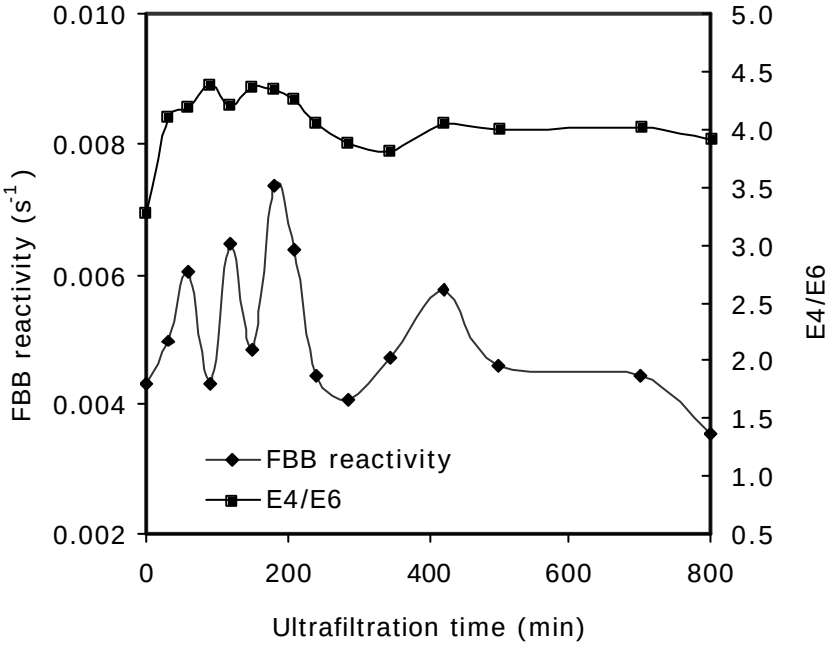

Figure 34. Changes in FBB reactivity and E_4/E_6 ratio of the permeate with UF time.

Effects of sonication on LDL

When the sonication was applied to the UF process, besides the dynamic filtration process, the static properties of the LDL feed could be affected by the sonication. To explain the sonication effect only on the LDL, the UF was turned off and the LDL loaded in the membrane cell was statically exposed to the ultrasound emitted from the ultrasonic bath for 45 min to 180 min. The effects of sonication on the properties of the LDL only, in terms of changes in UV-absorbency of the feed, E_4/E_6, FBB reactivity and pH, are shown in Figures 35-36.

Figure 35 shows that there was a very slight increase in the UV_{254} and UV_{340} absorbencies of the LDL with sonication. This suggests that the humic-like compounds of the LDL loaded in the membrane cell were not reduced by sonication. Conversely, some colloidal compounds were probably formed as a result of sonication under the given experimental conditions. The latter was confirmed by the decreased E_4/E_6-ratio of the LDL after sonication treatment (see Figure 36). A decrease in E_4/E_6-ratio indicates that larger molecular compounds and or more condensed aromatic compounds were formed in the LDL owing to sonication treatment. Formation of more condensed aromatic compounds was also in agreement with the increases in FBB reactivity of the LDL after sonication treatment. This is because that increases in FBB reactivity are associated with increases in 1-naphthol and other hydroxylated aromatic compounds. In contrast, the pH of the LDL hardly changed over 150 min of sonication. This suggested that the protonization or deprotonization properties of the LDL were not affected significantly by the sonication.

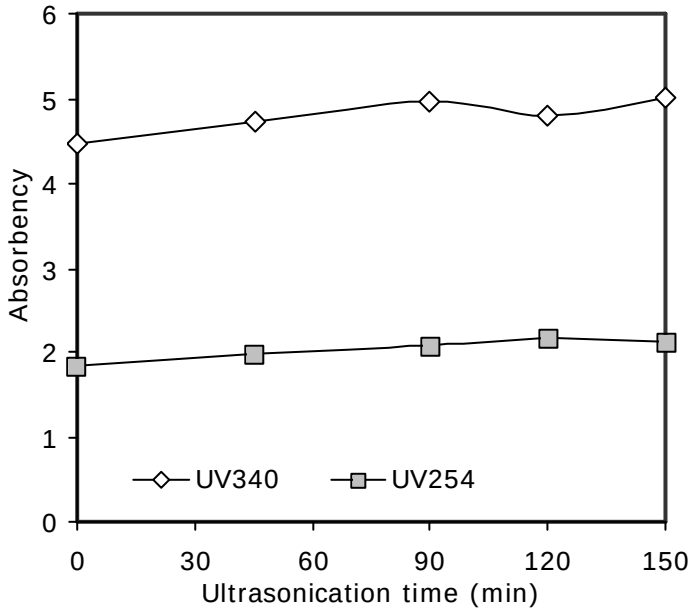

Figure 35. Changes in UV-absorbency of the feed LDL during sonication treatment.

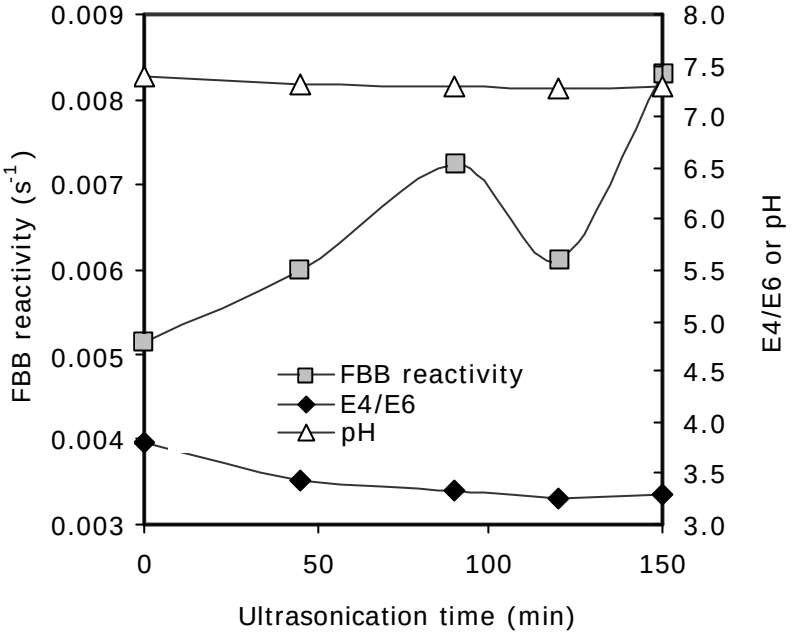

Figure 36. Changes in E_4/E_6 ratio, FBB reactivity and pH of the feed LDL with sonication time.

Effects of sonication on ultrafiltration

Effects of sonication on the dead-end UF performance were investigated by introducing the sonication into the UF process in on-line and off-line mode, through an ultrasonic bath or ultrasonic probe.

Changes in F_r with filtration time, with and without sonication, are shown in Figures 37-38. Results indicate that the introduction of sonication into the filtration process could prevent the decline in the permeate volume flux. Firstly, use of an ultrasonic bath appeared more efficient than an ultrasonic probe. This was probably owing to the different direction of propagation of the ultrasound from the sonic bath and probe transducers related to the permeate flow direction, i.e. the different sonic energy distributions on the membrane surfaces between the sonic bath and the probe. It had previously been noted that the enhancement of permeate volume flux reached a maximum as the ultrasound propagated in the same direction of the flow of the permeate and reached a minimum as the ultrasound propagated against the permeate flow (Lickiss, 1992). When the ultrasonic bath was used, the ultrasound propagated in the same direction of the permeate flow.

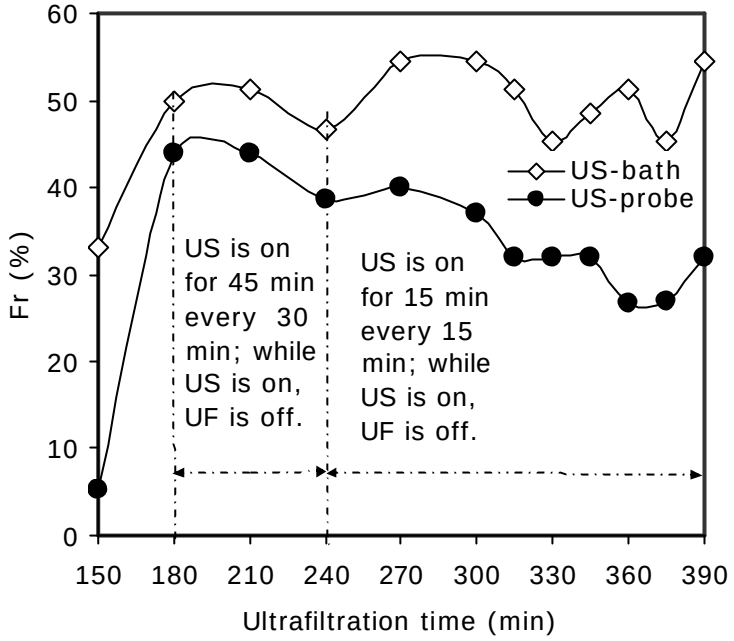

Figure 37. Changes in relative permeate flux (F_r) with off-line sonication.

The opposite was the case when the ultrasonic probe was used, where the ultrasound propagated against the permeate flow. Secondly, off-line sonication appeared more efficient than the on-line sonication. However, with longer periods of filtration, sonication appeared to be ineffective in the prevention of a decline in the permeate volume flux. This was probably because that there was a suction pressure on particles lying on a membrane surface, which, in the case of dead-end filtration, were packed randomly under convection flow condition.

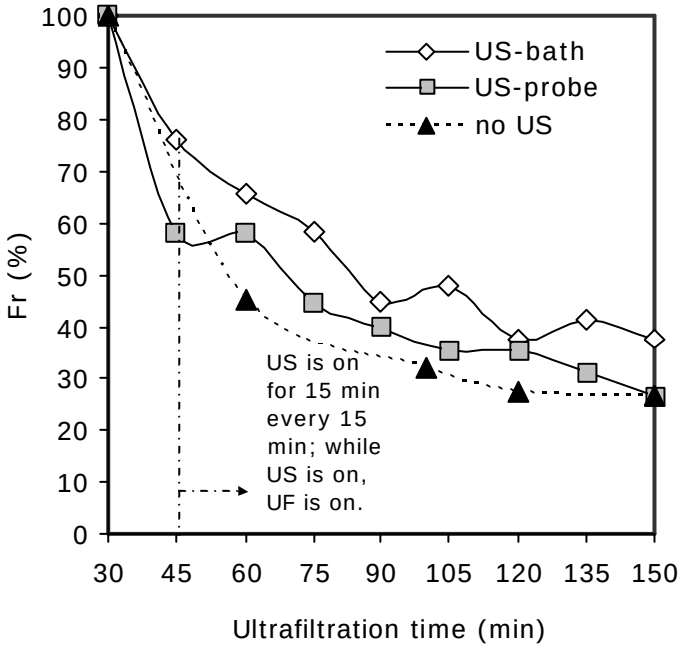

Figure 38. Changes in relative permeate flux (F_r) with on-line sonication.

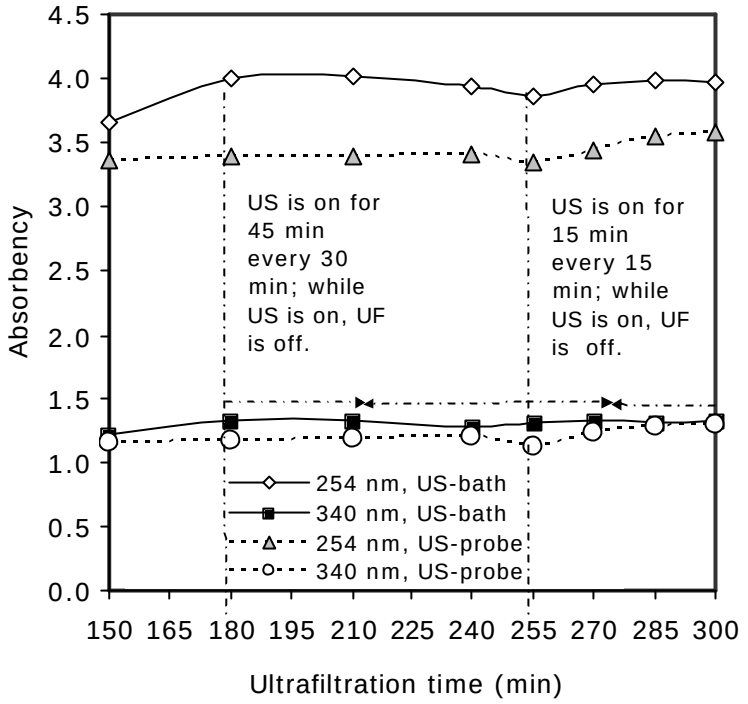

Figure 39. Changes in UV-absorbency of the permeate with off-line sonication.

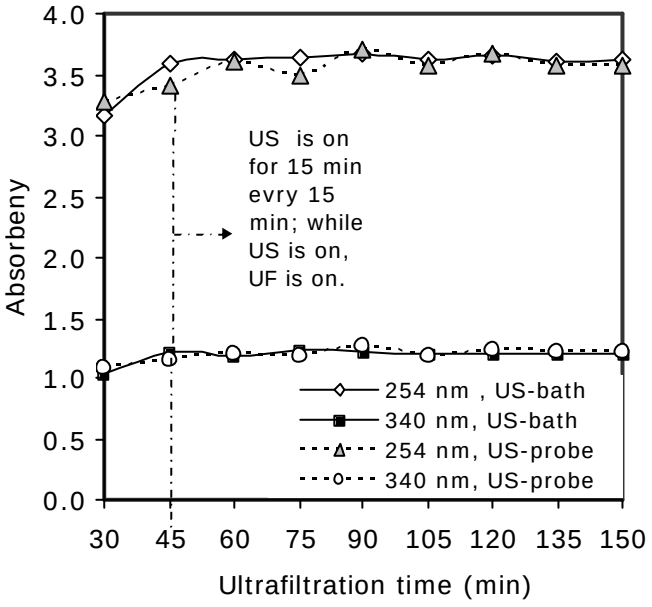

Figure 40. Changes in UV-absorbency of the permeate with on-line sonication.

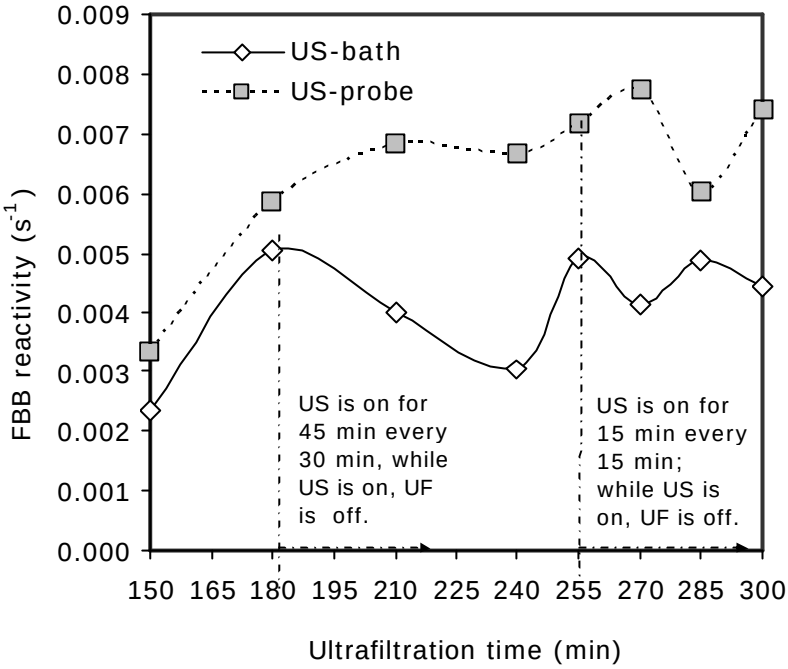

Figure 41. Changes in FBB reactivity of the permeate with off-line sonication.

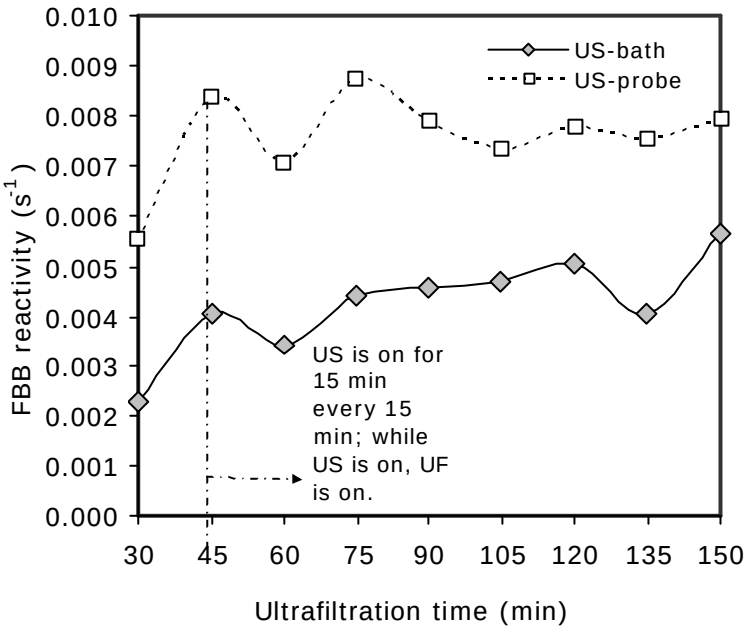

Figure 42. Changes in FBB reactivity of the permeate with on-line sonication.

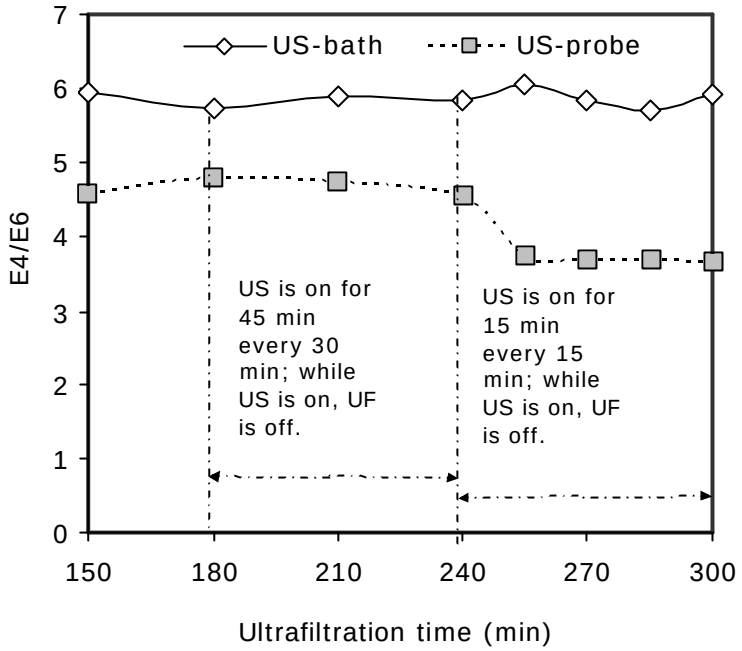

Figure 43. Changes in E_4/E_6 ratio with off-line sonication.

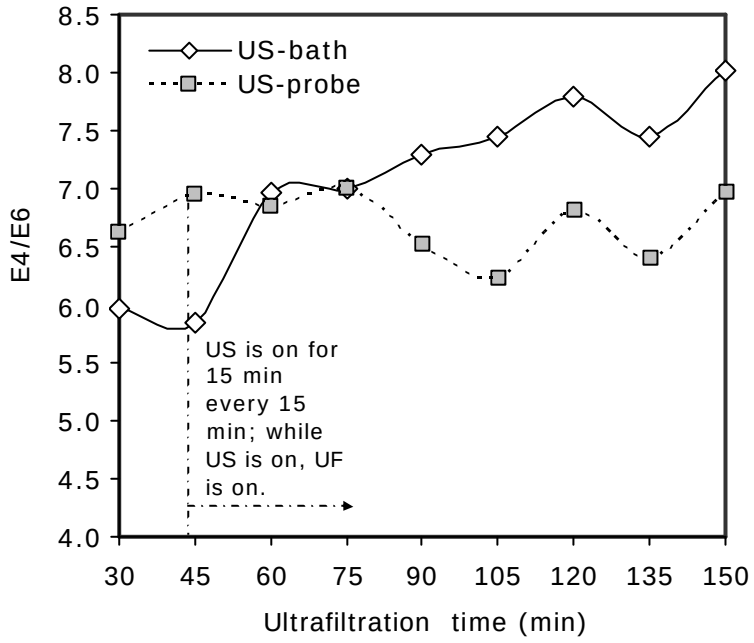

Figure 44. Changes in E_4/E_6 ratio of the permeate with on-line sonication.

Sonication could provide energy for these particles to realign and fill permeation gaps. Formation of a densely packed layer thus assisted by sonication during long periods of dead-end filtration could be one of the reasons why sonication failed to prevent the decline in the permeate volume flux at later stage of filtration.

Moreover, introducing on-line sonication in an early stage of filtration (see Figure 38) did not completely prevent a permeate flux decline. This was probably owing to that, instead of preventing concentration polarization and the formation of gel layers, on-line

sonication could speed up the adsorption or deposition of the humic-like compounds on the membrane surface during filtration.

Changes in the permeate water quality with filtration time in terms of UV-absorbency, FBB reactivity and E_4/E_6 ratio, with and without sonication, are shown in Figures 39-44. The results in Figures 39-40 show that the UV-absorbency of the permeate increased slightly with sonication. This suggests that some of the humic compounds passed through the membrane during ultrasonically assisted filtration, probably owing to the changes of the membrane permeability by the sonication. This was noticed in the study on the effects of low-frequency (47 kHz) ultrasonic waves on a poly(ether sulphone) (PES) membrane (Masselin et al., 2001). They have found that the PES was affected by the ultrasonic treatment, which led to an increase in pore radius for larger pores, and overall increases in pore density and porosity.

Figures 41 and 42 indicate that the FBB reactivity of the permeate generally increased with sonication. This was similar to the FBB reactivity profile of the LDL treated by sonication (Figure 36). The reason for the observation from above could be that sonication increased the content of FBB-reactive compounds in the LDL, and these compounds passed through the membrane easily (Figure 36). The increase in FBB reactivity of the permeate could result from the sonication effects on both the LDL feed and the membrane permeability.

Figures 43 and 44 show that the E_4/E_6 ratio of the permeate either increased, decreased or remained stable with filtration time, depending on the sonication mode. The E_4/E_6 ratio of the permeate generally remained the same or decreased with off-line sonication treatment (Figure 43), whereas the E_4/E_6 ratio of the permeate generally increased with on-line sonication treatment (Figure 44). Normally, the pore size of the fouled membrane decreases with the formation, deposition and condensation of a fouling layer on the membrane surface or even in the membrane pores as filtration proceeds. Only compounds smaller than the pore size of the fouled membrane were expected to pass through the membrane, hence, the E_4/E_6 ratio of the permeate was expected to increase gradually as fouling continued. A decrease in the E_4/E_6 ratio of the permeate with off-line sonication indicated that large compounds passed through the membrane during ultrasonically assisted filtration. This observation suggested that either some parts of the fouling layer or pore blockages of the membrane were probably reduced or the porosity of the membrane was enlarged by sonication. Hence, larger compounds, which were not supposed to pass through the fouled membranes, could do so after sonication.

On the other hand, as shown in Figure 43, the E_4/E_6 ratio of the LDL decreased with sonication time, indicating the formation of larger humic-like compounds or the condensation of aromatic compounds in the LDL during sonication. When the LDL was filtrated through the UF membrane, larger humic compounds formed as a result of sonication were retained by the membrane as foulants, while only small compounds passed through the membrane. In addition, sonication should preferably affect the mobility of larger molecules more than that of the smaller molecules. Thus, during on-line sonication filtration, larger molecules would be quickly transported to the membrane surface and block the membrane pores in the case of dead-end filtration. It was therefore found that the E_4/E_6 ratio of the permeate generally increased with on-line sonication filtration (Figure 44) and introducing on-line sonication from the early stage of filtration (see Figure 43) did not instantly prevent a permeate flux decline.

4.2.3. Mechanisms of ultrasonic effects on ultrafiltration

Enhancement of the permeate flux by sonication was considered to be a result of the enhancement of bulk mass transfer in the concentration polarization layer on the membrane surface (Chai et al., 1998; Kobayashi et al., 1999), probably by reducing the concentration polarization layer resistance and the localized solute concentration at the membrane surface. When a cavitating bubble oscillates near a solid surface, it does so asymmetrically and generates microjets (microcurrents) of high velocity. The high velocities thus generated can create vigorous streaming turbulence along the membrane surface, and this efficiently decreases the thickness of the boundary layers and diffusion resistances of the fouled membrane, therefore enhancing the rates of mass transfer through the membrane. Acceleration of mass diffusion with ultrasound is believed mainly a result of acoustic microcurrents in the liquid (acoustic streaming). The likely locus of the ultrasonic effect is the liquid-solid phase at the membrane interface (Band et al., 1997).

However, in practice, the interaction between ultrasonic waves and the dead-end ultrafiltration process would be much more complex, because the overall resistance to mass transfer through the membrane is caused by the combination of separate, but interactive processes, such as the formation of the concentration polarization, (gel layer) or cake layer (particulate), adsorption of solutes onto the external surface of the membrane, solute-solute adsorption and blockage of the membrane pores (Grund et al., 1992). It is therefore difficult to distinguish the exact effects of sonication on each of these processes. The improvement of the permeate volume flux by sonication during filtration could be one aspect of enhanced mass transfer. On the other hand, the sonication could preferably affect the mobility of larger molecules more than that of the smaller molecules. In this case, the enhanced mass transfer during dead-end UF could also lead to quick formation of the concentration polarization layer. It was thus found that sonication could not permanently prevent decline in the permeate flux as filtration proceeded. Further study needs to be carried out to determine the exact effect of ultrasound on different mass transfer stages of the UF by applying the sonication to the different fouling stages controlled respectively.

4.2.4. Conclusions regarding the ultrafiltration of LDL

The ES-MS spectra indicate that the organic compounds in the LDL feed are heterogeneous polymer-like structures, with predominantly low molecular masses. The poly(ether sulphone) UF membrane was easily fouled by the LDL. This was mainly the result of the formation of concentration polarization and gel layers.

Introducing sonication into UF processes could initially prevent or delay the permeate volume flux decline. However, the effects of sonication on UF of the LDL in dead-end filtration were complicated, depending on the mode of sonication and the configuration of the ultrasound source. Beside the dynamics of filtration, both the LDL feed in the filtration unit and the structure of the membrane could be affected by sonication. Use of the ultrasonic bath appeared to be more efficient than use of an ultrasonic probe. There was no evidence that the humic-like compounds in the LDL feed in the membrane holder were decomposed by sonication under the given experimental conditions. Off-line sonication appeared to be more efficient than on-line sonication. However, as filtration proceeded, sonication ceased to prevent the permeate flux from declining, especially when it was used on-line.
Sonication could enhance the bulk mass transfer of the LDL in the concentration polarization layer on the membrane surface, which can lead to an improvement in the permeate volume flux. On the other hand, the increased mass transfer could also cause

a rapid formation of a concentration polarization layer during dead-end filtration, hence in-process sonication could not permanently prevent the decline in permeate volume flux as filtration progressed and hence the effect of sonication on improving the ultrafiltration of the LDL in dead-end filtration mode was not evident in the long run.

4.3. LARGE-SCALE CYLINDRICAL CAPILLARY MEMBRANE UNIT FOR ULTRAFILTRATION OF NATURAL ORGANIC WATER (G in Table 2)

The source water used at this stage was a raw natural organic water from the Steenbras dam in Gordon's Bay. The water is of the acid moorland type, fairly highly coloured and is extremely soft and of low mineral content. The general physicochemical characteristics of the water are presented in Table 3.

Table 3. Physicochemical characteristics of the natural organic water sample from Steenbras Dam (the data are average values of the samples taken over 3 weeks).

Category	Parameters	Values
Physical	Total dissolved solids mg/L	35
	Conductivity @ 20 ^{0}C, mS/m	6.5-7.1
	pH	5.24-5.63
	Turbidity, NTU	1.44-2.32
	Colour, Plat.std	60-80
Organic	UV-absorbancy, 254 nm	0.38-0.41
	PV4 @27 ^{0}C, mg/L	6.7-6.9
Hardness	Total, $CaCO_3$ mg/L	7.2-8.1
Mineral	Alkalinity, $CaCO_3$ mg/L	2.0
	Chloride , Cl mg/L	17-18
	Sulphate, SO_4 mg/L	3.4-3.7
	Calcium, Ca mg/L	1.1-1.4
	Magnesium, Mg mg/L	1.06-1.16
	Sodium, Na mg/L	8.0-8.9
	Potassium, K mg/L	<0.50

4.3.1. Crossflow filtration

The feed solution was pumped under pressure into the membrane tubes as indicated in Figure 45. With the feed stream entering the modules, the solvent and small species are forced through the pores of the membrane (permeate), while larger particles are retained (retentate or concentrate). The filtered water exits as permeate, while the rest leaves the modules carrying impurities, as the concentrate stream. Some of the concentrate stream is recycled and some is discharged as retentate.

To obtain a basic ultrafiltration profile of the membrane system, a clean water (distilled water) flux profile was developed under various differential pressures (transmembrane pressures) before the actual water sample, natural organic water was filtered.

The feed pressures, concentrate pressures, permeate pressures, total feed flow rates, permeate flow rates (fluxes) were recorded at one-second intervals. The average values per minute or per 10 minutes were used to produce the permeate flux profile and to calculate transmembrane pressures (TMP).

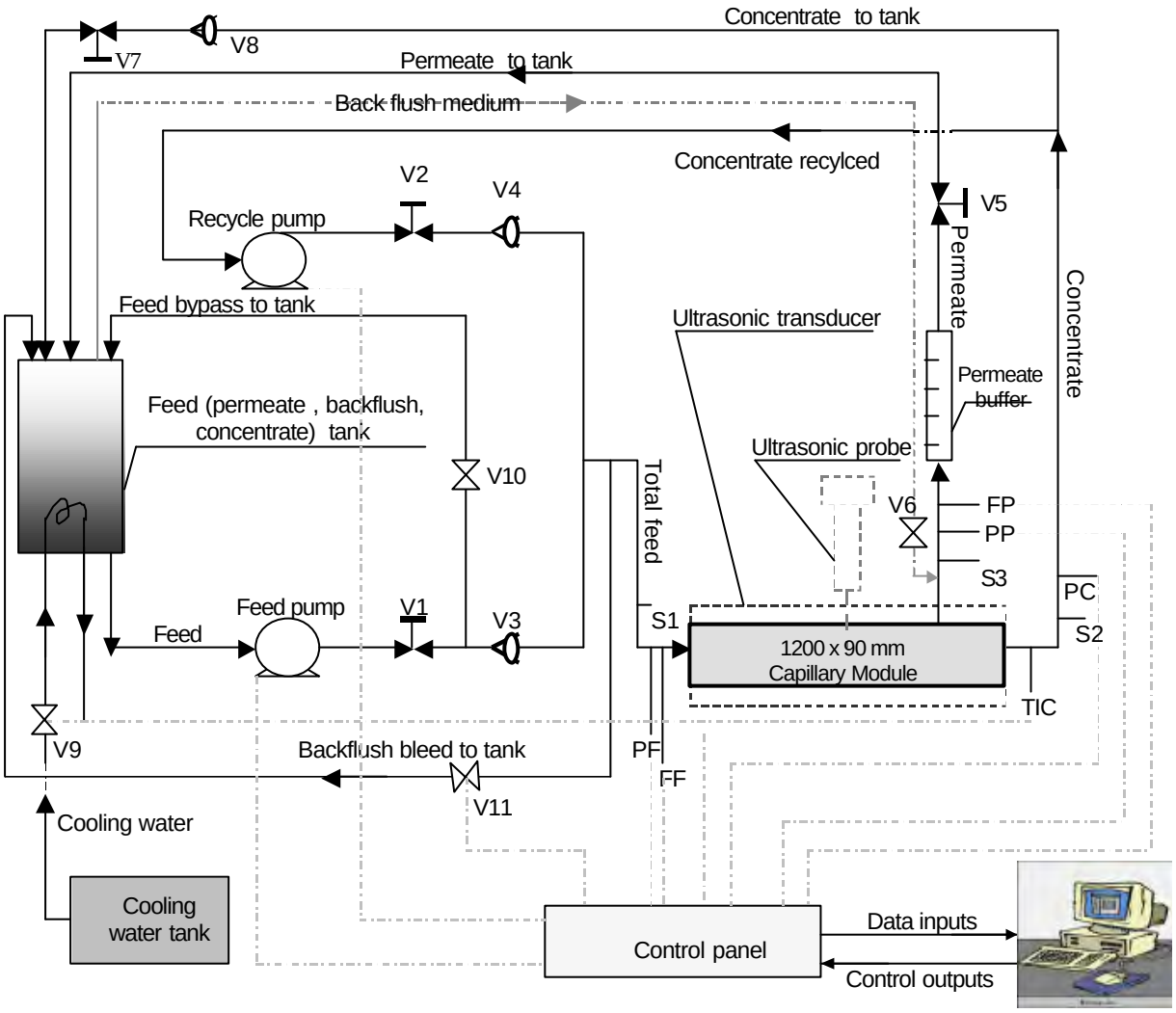

Valve	Function	Control Actuator
V1	Primary feed flow throttle	Manual
V2	Recycle flow throttle	Manual
V3,V4,V8	None-return valves to prevent back-flow	Spring loaded
V5	Permeate throttle (Trans-membrane pressure regulator)	Manual
V6	Back-flush flow regulator	Manual
V7	Concentrate backpressure regulator	Manual
V9	Cooling water flow regulator	Solenoid (liquid)
V10	Feed pressure regulator	Manual
V11	Back-flush bleed regulator	Solenoid (liquid)
PF	Feed manifold pressure	
FF	Combined (total) feed flow	
PP	Permeate pressure	
FP	Permeate flow rate	
PC	Concentrate manifold pressure	
TIC	Thermal induced couple (Temperature probe)	
S1, S2, S3	Total feed, concentrate, permeate sampling ports	

Figure 45. The diagram of large scale capillary membrane filtration.

4.3.2. Ultrasonication cleaning

A number of laboratory studies have found that applying the ultrasonication cleaning simultaneously with filtration did not result in significant enhancement of the permeate flux (Chai et al., 1998; Kobayashi et al., 1999). Therefore, we did not employ this cleaning method on a large scale system. Instead, we terminated filtration while the contaminated membranes were cleaned with ultrasonication.

Four different cleaning modes were investigated: Ultrasonication with both feed and recycle flow off, followed by forward distilled water flushing, namely US (1); ultrasonic cleaning with feed flow off, recycle flow on at the flow rate of 5467-5500 L/h, followed by forward distilled water flushing, namely US (2); ultrasonic cleaning with feed flow on at the flow rate of 280-300 L/h, recycle flow off, followed by forward distilled water flushing, namely US (3); and ultrasonic cleaning with both feed flow and recycle flow on, at the flow rate of 6280-6320 L/h, followed by forward distilled water flushing, namely US (4). Ultrasonication was applied to the membrane system via each of 5 holes traversing the module shell (10 minutes at each hole at a duty cycle of 50% and amplitude output of 10).

4.3.3. Large-scale capillary membrane unit with natural organic water (NOM)

Four different cleaning modes were investigated: Ultrasonication with both feed and recycle flow off, followed by forward distilled water flushing, namely US (1); ultrasonic cleaning with feed flow off, recycle flow on at the flow rate of 5467-5500 L/h, followed by forward distilled water flushing, namely US (2); ultrasonic cleaning with feed flow on at the flow rate of 280-300 L/h, recycle flow off, followed by forward distilled water flushing, namely US (3); and ultrasonic cleaning with both feed flow and recycle flow on, at the flow rate of 6280-6320 L/h, followed by forward distilled water flushing, namely US (4). Ultrasonication was applied to the membrane system via each of 5 holes traversing the module shell (10 minutes at each hole at a duty cycle of 50% and amplitude output of 10). The effects of transmembrane pressure (TMP) under a constant crossflow rate on the permeate flux productivity with distilled water are shown in Table 4.

Table 4 shows that under a controlled crossflow rate, the permeate flux of pure water increased with an increased in transmembrane pressure. Therefore, the transmembrane pressure was controlled between 120 kPa-125 kPa throughout the filtration experiments.

Table 4. The permeate flux of distilled water under various transmembrane pressures.

Crossflow rate (L/h)	TMP (kPa)	Permeate flux (L/h)
6370	105	119.5
6342	121	152.6
6329	125	158.4
6349	132	175.1

To ensure good control of this operation module, the membrane system was operated with distilled water under constant crossflow conditions over an extended period. The transmembrane pressure (TMP) and the permeate flux profile are shown in Figure 46.

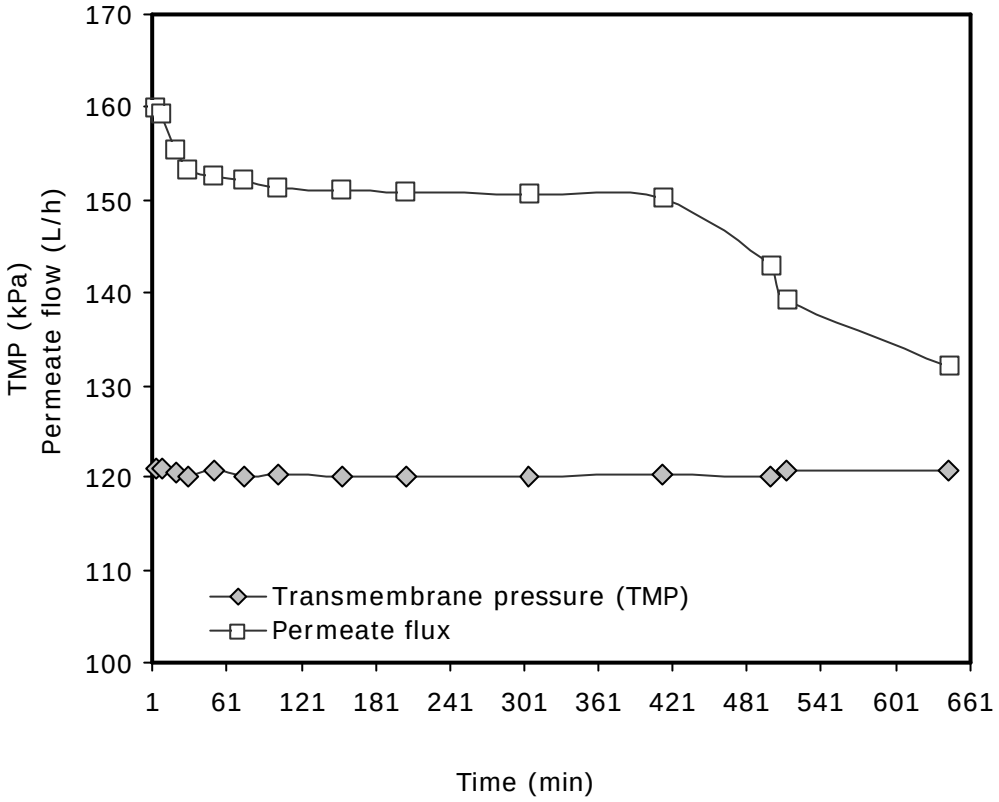

Figure 46. Profiles of the transmembrane pressure (TMP) and permeate flux during filtration of distilled water (large scale system, cross-flow rate 6320-6340 L/h).

Figure 46 shows that the transmembrane pressure and the permeate flux remained very stable during 30-420 min of filtration, although the permeate flux showed some decline after 500 min of filtration. This suggests reliable performance of the membrane under constant transmembrane pressures. Subsequent filtration experiments were therefore conducted under constant transmembrane pressure and constant crossflow rate, unless otherwise indicated.

The ultrafiltration profiles of the membrane system with distilled water and natural organic water are shown in Figure 47. It can be seen that the permeate flux of the natural organic water declined with filtration time, while the permeate flux of the distilled water remains stable during filtration. This indicated that membrane was contaminated or fouled by the natural organic water.

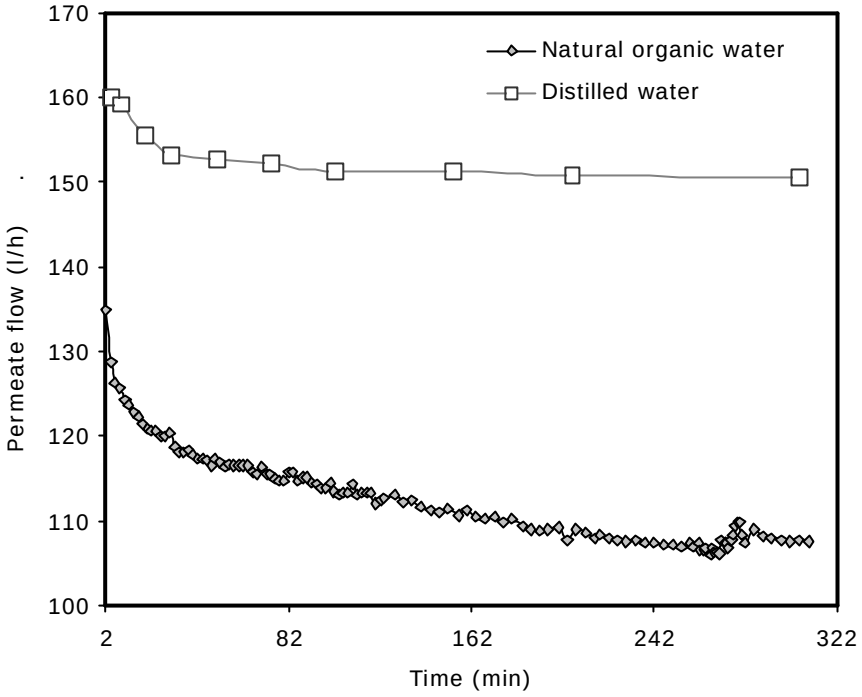

Figure 47. Profiles of the permeate flux of distilled water and natural organic water (large scale system, cross-flow rate 6320-6340 L/h).

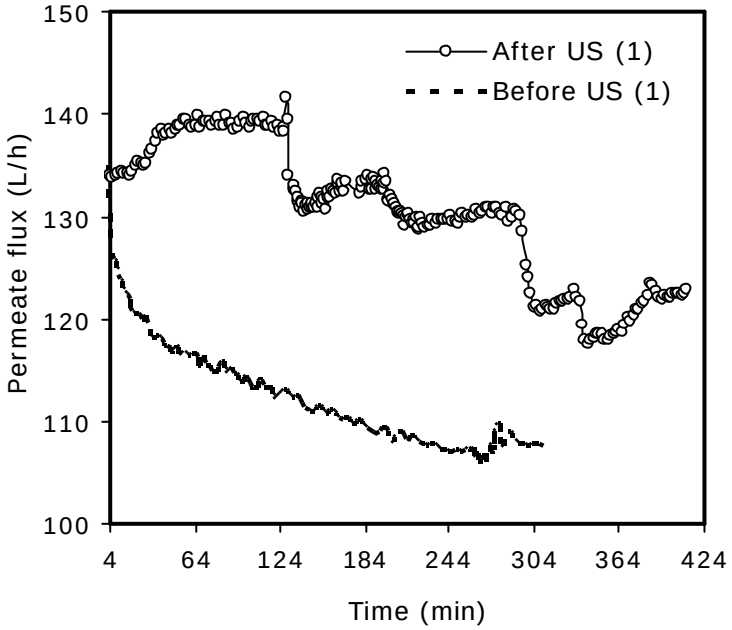

Figure 48. Effects of ultrasonication (module US (1)) on the permeate flux (large scale system, cross-flow rate 6300-6400 L/h, TMP 122-123 kPa, pH 4.85-5.04).

The cleaning effects of ultrasonication mode, US(1), on the membranes contaminated with natural organic water are shown in Figure 48. The permeate flux of the membrane increased markedly after exposure to the ultrasonication.

Likewise, the cleaning effects of ultrasonication module, US(2), on the membranes contaminated with natural organic water are shown in Figure 49. The permeate flux of the membrane was noticeably enhanced after exposure to the ultrasonication. The enhancing effect appeared more promising than with the US(1) mode. The extent and the pattern of difference in UV-absorbency, turbidity and conductivity between the permeate stream and the concentrate-feed stream also did not show evident changes before and after the ultrasonication. However, it could be noticed that the turbidity of the permeate after ultrasonication increased slightly at some stage of filtration. This suggests that some compounds which were supposed to be retained by the membrane passed through the membrane after exposure to the enhanced ultrasonication. In this case, the permeate quality was impaired.

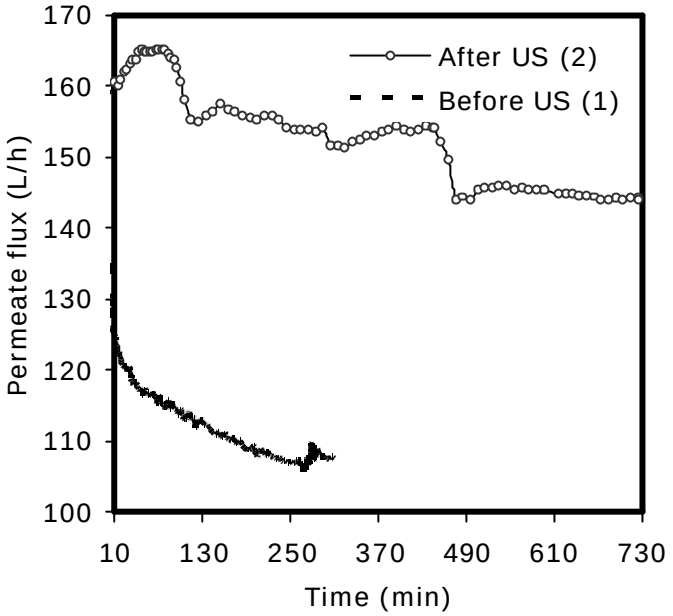

Figure 49. Effects of ultrasonication (module US (2)) on the permeate flux (large scale system, cross-flow rate 6300-6400 L/h, TMP 122-123 kPa, pH 4.93-5.16).

The cleaning effects of ultrasonication module, namely US(3), on the membrane system contaminated with natural organic water are shown in Figure 50. Again, the permeate flux of the membrane increased noticeably after exposure to ultrasonication. The increase of permeate flux appeared similar to the increase of the flux when the US(2) mode was used. This suggests that using the feed flow or recycle flow during ultrasonication did not make much difference in improving the filtration performance of the membrane. The extent and the pattern of difference in UV-absorbency, turbidity and conductivity between the permeate steam and the concentrate-feed steam also did not show evident changes before and after the ultrasonication. However, similar to US(1) mode, the turbidity of the permeate after ultrasonication showed a slight increase, indicating that some compounds which were supposed to be retained by the membrane passed through after exposure to the enhanced ultrasonication.

The increase in permeate flux associated with ultrasonication mode US(4), is shown in Figure 51. The increase of permeate flux appeared to that related to the US(2) and US(3) modes. This implies that the increase of fluid flow rate inside the membrane by combing the feed flow and recycle flow did not necessarily improve membrane defouling during ultrasonication. Similar to the other modes, a slight increase in turbidity also indicated the passage of some compounds through the membrane after exposure to the ultrasound.

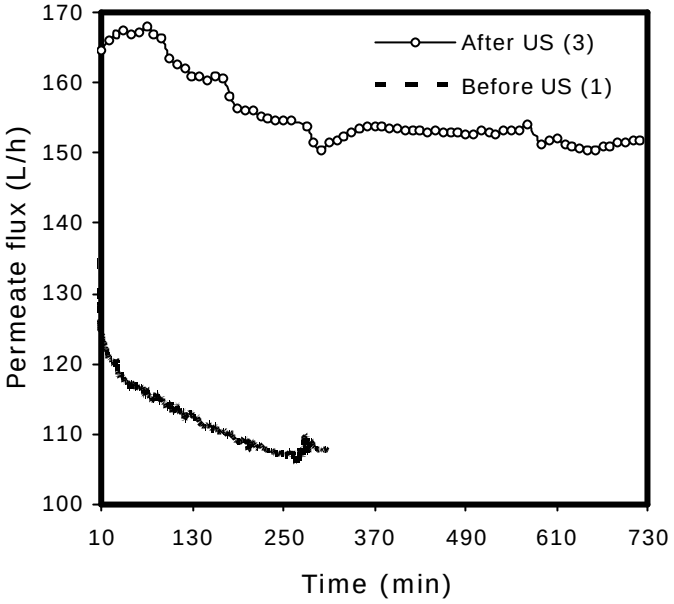

Figure 50. Effects of ultrasonication (module US (3)) on the permeate flux (large scale system, cross-flow rate 6300-6400 L/h, TMP 122-123 kPa, pH 4.92-5.05).

Finally, the cleaning effect of compressed air back pulse (108-110 kPa, for 10 min) on the membrane system contaminated with natural organic water is shown in Figure 52. The permeate flux of the membrane increased exceptionally after 80 min of filtration after introduction of the compressed air pulse. At the same time, the UV-absorbency, turbidity and conductivity of the permeate all appeared much higher than those of the permeate before exposure to the compressed air pulse. This suggests that some of the membrane fibres might have been damaged by the compressed air pulse. This was subsequently confirmed by visual inspection, which showed to broken fibres.

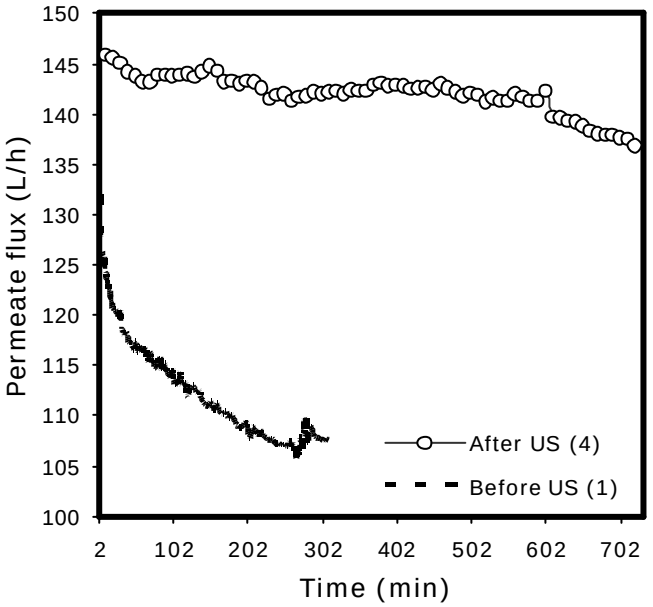

Figure 51. Effects of ultrasonication (module US (4)) on the permeate flux (large scale system, cross-flow rate 6300-6400 L/h, TMP 122-123 kPa, pH 4.79-4.88).

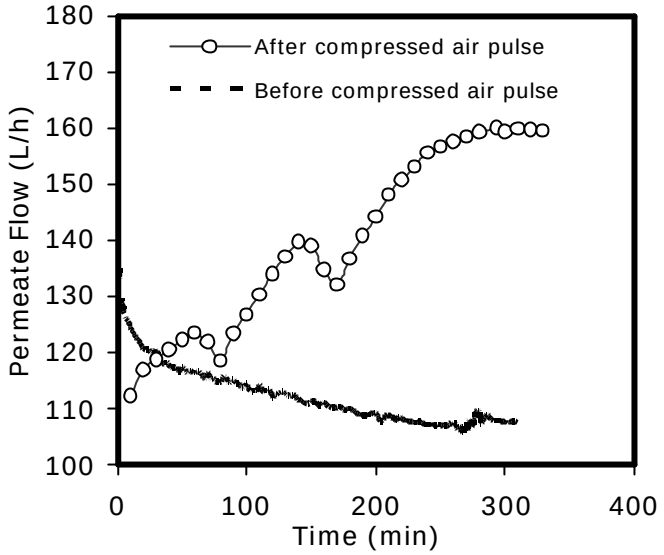

Figure 52. Effects of fibre damage as a result of compressed air pulsing (108-110 kPa, 10 min) on the permeate flux during filtration (large scale system, cross-flow rate 6300-6400 L/h, TMP 122-123 kPa, pH 4.72-4.78).

4.3.4. Conclusions regarding ultrafiltration of NOM effluent

The results presently obtained from larger-scale experiments indicated that:

- Ultrasonication again appears to be an effective cleaning technique to enhance the flux of the membrane system.

- The quality of the filtration products in terms of the differences in UV-absorbency, turbidity and conductivity between the permeate steam and the concentrate-feed steam did not change before and after ultrasonication.

The intensity of the ultrasonication applied to the membrane fibre needs to be investigated further to ensure an adequate permeate, with a concomitant increase in the permeate flux.

4.4. SMALL-SCALE CAPILLARY MEMBRANE UNIT WITH NATURAL ORGANIC MOUNTAIN WATER FROM STEENBRAS DAM (GORDON'S BAY) (H in Table 2)

4.4.1. Materials and Methods

The UF membranes were poly(ether sulphone) (PES) capillary membranes with molecular weight cut-off between 30-40 kDa. The membranes were previously fouled by the natural organic water from the Steenbras Dam near Gordon's Bay. The water is of the acid moorland type, fairly highly coloured and is extremely soft and of low mineral content.

Ultrasound was generated via two laboratory scale horn ultrasonic transducers with different ultrasonic frequencies (P1 and P2 referred to in Table 2). In addition, the membrane cells were also subjected to mechanical vibration, realized with a laboratory Vortex-Genie 2 Vortex agitator (Scientific Industries INC., NY, USA).

The experimental setup is shown in Figure 53. A Watson-Marlow peristaltic pump 503 S, Watson-Marlow Limited, Cornwall, UK, was used to pump the effluent from the feed tank through the bench-scale membrane filtration unit.

Each experiment commenced with pure water being circulated through the system at a fixed flow rate and applied pressure for about half an hour to compress the membrane and to build up a stable flow field. The pure water was then replaced by effluent. The permeate flux was measured by an electrical balance and the accumulated mass of the flux over 30 min of filtration was used to assess the vibration and ultrasonication effects. The pump-feeding rate was controlled at 111-112 RPM and the operating pressure was controlled at 100-105 kPa. The filtration was carried out in crossflow module.

Each ultrasonication or vibration treatment was operated in two modes, on-line and off-line, for the duration of 10 min. The off-line treatment was followed by a 2-min forward-flush with the filtration water before the 30 min of assessment filtration was taken.

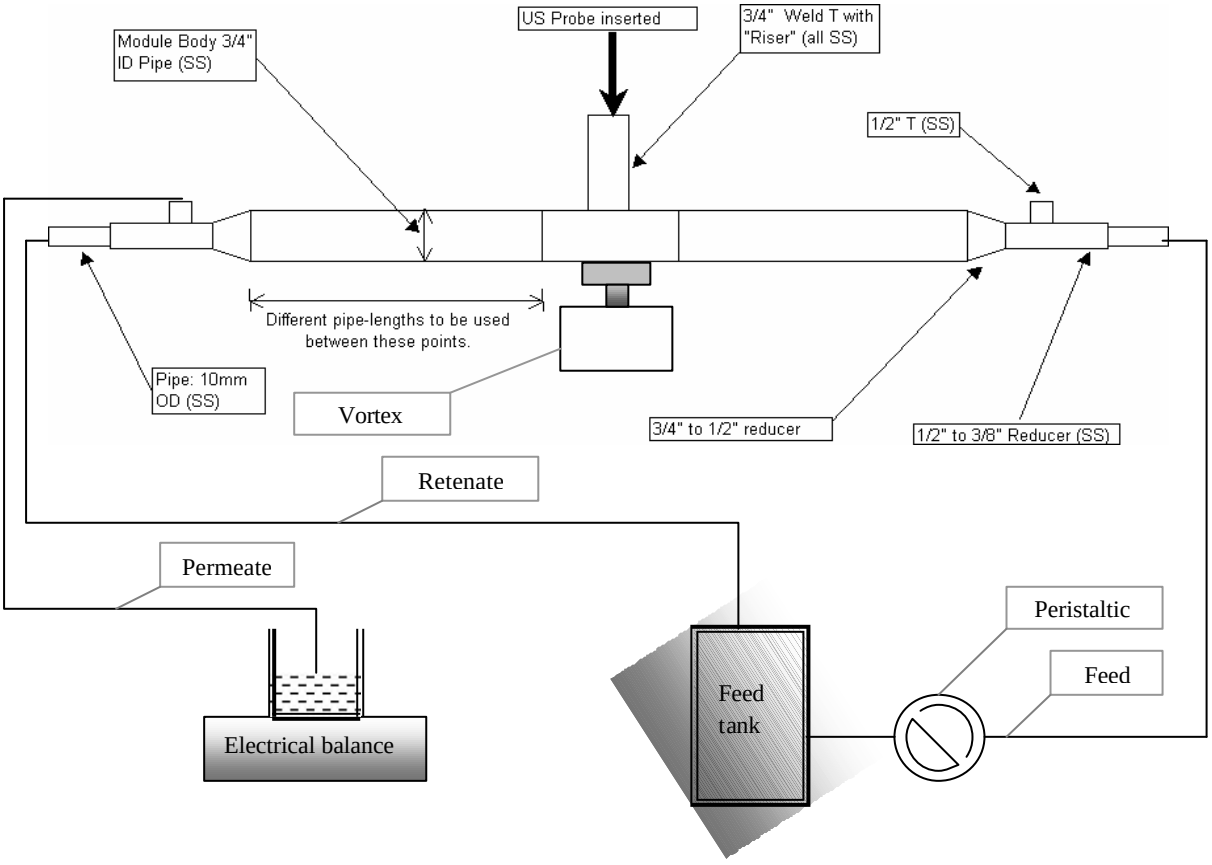

Figure 53. Schematic diagram of the bench-scale UF system with vibration and ultrasonication treatment.

4.4.2. Conclusions

The mechanical vibration and ultrasonication was performed on cleaning of an ultrafiltration membrane fouled by natural organic water. The results suggested that in general the low frequency vibration and high frequency ultrasonication showed a comparable effect on membrane defouling or cleaning. The off-line cleaning module with forward flushing performed better than the on-line cleaning module, while on-line vibration gave better results than on-line ultrasonication.

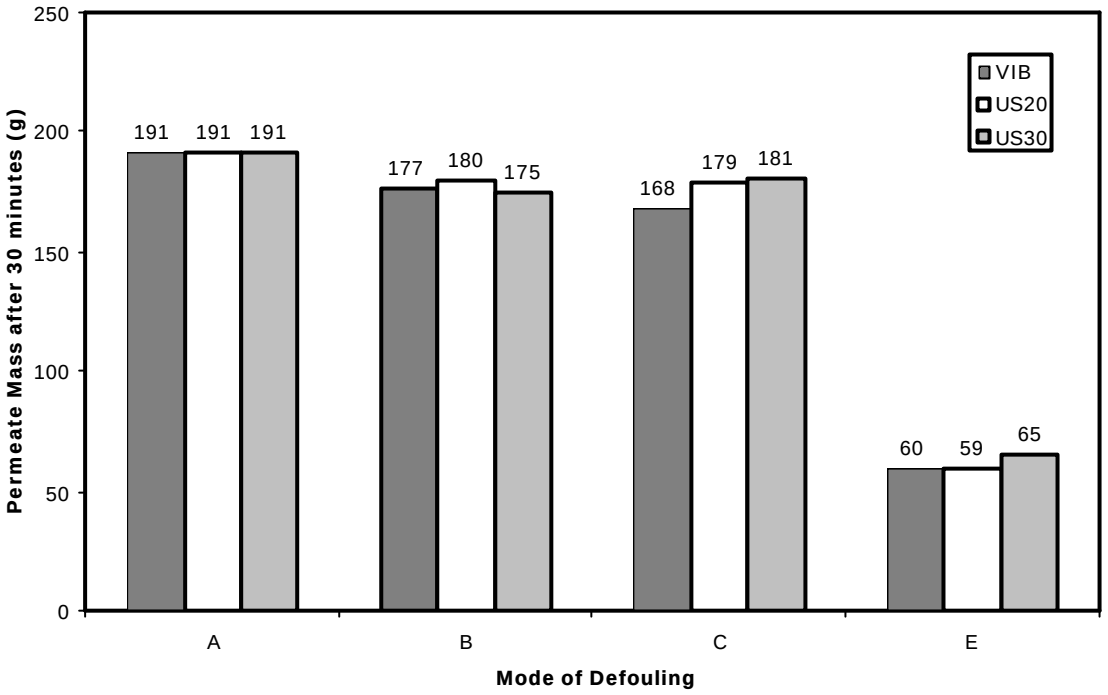

Figure 54. Effect of different modes of vibration (defouling) on permeate flow with water from the Steenbras dam as feed.

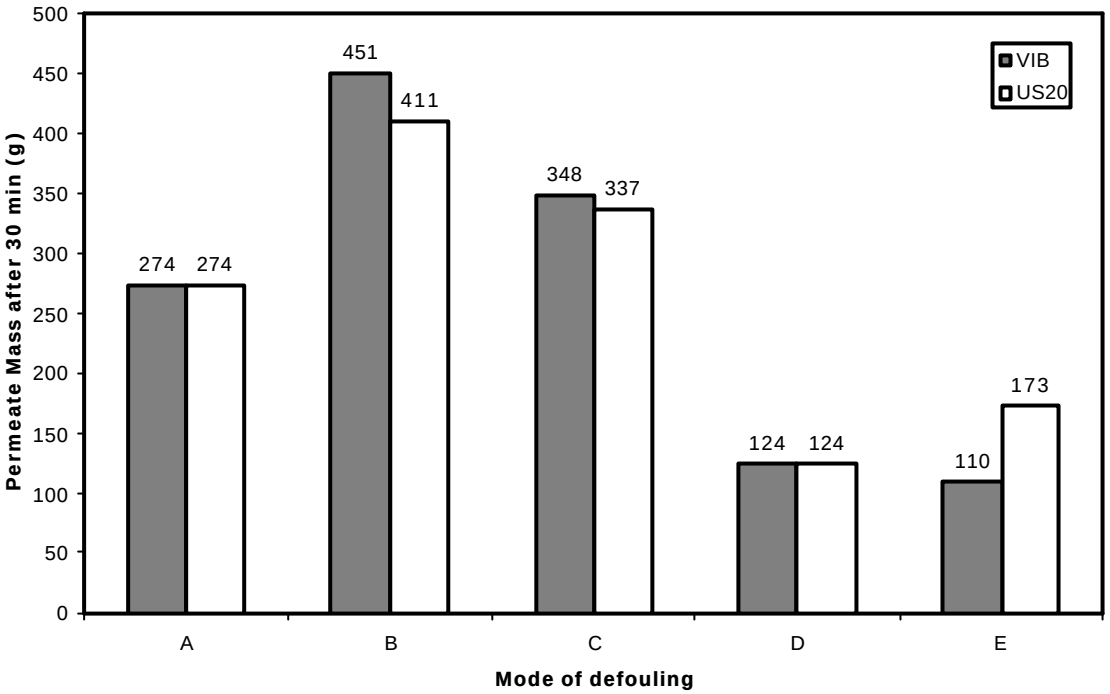

Figure 55. Effect of different modes of vibration (defouling) on permeate flow with distilled water as feed.

	Membrane:	UF membrane fouled by Steenbras dam water
	Filtration module :	Crossflow, 100-105 kPa
	Pump feeding rate:	111-112 RPM
Feed: Distilled Water	Treatment conditions	Permeate (in 30 min):
A	Before vibration	274.4 (g)
B	After 10 min off-line vibration	450.5 (g)
C	After 10 min on-line vibration	348.4 (g)
D	10 min filtration without vibration	123.7 (g)
E	10 min filtration with on-line vibration	110.1 (g)
A	Before 20 kHz ultrasonication	274.4 (g)
B	After 10 min off-line 20 kHz ultrasonication	410.8 (g)
C	After 10 min on-line 20 kHz ultrasonication	337.2 (g)
D	10 min filtration without ultrasonication	123.7 (g)
E	10 min filtration with on-line 20 kHz ultrasonication	173.4 (g)
Feed: Steenbras dam Water	Treatment conditions	Permeate (in 30 min):
A	Before vibration	191.2
B	After 10 min off-line vibration	176.5
C	After 10 min on-line vibration	168
B	After 10 min off-line 20 kHz ultrasonication	179.6

C	After 10 min on-line 20 kHz ultrasonication	179.2
B	After 10 min off-line 30 kHz ultrasonication	174.7
C	After 10 min on-line 30 kHz ultrasonication	180.8
E	10 min filtration with on-line vibration	59.6
E	10 min filtration with on-line 20 kHz ultrasonication	59.3
E	10 min filtration with on-line 30 kHz ultrasonication	65.2

Feed:

Steenbras dam water	Treatment conditions	Permeate (in 30 min):
A	Before vibration	100.00
B	After 10 min off-line vibration	108.33
C	After 10 min on-line vibration	105.06
B	After 10 min off-line 20 kHz ultrasonication	93.54
C	After 10 min on-line 20 kHz ultrasonication	100.22
B	After 10 min off-line 30 kHz ultrasonication	102.58
C	After 10 min on-line 30 kHz ultrasonication	96.63
E	10 min filtration with on-line vibration	303.36
E	10 min filtration with on-line 20 kHz ultrasonication	100.51
E	10 min filtration with on-line 30 kHz ultrasonication	90.95

5. ASSESSMENT OF DAMAGE CAUSED BY ULTRASONICATION

5.1. SMALL-SCALE CAPILLARY MEMBRANE UNIT (E and F in Table 2)

Experiments to assess the potentially damaging effect of ultrasound on ultrafiltration membranes were conducted with ultrapure (Milli-Q) water and water containing Congo Red dye in a small cylindrical unit that housed poly(ether sulphone) capillary tubes. A bench scale membrane module (Figures 56 and 57) was designed to take the IKA U50 7 mm diameter ultrasonic probe. The operating frequency of the probe was fixed at 30 kHz.

The module held 10 poly(ether sulphone) hollow fibres, which were obtained from the Institute of Polymer Science at the University of Stellenbosch in South Africa. Permeate collected on the shell side of the module and was collected from the permeate port closest to the feed entrance. The ultrasonic probe was inserted at the central T junction shown in Figure 56. The first ½" of the T junction acted as the permeate port. Both the central T junction and the second ½" T were open to the atmosphere, while the shell-side was at atmospheric pressure. The operating pressure of the hollow fibres was 100 kPa (g), while the maximum design pressure of the fibres was 200 kPa (g). The pressure was regulated via a backpressure valve on the retentate outlet. The hollow fibre bundle was 345 mm long (excluding the epoxied ends that were 70 mm in length each). The total length of the module was 485 mm. A Watson-Marlow peristaltic pump was used to circulate the feed.

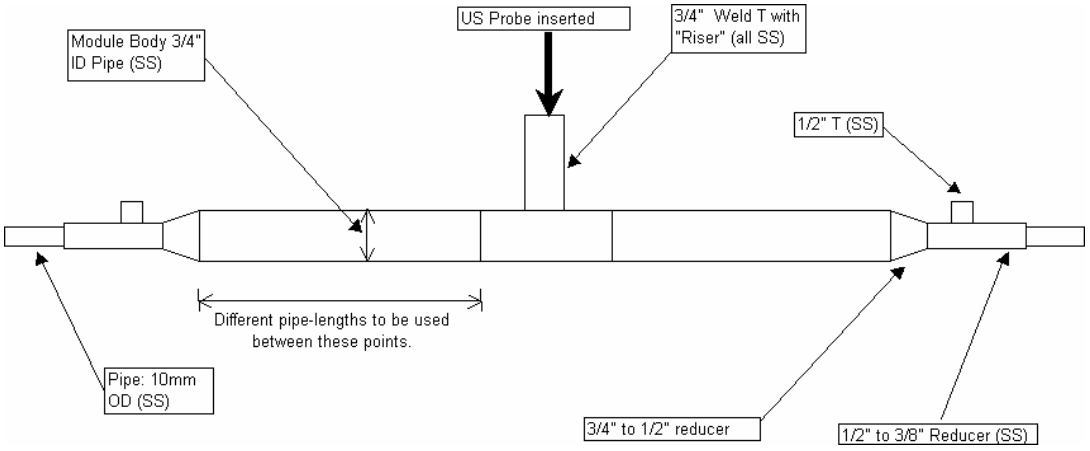

Figure 56. Diagram of the bench-scale capillary ultrafiltration module.

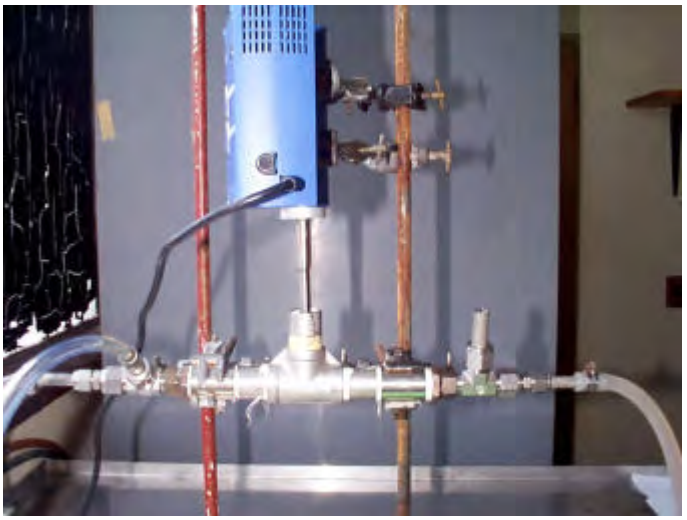

Figure 57. Photograph of the bench-scale module and probe.

5.1.1. Membrane Preparation

The hollow fibres were received in dry form and had to be prepared before any work could be done with them. Ultra-pure water was pumped through the membrane at 50 kPa (g). The first 3 L of retentate was discarded as this contained organics that had been flushed out of the membrane. After 1 h the pressure was raised to 100 kPa (g) and ultrapure water was circulated through the membrane for up to 24 h.

After completion of the preparatory phase, permeate was collected for 1 h and the volume collected was used to calculate the clean water flux of the membrane in litres per meter squared per hour ($Lm^{-2}h^{-1}$). For the PES membranes, typical values ranged from 50 to 100 $Lm^{-2}h^{-1}$.

5.1.2. Tests with Congo Red

The feed was made up of approximately 9 L of distilled water with less than 0.01 g of Congo Red dye. This feed was pumped through the membrane module for 5 to 7 h, taking hourly flux and retentate flow rate measurements until the flux had become more or less stable. After this, the ultrasonic probe was inserted and ultrasonication commenced. The bundle of hollow fibres was ultrasonicated for a total of 6 h at the full amplitude and full cycle of the probe. Ultrasonication was not applied continuously over the whole period of filtration, but was applied in intervals of one hour at a time during filtration. The feed temperature was measured at the start and finish of every ultrasonication interval. Permeate and retentate temperatures were recorded every 10 minutes while ultrasonication was taking place. Between ultrasonication intervals, feed was circulated through the module for 30 minutes at a time. Whenever coloured permeate was observed the experiment was terminated, as coloured permeate was regarded as an indication of damage to the membrane. After the completion of each experimental run, the hollow fibre bundle was removed for further examination.

5.1.3. Tests with Ultra-Pure Water

Milli-Q water (distilled and deionized) was used as the feed. The water used in experimental runs was obtained from the Biochemistry department at the University of Stellenbosch. Feed was pumped through the membrane for 10-20 hours, taking hourly flux measurements until the flux had stabilized. After this, the ultrasonic probe was inserted and ultrasonication commenced. The bundle of hollow fibres was ultrasonicated for a total of 6 hours at full amplitude and full cycle of the probe. As before, ultrasonication took place over discrete time intervals during filtration. The feed temperature was measured at the start and end of every ultrasonication interval and permeate temperatures were recorded every 10 minutes during ultrasonication. Between each ultrasonication interval, feed was circulated through the module for 30 minutes. An abnormal increase in permeate flux was regarded as an indication of damage to the membrane. After the completion of the each experimental run the hollow fibre bundle was removed and the hollow fibres were examined under a microscope.

5.2. VISUAL TESTS WITH CONGO RED

5.2.1. Visual Test 1

Feed was pumped through the module over a period of 5 hours, during which no sonication took place. After 5 hours, ultrasonication was introduced to the system, but the test was terminated 10 minutes after switching on the ultrasound when a hollow fibre ruptured. This occurred when the tip of the sonotrode touched the hollow fibre bundle. The damage to the membrane was visible to the naked eye and was in the middle of the strand in line with the insertion point of the sonotrode.

5.2.2. Visual Test 2

Feed was pumped through the module over a period of 5 hours, during which no sonication took place. This test was terminated 9.5 minutes after switching on the ultrasound when two hollow fibres were ruptured. This happened when the tip of the sonotrode touched the hollow fibre bundle. The damage to the hollow fibres was visible to the naked eye and was in the middle of the strands in line with the insertion point of the sonotrode.

5.2.3. Visual Test 3

As before, feed was pumped through the module over a period of 5 hours, during which no sonication took place. This was followed by sonication over a period of 7 hours. From Figure 58 it can be seen that during the first five hours (in the absence of sonication) the flux decreased with time. Within the first hour of sonication, the flux increased markedly, but then gradually decreased again, as indicated in Figure 58. Permeate and retentate temperatures were also recorded. The ultrasound caused a modest increase in these temperatures, never exceeding 4 °C. All the permeate samples were clear and when the hollow fibres were examined under an optical microscope, no damage to the membranes surface could be observed.

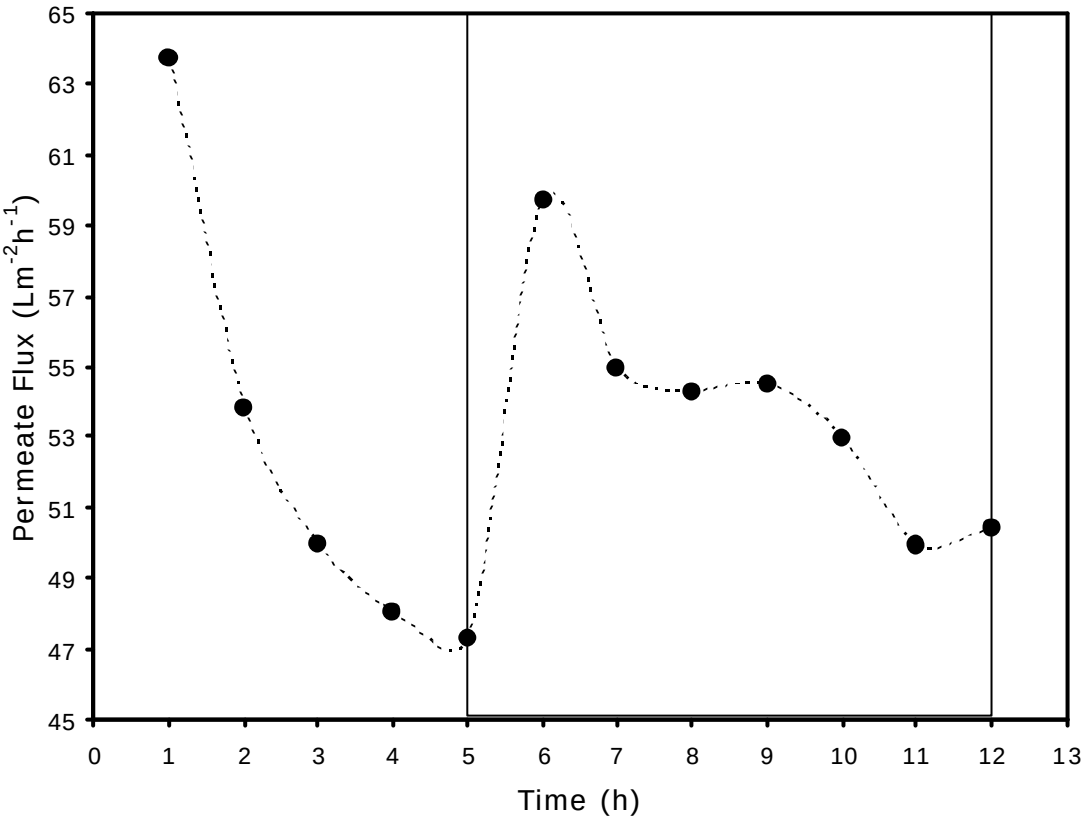

i

Figure 58. Permeate flux of water containing 0.11 wt% Congo Red dye (Visual Test 3). Shaded time intervals indicate periods of sonication.

5.2.4. Visual Test 4

Feed was pumped through the module in the absence of sonication for a total of 5 hours. This was followed by sonication in hourly intervals for a total time of 5 hours. Every sonication interval was followed by a 30 min interval where feed was pumped through the module in the absence of sonication. During the first 5 hours (in the absence of sonication) the flux was fairly constant at low values (Figure 59). During the first sonication-interval the flux increased markedly. During the 30-minute recovery period the flux decreased again, but not to the same level as was recorded during the first 5 hours. Once the ultrasound was switched on again, the flux increased again. The sonicated flux values remained fairly constant.

Sonication appeared to have increased the permeate flux, as the average sonicated flux was 31% higher than the average unsonicated flux, and 40% higher than the average value of the unsonicated flux recorded during the first 5 hours. The last flux value is abnormally high – at this point coloured permeate was obtained, an indication of damage to the membrane, which was subsequently confirmed by microscopic analysis. This damage again appears to have been caused by the sonotrode coming into contact with the fibre.

The ultrasound caused a modest increase in temperature of less than 3 °C in the permeate and less than 1.5 °C in the retentate. This minimal temperature increase indicates that temperature could not have been the most important driving force behind the observed enhancement of the flux.

It appears as if phenomena other than defouling may also have occurred during sonication, since the generally higher flux values observed during sonication are not consistent with the effect expected with the removal of foulants from the membrane. Similar trends were identified in the other visual tests described here, as can be seen in Figure 58 as well.

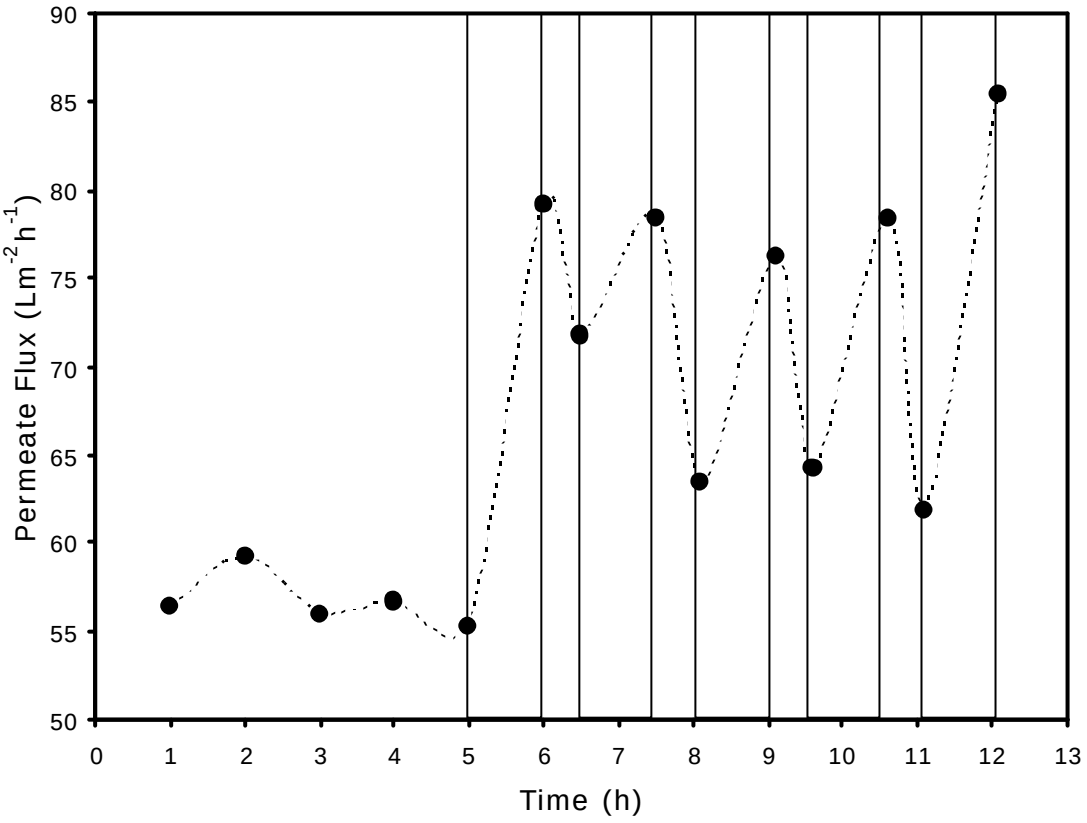

Figure 59. Permeate flux of water containing 0.11 wt% Congo Red dye (visual test 4).

5.2.5. Visual Test 5

Feed was pumped through the module in the absence of sonication for a total of 6 hours. This was followed by sonication for one hour followed by a 30 min interval where feed was pumped through the module in the absence of sonication. During the sonication interval the flux increased dramatically and at the end of the 30-minute recovery period coloured permeate was obtained.

5.2.6. Visual Test 6

Feed was pumped through the module in the absence of sonication for a total of 8.5 hours. This was followed by sonication in hourly intervals for a total time of 6 hours. As with the previous test, each sonication interval was followed by a 30 minute interval, where the feed was pumped through the module in the absence of sonication.

During the first 8.5 hours (in the absence of sonication) the flux varied with time, as indicated in Figure 60. During the first sonication interval the flux increased. During the 30-minute recovery period the flux decreased again, but not to the same level as was recorded during the first 8.5 hours. This pattern was repeated during subsequent cycles of ultrasonication and operation without ultrasound.

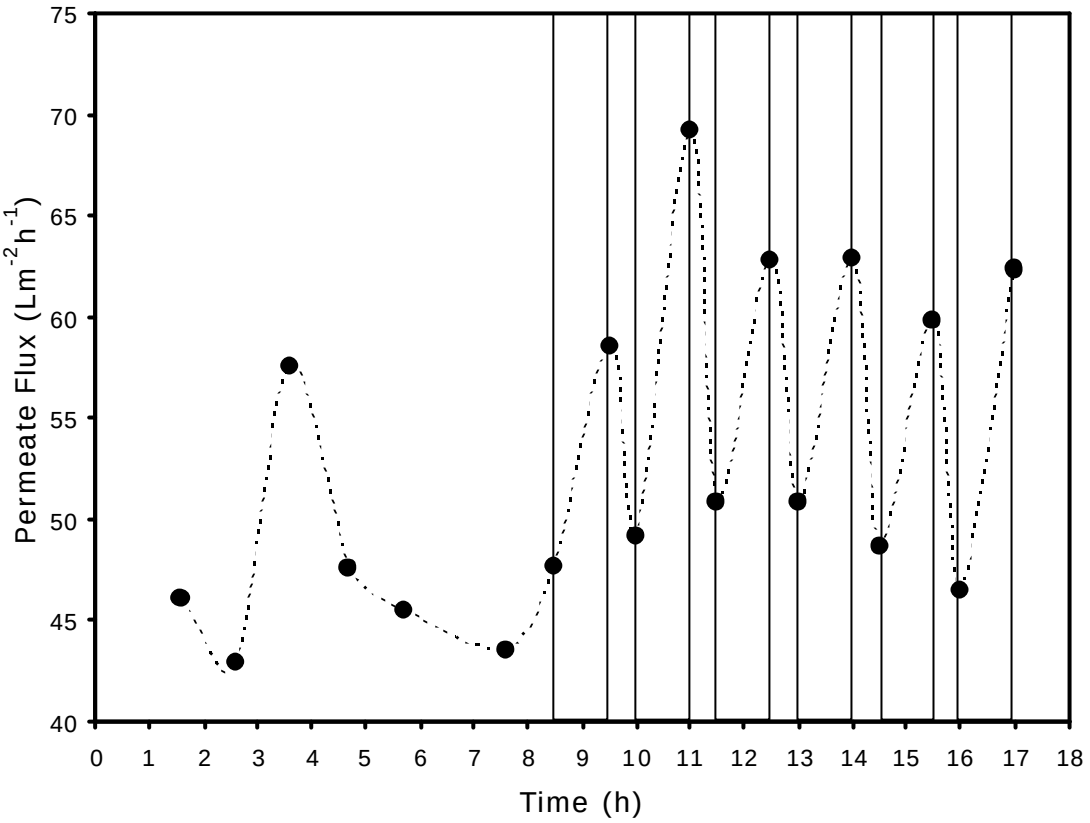

Figure 60. Permeate flux of water containing 0.11 wt% Congo Red dye (Visual Test 6). Shaded areas indicate periods of sonication.

No indications of damage to the membrane could be observed from either the colour of the permeate or visual examination of the membrane fibres. The ultrasound increased the permeate and retentate temperatures to maximum values of 6 °C and 3 °C respectively. Again, this was not sufficient to fully explain the increase in the observed flux enhancement.

5.3. TESTS WITH ULTRAPURE WATER

Milli-Q water (distilled and deionized) was used as the feed. Generally, an abnormal increase in the permeate flux was regarded as an indication that damage to the membrane had occurred. Three experimental runs were carried out.

5.3.1. Milli-Q Water Test 1

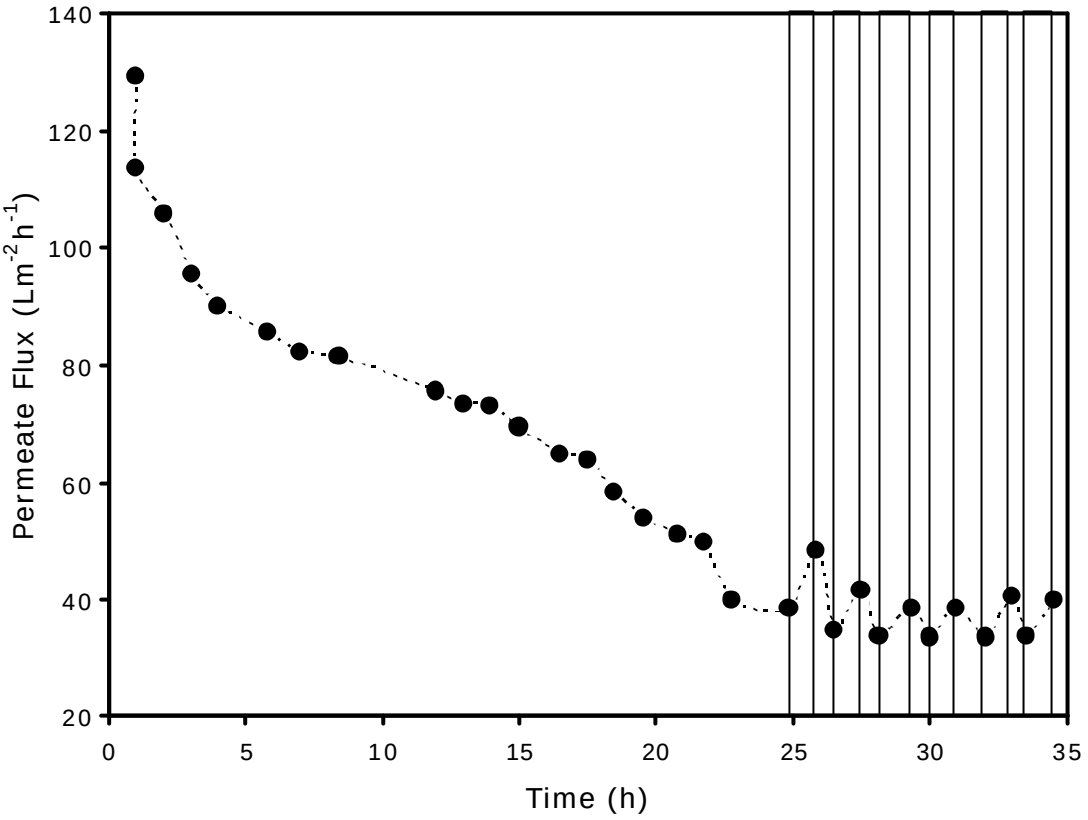

Figure 61. Permeate flux of ultrapure water (Visual Test 1)

Feed was pumped through the module in the absence of sonication for a total of 25 hours. This was followed by sonication in hourly intervals for a total time of 6 hours. Every sonication interval was followed by an approximately 30-minute interval where feed was pumped through the module in the absence of sonication.

The unsonicated flux decreased from approximately 56 to 46 $Lm^{-2}h^{-1}$ with time. Once sonication commenced, the flux stabilized, again showing the patterns of increase and decrease after sonication and in the absence of sonication respectively, but to a lesser extent than what was observed with the Congo Red dye.

No abnormal increases could be detected in the permeate flux. The increase in flux during sonication cannot be attributed to cleaning, since ultra-pure water was used as the feed. Instead, the increase in flux could possibly be attributed to ultrasound having an enhancing effect on mass transfer. The permeate temperature was monitored during each experimental run, indicating a maximum increase of 3.5 ºC, which does not fully explain the observed increase in the permeate flux.

5.3.2. Milli-Q Water Test 2

Feed was pumped through the module in the absence of sonication for a total of 14.4 hours. This was followed by sonication in hourly intervals for a total time of 6 hours. Every sonication interval was followed by a 60 minute interval, where feed was pumped through the module in the absence of sonication. Essentially the same effects were observed as was the case with Test 2.

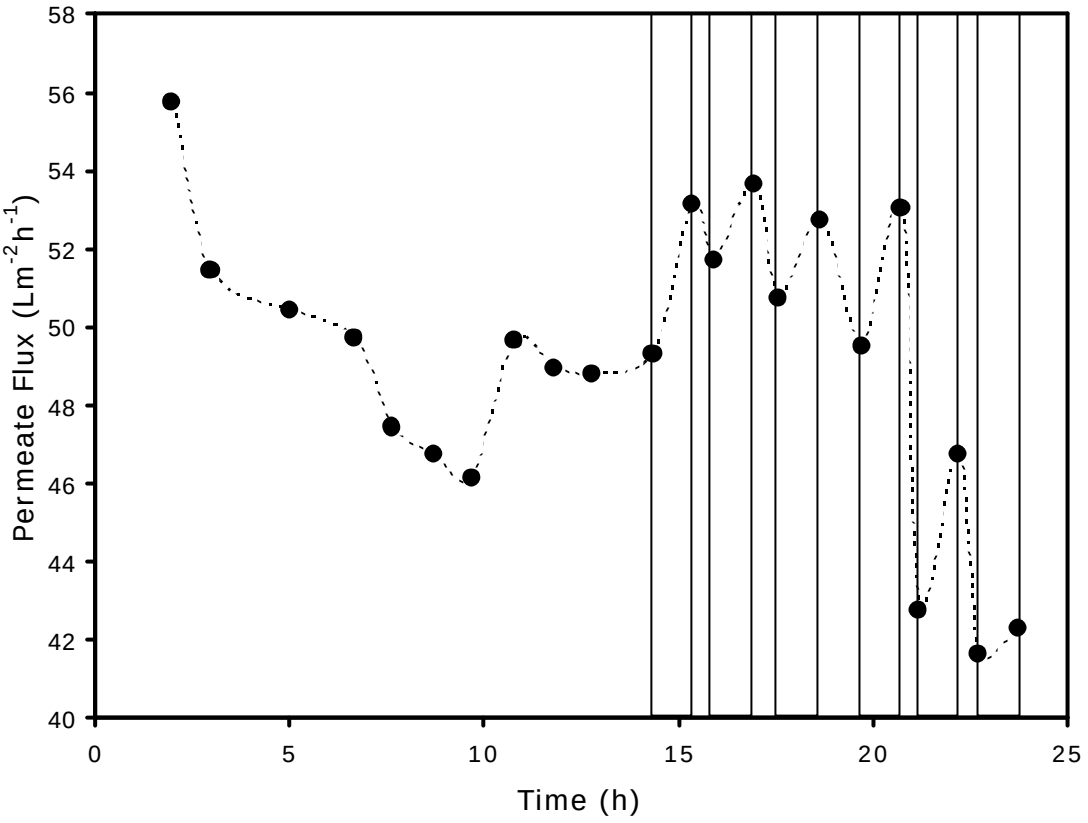

Figure 62. Permeate flux of ultrapure water (Visual Test 2).

5.3.3. Milli-Q Water Test 3

Feed was pumped through the module in the absence of sonication for a total of 10.3 hours. This was followed by sonication in hourly intervals for a total time of 6 hours. Every sonication interval was followed by a 30-90 minute interval where feed was pumped through the module in the absence of sonication. Again the same effects were observed as was the case with Tests 1 and 2.

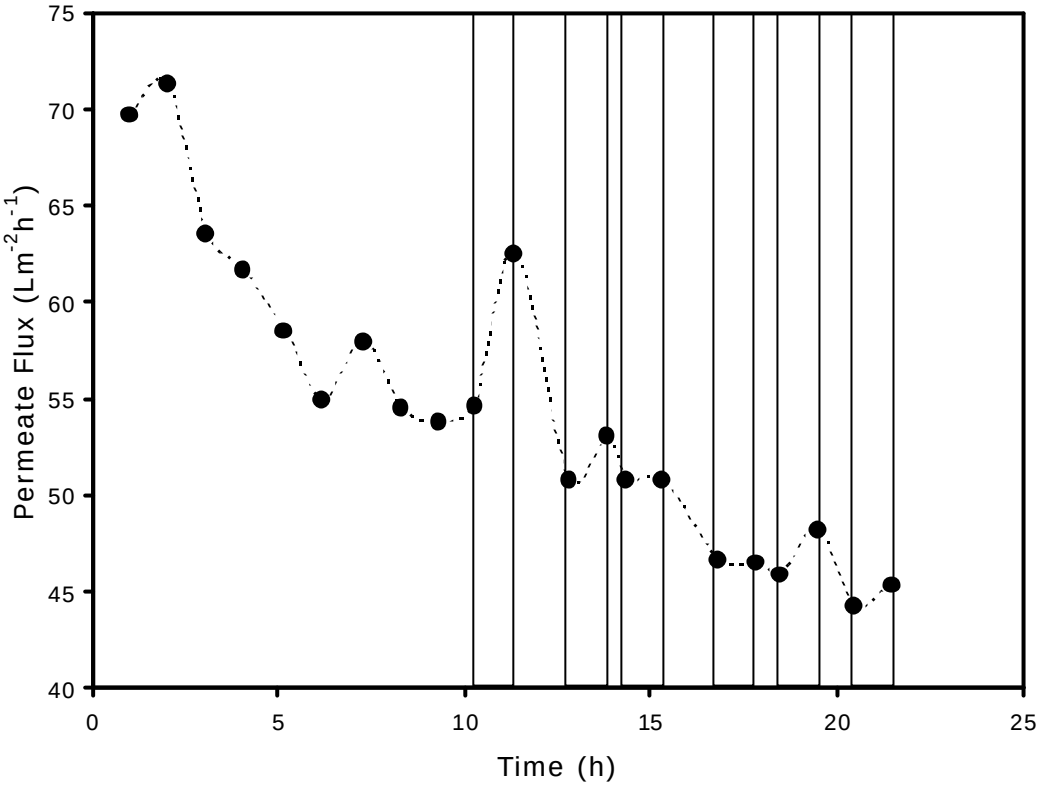

Figure 63. Permeate flux of ultrapure water (Visual Test 3).

5.4. CONCLUSIONS

- No membrane damage was apparent during the crossflow filtration experiments with water containing Congo Red dye and ultrapure water, except where the sonotrode of the ultrasonicator was in contact with the membrane fibres.

- In the distilled water containing approximately 0.11 wt% Congo Red dye, ultrasonication enhanced the permeate flux with approximately 30-40%. This improvement could not be explained completely in terms of the defouling of the membranes and some other phenomenon must also have occurred.

- In every visual test with the Congo Red dye, the sonication led to increased permeate and retentate temperatures, but since these temperature increases were not excessive as far as their effect on the viscosity of the fluids were concerned, the flux enhancement could also not be explained in terms of the increased temperatures (lower viscosities). An increase of approximately 6 °C at ambient temperatures would lead to an approximate decrease of 10% in the viscosity of the fluids concerned (water).

- With ultrapure water as feed, the flux was not enhanced significantly. This was expected, as there were no or very little foulant that could be removed. The slight flux enhancement (6% for Milli-Q test 2 and 4% for test 3) could possibly be attributed to enhanced mass transfer owing to microstreaming associated with the ultrasound. The fact that the flux kept declining during the Milli-Q water tests suggested that a possible increase in the pore size of the membranes was also unlikely, as was the effects associated with a rise in the temperature of the flux.

6. TECHNO-ECONOMIC CONSIDERATIONS IN THE SCALE-UP OF ULTRASONIC DEFOULING OF MEMBRANE SYSTEMS

In this section the economic aspects of crossflow capillary ultrafiltration is considered, where ultrasound is used to defoul the membranes, instead of backflushing. The analysis is based on the experimental data related to the filtration of water containing natural organic substances in the large-scale membrane filter, as discussed previously.

6.1. COST MODEL FOR CONVENTIONAL ULTRAFILTRATION

An approach similar to that by Davis (1997) was followed, where the cost of treating the water can be divided into capital and operational costs. Capital costs represent the investment required to establish a given capacity for the production of treated water. This includes costs such as land, engineering, construction and installation. It is common practice to annualize the initial cost incurred in the erection of the facility when calculating the investment required per unit volume of plant capacity ($/m^3).

Operational costs include all the expenses associated with plant operation and maintenance, such as energy consumption, membrane replacement and labour. For the purposes of this analysis, the treatment and disposal of waste arising from the process is considered negligible, although this cost is highly dependent on the nature of the feed and the location of the plant. At any rate, the waste disposal cost of the conventional filtration with backflushing should be roughly similar to that of filtration with ultrasonication.

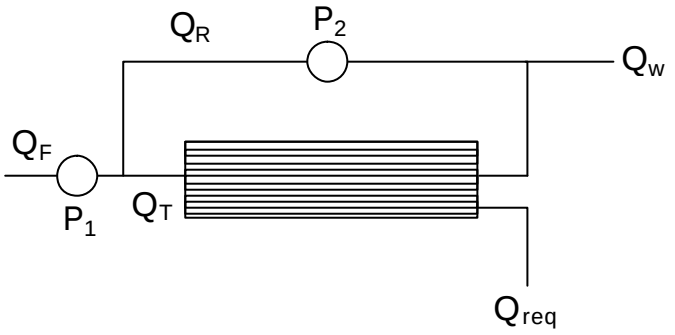

Figure 64. Schematic of the crossflow ultrafiltration water treatment system.

The model is based on the simple schematic shown in
Figure 64. Water from a natural source is pumped through the membrane module at a pressure of P_1. The concentrate is recycled through pump 2 at a rate depending on the design crossflow velocity (i.e. flow through a large cylindrical module containing tubular membrane elements).

6.1.1. Calculation of capital costs

Capital costs are subdivided into costs associated with the membranes and costs not associated with the membranes. The membrane costs include the initial cost of the membrane modules and are calculated by

$$C_{mem} = C_{mod}N_{mod} \quad (1)$$

where Cmod is the cost of a single module and N_{mod} is the number of modules required on the plant. N_{mod} is calculated from (2) (Pickering and Wiesner, 1993)

$$N_{mod} = \text{int}(A_{req}/A_{mod} + 1) \quad (2)$$

where A_{req} is the required total membrane area for the design flow and A_{mod} is the membrane area of the module.

A_{req} is calculated from the flow rate Q_{req} at the plant design capacity and J_{net} is the permeate flux of the membrane.

$$A_{req} = Q_{req}/J_{net} \quad (3)$$

The non-membrane costs are calculated from the model proposed by Pickering and Wiesner (1993) based on industrial data from membrane, engineering and construction companies, covering costs associated with engineering, construction and installation

$$C_{n\text{-}mem} = \$1.50 \times 10^5 N_{mod}^{0.74} \quad (4)$$

The total capital cost (CC) is amortized over the design life of the plant to give an annualized cost, i.e.

$$CC = (C_{mem} + C_{n\text{-}mem})AF/Q_{req} \quad (5)$$

The amortization factor is given by

$$AF = i(1+i)^T/[(1+i)^T - 1] \quad (6)$$

where T is the plant life and I the annual discount rate for capital investment.

6.1.2. Calculation of operating costs

The following operating costs are considered, viz. energy costs (pumping of the feed, pumping of recycling concentrate, and pumping during backflushing), membrane replacement, maintenance and labour.

Cost of pumping feed

The energy associated with of pumping the feed from ambient pressure P_0 to P_1 can be estimated by

$$E_1 = (P_1 - P_0)(Q_F/\eta_1)/Q_{req} \quad (7)$$

where η_1 is the efficiency of the pump, Q_F the feed flow rate drawn into the plant, differing from the plant capacity by Q_W, as indicated in Figure 64.

Cost of pumping recycle

The energy required to recycle the feed will depend directly on the pressure drop through the module (P_{mod}) on the concentrate side. This can be estimated by

$$P_{mod} = 2L_{mod}\rho u^2 f_f/d_{elem} \quad (8)$$

with L_{mod} the length of the module, ρ the density of the fluid, u the average crossflow velocity within the membrane elements and d_{elem} the diameter of the membrane elements. The Fanning friction factor can be estimated by

$$f_f = 16/Re \ (Re < 4000) \quad (9)$$
$$f_f = 0.0791/Re^{1/4} \ (Re \geq 4000) \quad (10)$$

The Reynolds number (Re) is calculated from the diameter of the element and the average crossflow velocity, $Re = \rho u d_{elem}/\mu$, with μ the viscosity of the fluid.

With the pressure drop ($P_{mod} - P_0$) known, the energy required to pump the recycled concentrate is

$$E_2 = (P_{mod} - P_0)(Q_R/\eta_2)/Q_{req} \quad (11)$$

where QR is the recycle flow rate, η_2 is the efficiency of the recycle pump. The recycle flow rate is obtained from the mass balance

$$Q_R = Q_T - Q_{req} - Q_W \quad (12)$$

where Q_W is the waste flow rate and Q_T is the total flow rate entering the module. Q_T is determined by fixing the crossflow velocity within the capillaries

$$Q_T = uA_0 N_{mod} N_E \quad (13)$$

where A_0 is the cross-sectional area of the membrane element and N_E the number of elements per module. The waste concentrate is fixed by the plant recovery, R

$$Q_W = Q_F(1 - R) \quad (14)$$

Cost of backflushing

The energy required to pump the fluid involved in backflushing is

$$E_{BF} = (P_{BF} - P_0)(Q_{BF}/\eta_{BF})/Q_{req} \quad (15)$$

Q_{BF} is estimated from

$$Q_{BF} = J_{BF} A_{mod} N_{mod} \quad (16)$$

Since backflushing occurs only during part of the cycle, the energy required is weighted by the backflushing duration time

$$E_{BF}' = E_{BF} t_{BF} / t_{CYC} \quad (17)$$

where t_{CYC} is the duration of the operating cycle (backflush + forward operation).

The cost associated with the total energy is subsequently calculated as

$$C_E = C_{kWh}(E_1 + E_2 + E_{BF}') \quad (18)$$

where C_{kWh} is the cost per kilowatt-hour ($/kWh).

Cost of membrane replacement

Although the membrane is a capital item, the cost associated with the replacement of the membrane is treated as an operating cost, instead of a periodic investment of capital. The assumption is that the membranes are replaced at fixed intervals (as recommended by the manufacturer). The cost of the membrane replacement is then annualized over one replacement period by means of an amortization factor (A_{FM})

$$A_{FM} = i_M / [(1+i_M)^{ML} - 1] \quad (19)$$

with ML the membrane lifespan in years and iM the annual discount rate for replacement of the membrane. The annual cost of replacing the membrane is then calculated from

$$C_{MR} = C_{mod} N_{mod} AF_M / Q_{req} \quad (20)$$

Cost of labour and maintenance

The maintenance cost is estimated by an annualized 1.5% of the non-membrane cost (Owen et al., 1995). The required labour costs are estimated from data for man-hour requirements for fluid processing plants (Peters and Timmerhaus, 1991).

The total cost for treating the water is found by adding the capital and operating costs.

6.2. COST MODEL FOR ULTRASONIC DEFOULING

The cost model for the treatment of water with ultrasound defouling of the membranes is similar to the cost model for the conventional treatment of the water with backflushing, except that the cost of the ultrasonic equipment has to be added on top of the existing capital costs, while the electrical energy required to run the ultrasonic equipment has to be added to the operational cost outlined above. These additional costs are offset by the increased productivity of the membranes, leading to smaller filtration plants.

Capital cost of ultrasonic equipment

The capital cost (CC_{US}) of the ultrasonic equipment (transducers + generators) are estimated as follows

$$CC_{US} = C_T N_T N_{mod} \quad (21)$$

where C_T is the cost of a transducer unit, N_T is the number of transducers required per module and N_{mod} is the number of modules required to meet the required plant capacity. The number of transducers required per module is estimated from the required power for acoustic cavitation in fluids (50-100 W/gallon) reported in the literature, assuming that the nominal power output of a transducer is 50 W and that each transducer can cavitate approximately 2 x 10^{-3} m^3 of fluid.

$$N_T = \text{int}(V_{mod}/0.002+1) \quad (22)$$

Operating cost of ultrasound

The operating cost is based on the power required to cavitate a unit volume of fluid (W_{cav}) as reported in the literature for ultrasonic cleaning systems (50-100 W/gallon as above, or 13020 W/m^3)

$$W_{mod} = W_{cav}V_{mod} \quad (23)$$

This is equivalent to the number of transducers per module multiplied by the nominal power requirement of each transducer. The total energy consumed by the ultrasound equipment is then simply annualized by multiplying with the number of seconds per annum to get

$$E_{US} = 31557600W_{mod}N_{mod} \quad (24)$$

The cost is then

$$C_{US} = E_{US}C_{kWh} \quad (25)$$

after converting to kWh, with C_{kWh} the price of electricity (0.1 $/kWh). Finally, since experiments have shown that continuous ultrasonication is not necessary, the actual cost can be found by correcting CUS with the duty cycle of the ultrasonication, i.e. the fraction of time (t_{US}) ultrasound is actually used during cleaning.

$$C_{US}' = C_{US}t_{US} \quad (26)$$

6.3. ANALYSIS AND DISCUSSION

The conventional and ultrasonic equipped systems were compared for large and smaller scale plants treating 5 000 000 and 500 000 gallons of water per day respectively. The parameters for the analysis are summarized in Table 5.

Table 5. Parameters used in economic analysis of water treatment systems.

Parameter	Value	Units	Description
J_{net}	0.00139	$m^3 m^{-2} s^{-1}$	net volumetric membrane flux (permeate flux)
Q_{req}	0.222	$m^3 s^{-1}$	required flow rate at plant design capacity
d_M	0.09	m	module diameter
P_1	250000	Pa	pressure difference
P_0	100000	Pa	atmospheric pressure
η_1	0.4	-	pump efficiency
Q_F	0.244	$m^3 s^{-1}$	feed flow rate to plant
L_{mod}	1.2	m	length of module
ρ	1050	$kg m^{-3}$	density of water to be treated
η	0.001	Pa.s	viscosity of fluid
d_{elem}	0.001	m	diameter of an element
η_2	0.4	-	efficiency of recycle stream pump
N_E	884	-	number of elements per module
R	0.9	-	plant recovery
P_{BF}	260000	Pa	backflushing pressure
η_{BF}	1	-	backflush pump efficiency
J_{BF}	0.00139	$m^3 m^{-2} s^{-1}$	concentrate flux relevant to backflushing
t_{BF}	0.1	-	backflush duration time (10% of cycle flow time)
t_{US}	0.05	-	cycle time

Table 6. Cost factors used in economic analysis of water treatment systems.

Parameter	Value	Units	Description
T	20	y	plant life
i	0.08	-	annual discount rate
T_{US}	20	y	equipment life
i_{US}	0.08	-	annual discount rate
C_{kWh}	2.78E-08	$\$J^{-1}$	electricity cost (= \$0.1/kWh)
C_{USunit}	6000	\$	capital cost per transducer unit
ML	8	years	recommended membrane life
L	0.07	$\$h^{-1}$	cost of labour per hour of plant operation

With the parameters in Tables 5 and 6, the processing cost can be calculated as a function of permeate flux with or without the use of ultrasound. When the ultrasound is used, the overall efficiency of the membranes is increased, so that fewer membrane modules are needed to meet the required production. This comes at the expense of the capital and operating cost associated with the ultrasonic equipment.

Figures 65 and 66 show the cost of treatment for the large (0.222 m^3/s) and small scale (0.0222 m^3/s) plants. In this scenario, the overall increase in the efficiency of the membranes, owing to ultrasonic anti-fouling measures is 50% (estimated from experimental data – see for example Figure 51). Figures 67 (large scale) and 68 (small scale) show the allocation of costs in the above scenarios. On both the large and small-scale plants, the membrane costs are dominant, when no ultrasound is used.

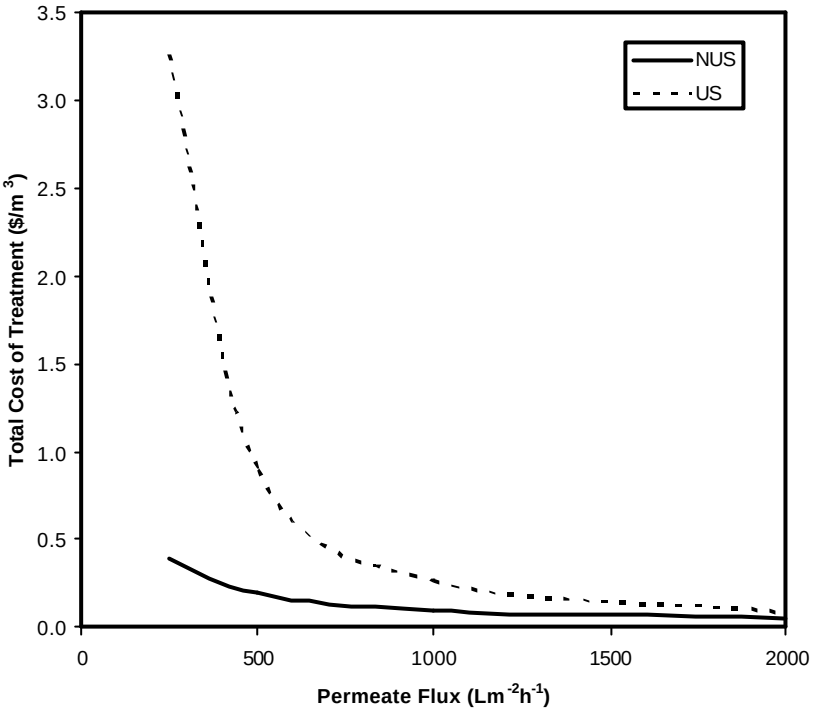

Figure 65. Water treatment cost versus permeate flux for a 0.222 m^3/s (5 million gallons per day) facility with sonication (broken line) and without (solid line).

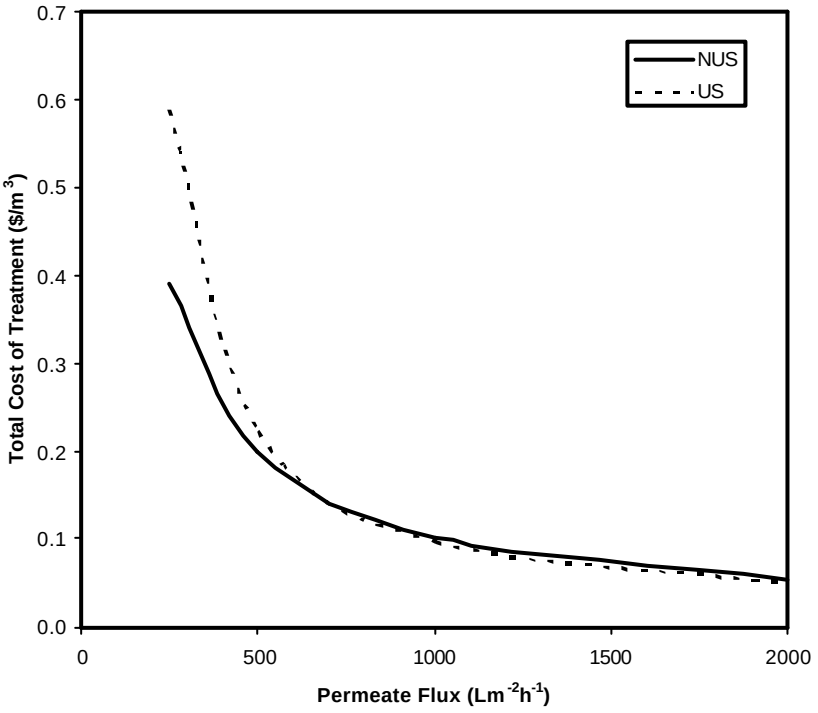

Figure 66. Water treatment cost versus permeate flux for a 0.0222 m^3/s (0.5 million gallons per day) facility with sonication (broken line) and without (solid line).

When ultrasound is used, the capital cost of the ultrasonic equipment becomes the most important on the large-scale plant, but markedly less so on the smaller-scale plant. These results suggest that the use of ultrasound for defouling or prevention of membrane fouling may be feasible on water treatment plants with relatively small capacities (< 0.0222 m^3/s). Naturally, these conclusions depend on the assumptions of the model. For example, if the estimated membrane replacement costs are reduced by 50%, the use of ultrasound will result in a less competitive design, on both small and large-scale plants. At a small scale, less expensive ultrasonic equipment will not make much of a difference to the costs, but the opposite may also render the ultrasound system less competitive.

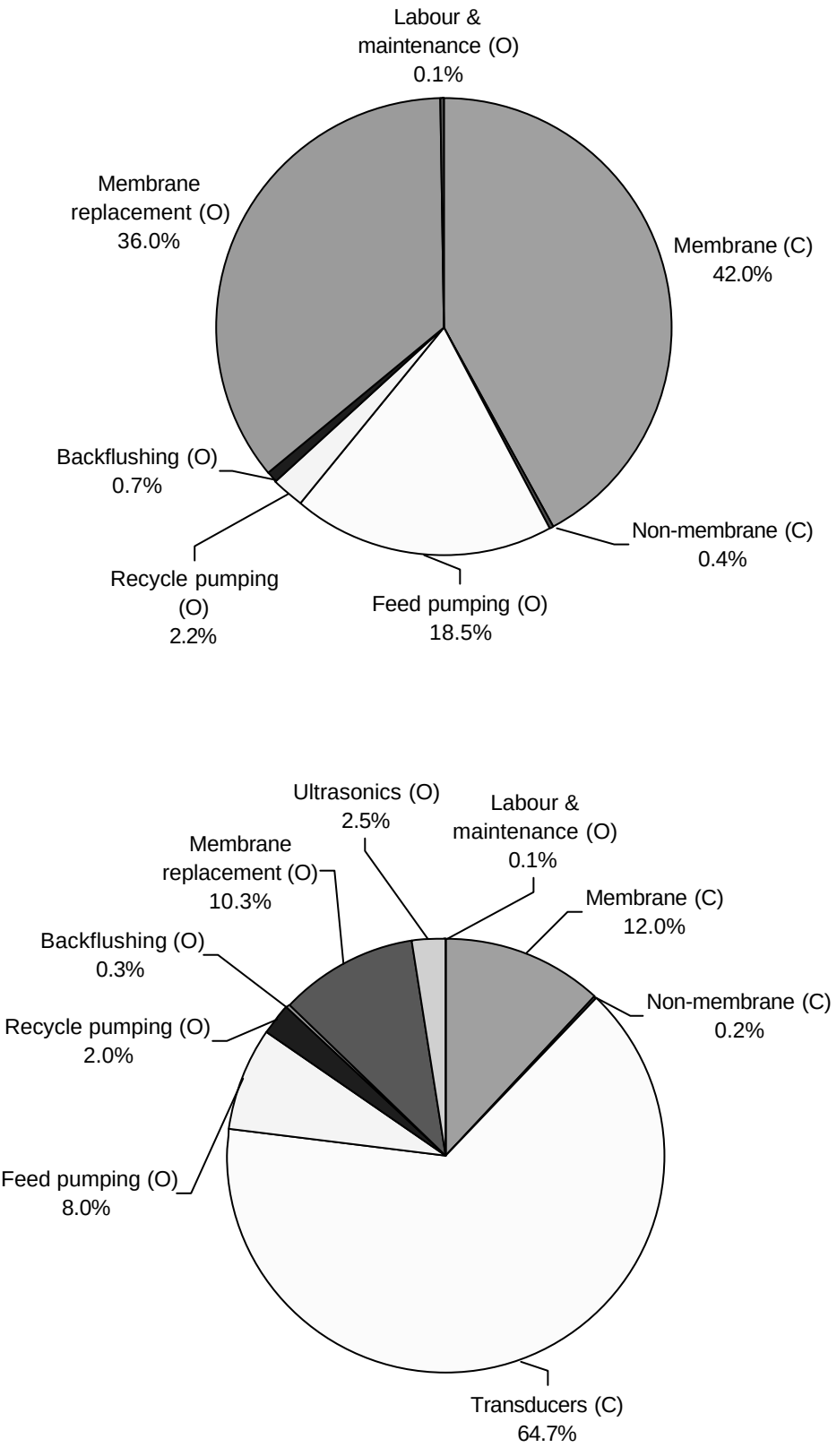

Figure 67. Breakdown of total cost without sonication ($0.0622/m^3) (top) and with sonication ($0.144/m^3) (bottom) at a permeate flux of 2000 L/m^{2}h for a 0.222 m^3/s.

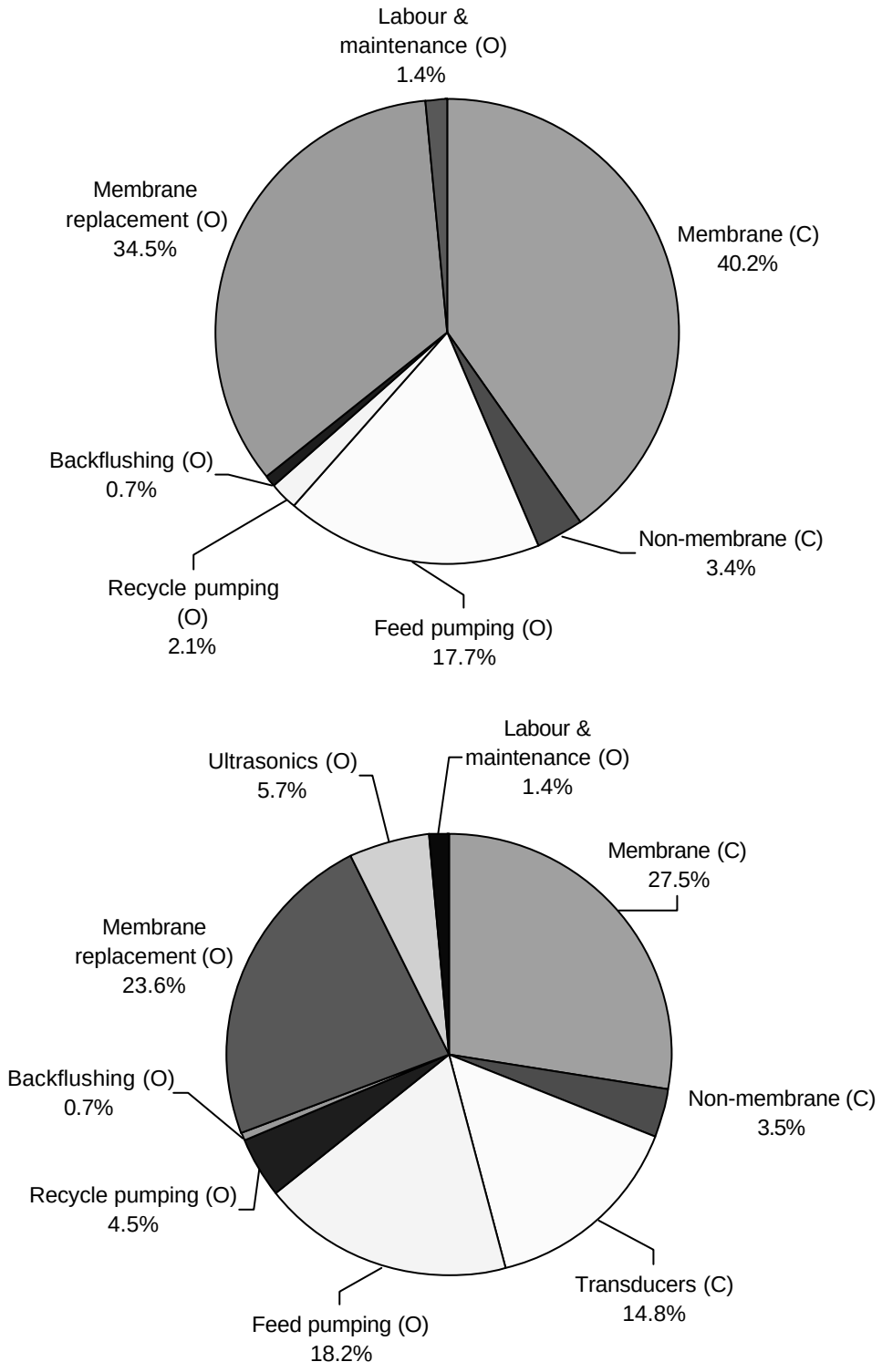

Figure 68. Breakdown of cost without sonication ($0.065/m^3$) (top) and with sonication ($0.0.063/m^3$) (bottom) at a permeate flux of 2000 L/m^2h for a 0.0222 m^3/s.

7. SUMMARY AND CONCLUSIONS

- The literature review clearly indicated that foulants can be removed by ultrasound over a wide range of process conditions, frequencies (from 20–100 kHz) and specific power inputs (nominally ranging from 0.5-83 W/cm^2). There are some indications from limited work that relatively low frequencies (20-28 kHz) provide the best results. All the experiments referred to in the literature were conducted with laboratory-scale sonication systems and these results were largely confirmed by laboratory experiments with small-scale and larger-scale membrane units.

- The influence of ultrasonic frequencies in particular need to be investigated further, bearing in mind that these are likely to be highly system specific and/or sensitive to operating conditions. A systematic study in this regard was not possible, since the frequencies of sonication equipment is generally fixed and such a study would require a series of different sonicators altogether.

- No membrane damage could be observed as a result of ultrasonication. The literature is divided on this issue, but it appears as if membrane damage is unlikely to occur, as long as sufficient flow conditions are maintained during sonication.

- Moreover, it was found that continuous on-line ultrasonication to remove foulants from membranes is not necessary. For all practical purposes, similar results could be obtained by means of intermittent sonication. Experiments have also shown that even better results can be obtained by using ultrasound in conjunction with chemical cleaning of the membranes. This was confirmed by several other studies described in the literature.

- In addition, experiments have confirmed that the ultrasonic energy decreases rapidly with distance from the source, suggesting that depending on the configuration of the plant, membrane modules would each probably require multiple transducers when equipped with ultrasound defouling systems.

- On the basis of these and other findings in the literature, ball park estimates suggest that the feasibility of using ultrasound on a large-scale to reduce or prevent fouling of membranes depends on the capital cost of the ultrasonic equipment, rather than its operating cost. These estimates depend on a number of assumptions that may very widely for individual cases.

8. RECOMMENDATIONS FOR FUTURE WORK

On the basis of the results and analyses discussed above, the following recommendations can be made.

- Since the sonicators used in the experiments were laboratory scale systems, further experiments need to be conducted with industrial scale systems. More specifically, the integration of these systems with existing membrane modules should be considered in line with some of the latest advances in sonochemical reaction systems, where multi-transducer multi-frequency systems are proposed. This would give a better indication of some of the important issues surrounding the capital and operating cost associated with ultrasonication.

- Moreover, the economic feasibility of using ultrasound to combat membrane fouling should be verified experimentally by running a filtration unit in a closed circuit, using both conventional means and ultrasound to clean the membranes in order to experimentally verify the cost, also in terms of the disposal the chemicals, where used for cleaning.

- In additional, the cost model used in this investigation needs to be refined, either by use of existing cost estimation software or by more detailed modeling in order to compare different designs and operating strategies more accurately.

- On a final note: one of the crucial issues throughout the project concerned the determination of critical parameters associated with sonication, such as the minimum power required per unit volume of effluent or membrane surface area, the optimal sonication frequency, parameters such as sweep control, duty cycles, etc. These issues are just as important in the wider field of sonochemistry, where the basic theory is well established, but where the lack of reliable measurement of acoustic cavitation is still a major stumbling block in more advanced reactor design, control and optimization. Advances in the development of sensors capable of measuring acoustic cavitation should therefore also give significant impetus to the development of more cost-effective industrial sonication systems.

REFERENCES

Band, M., Gutman, M., Faerman, V., Korngold, E., Kost, J., Plath, P.J. and Gontar, V. (1997) Influence of specially modulated ultrasound on the water desalination process with ion-exchange hollow fibres, *Desalination*, 109, 303-313.

Chai, X., Kobayashi, T. and Fujii, N. (1998) Ultrasound effect on crossflow filtration of polyacrylonitrile ultrafiltration membranes, *Journal of Membrane Science*, 148, 1998.
Chai, X., Kobayashi, T. And Fujii, N. (1999) Ultrasound-associated cleaning of polymeric membranes, *Separation and Purification Technology*, 15(2), 139-146.

Cui, Z.F. and Wright, K.I.T. (1994) Flux enhancements with gas sparging in downwards crossflow ultrafiltration: Performance and mechanism, *Journal of Membrane Science*, 90, 183-189.

Davis, R.H. 1997. Novel membrane process with rapid backpulsing for water treatment. Water Treatment Technology Program Report No 18, US Department of the Interior, USA.

Dekker, M. and Boom, R. (1995) Improving membrane filtration processes, *Trends in Biotechnology*, 13, 129-131

Gogate, P.R., Mujumdar, S. and Pandit, A.B. (2003) Large-scale sonochemical reactors for process intensification, *Journal of Chemical Technology and Biotechnology*, 78(6), 685-693.

Harvey, R. (1965) *US Patent No. 3 206 397.*

Howkins, S.D. (1969) Diffusion rates and the effect of ultrasound, *Ultrasonics*, 129-130.
Kobayashi, T., Chai, X. and Fujii, N. (1999) Ultrasound enhanced cross-flow membrane filtration, *Separation and Purification Technology*, 17, 31-40.

Kobayashi, T., Kobayashi, T., Hosaka, Y. and Fujii, N. (2003) Ultrasound-enhanced membrane-cleaning processes applied water treatments: Influence of sonic frequency on filtration treatments, *Ultrasonics*, 41, 185-190.

Kost, J. and Langer, R. (1988) Ultrasound enhancement of membrane permeability, *US Patent No. 4 780 212*.

Krautkrämer, J. and Krautkrämer, H. (1969) *Ultrasonic Testing of Materials*. Springer-Verlag, Berlin/Heidelberg, Germany.

Lenart, I. and Auslander, D. (1980) *Ultrasonics*, 9, 216.

Li, H., Ohdaira, E. and Ide, M. (1995) Enhancement in diffusion of electrolyte through membrane using ultrasonic dialysis equipment with plane membrane, *Japanese Journal of Applied Physics*, 35(5B), 2725-2729.

Li, H., Ohdaira, E. and Ide, M. (1996) Effect of ultrasonic irradiation on permeability of dialysis membrane, *Japanese Journal of Applied Physics*, 35(5B), 3255-3258.

Li, J. and R. D. Sanderson (2003) Water Commission Research Report. 2003.

Li, J., Hallbauer, D.K. and Sanderson, R.D. (2003) Direct monitoring of membrane fouling and cleaning during ultrafiltration using a non-invasive ultrasonic technique, *Journal of Membrane Science*, 215, 33-52.

Li, J., Sanderson, R.D. and Jacobs, E.P. (2002). Ultrasonic cleaning of nylon microfiltration membranes fouled by paper Kraft paper mill effluent. *J. Membr. Sci.* 205, 247-257.

Lickiss, P.D. (2000) *The New Chemistry*, Cambridge University Press, Cambridge (2000).
Liu, G., Liu, Y., Ni, J., Shi, H. and Qian, Y. (2004) Treatability of Kraft spent liquor by microfiltration and ultrafiltration, *Desalination*, 160(2), 131-141.

Löning, J.M., Horst, and Hoffmann, U. (2000) Proceedings of the 7th Meeting of the European Society of Sonochemistry, 197.

Lu, W.M. and Ju, S.C. (1989) Selective particle deposition in crossflow filtration. *Sep. Sci. Technol.* 24, 517–540.

Maartens, A., (1998) *Ultrafiltration Membranes: A Biological Approach to Foulants Charaterisation and Cleaning*. Ph.D. Dissertation, University of Stellenbosch, Stellenbosch, South Africa.

Madaeni, S.S. and Mansourpanah, Y. (2004) Chemical cleaning of RO membranes fouled by whey, *Desalination*, 161(1), 13-24.

Mairal, A.P. (1998) Ph.D. Dissertation, University of Colorado at Boulder, CO, USA.

Mason, W.P. (1958) *Physical Acoustics and the Properties of Solids*, Van Nostrand, New York, USA.

Mason, T. (1992) Ultrasound in Industrial Processes: The problems of scale-up. In *Current Trends in Sonochemistry*, Price, G. (ed), The Royal Society of Chemistry, Cambridge, UK.

Masselin, I., Chasseray, X., Durand-Bourlier, L., Lainé, J.-M., Syzaret, P.-Y., and Lemordant, D. (2001) Effect of sonication on polymeric membranes, *Journal of Membrane Science*, 181, 213-220.

McCausland, L.J., Cains, P.W. and Martin, P.D. (2001) Use the power of sonocrystallization for improved properties, *CEP Magazine*, July, 56-61.

Meier-Haack, J., Booker, N.A. and Carroll, T. (2003) A permeability controlled microfiltration membrane for reduced fouling in drinking water treatment, *Water Research*, 37, 585-588.

Mujamdar, S., Senthil Kumar, P. and Pandit, A.B. 1998. Effect of liquid-phase properties on ultrasound intensity and cavitational activity. *Ultrasonics Sonochemistry*, 5, 113-118.

Muraldidhara, H.S., Senapati, N., Ensminger, D. and Chauhan, S.P. (1986) Electro-Acoustic Separation Process for Fine Particle Suspension, *Filtration & Separation*, 351-353.

Muthukumaran, S., Yang, K., Seuren, A., Kentish, S., Ashokkumar, S., Stevens, G.W. and Grieser, F. (2004) The use of ultrasonic cleaning for ultrafiltration membranes in the dairy industry, *Separation and Purification Technology* (In press).

Nilsson, J.L. (1990) Protein fouling of UF membranes: Causes and consequences, *Journal of Membrane Science,* 52, 121-142.

Nosov, V.A. (1965) *Ultrasonics in the Chemical Industry*, New York, USA.
Parameshwaran, K., Fane, A.G., Cho, B.D. and Kim, K.J. (2001) Analysis of microfiltration performance with constant flux processing of secondary effluent, *Water Research*, 35(18), 4349-4358.

Peterson, M.N.A. (1967) Ultrasonic Sieving, *U.S. Patent 3 305 481*, February 21.
Piazza, T. and Puskas, W. L. (2002) *The Ideal Ultrasonic Parameters for Delicate Parts. Cleaning* (www.blackstone-ney.com)

Reihanian, H., Robertson, C.R. and Michaels. (1983) Mechanisms of polarization and fouling of ultrafiltration membranes by proteins. *Journal of Membrane Science*, 16, 237-258.

Schäfer, A.I., Fane, A.G. and Waite, T.D. (2001) Cost factors and chemical pretreatment effects in the membrane filtration of waters containing natural organic matter, *Water Research*, 35(6), 1509-1517.

Semmelink, A. (1970) Application of ultrasonic energy to filtering of liquids, paper read at *IEEE Ultrasonics Symposium, 1970*.

Semmelink, A. (1973) Ultrasonically enhanced liquid filtering, *Ultrasonics International Conference Proceedings, 1973*.

Simon, A., Penpenic, L, Gondrexon, N., Taha, S and Dorange, G. (2000) A comparative study between classical stirred and ultrasonically-assisted dead-end ultrafiltration, *Ultrasonics Sonochemistry*, 7, 183-186.

Singh, N. And Cheryan, M. (1998) Process design and economic analysis of a ceramic membrane system for microfiltratoin of corn starch hydrosylate, *Journal of Food Engineering*, 38, 57-67.

Takata, K., Yamamoto, K., Bian, R. and Watanabe, Y. (1998) Removal of humic substances with velocity shear induced processing membrane filtration, *Desalination*, 117, 273-282.

Tarleton, E.S. (1988) How electric and ultrasonic fields assist membrane filtration. *Filtration & Separation,* 25(6), 402-406.

Tarleton, E.S. and Wakeman, R.J. (1990) Microfiltration enhancement by electrical and ultrasonic force fields, *Filtration & Separation*, 27(3), 192-194.

Tarleton, E.S. and Wakeman, R.J. (1992) Electro-Acoustic Crossflow Microfiltration, *Filtration & Separation*, 29(5), 425-431.

Van Dulm, P., and Norde, W. (1983) The adsorption of human plasma albumin on solid surfaces, with special attention to the kinetic aspects, *J. Colloid Inter. Sci.* 91(1), 248-255.

Vyas, H.K., Bennett, R.J. and Marshall, A.D. (2001) Cake resistance and force balance mechanism in the crossflow microfiltration of lactalbumin particles. *J. of Membrane Science,* 192, 165–176.

Wakeman, R.J. and Smythe, M.C. (2000) Clarifying filtration of fine particle suspensions aided by electrical and acoustic fields, *Chemical Engineering Research and Design*, 78(A1), 125-135.

Wakeman, R.J. and Smythe, M.C. (2000) The use of acoustic fields as a filtration an dewatering aid, *Ultrasonics*, 38, 657-661.

Wakeman, R.J. and Tarleton, E.S. (1991) An experimental study of electroacoustic crossflow microfiltration. *Trans. I Chem. E* 69 Part A, 386–397.

Williams, C. and Wakeman, R.J. (2000) Membrane fouling and alternative techniques for its alleviation. *Membrane Technology*, 124, 4-14.

Yazen, X.J., Dodds, L. and Leclerc, D. (1995) Cake characteristics in crossflow and dead-end microfiltration. *Filtr. Sep.* 32, 795–798.

Zhu, C., Liu, G.L., Cheung, C.S., Leung, C.W. and Zhu, Z.C., (1999) Ultrasonic stimulation on enhancement of air gap membrane distillation. *Journal of Membrane Science*, 161(1-2), 85–93.

APPENDIX A:

TRANSMISSION OF SOUND WAVES IN SOLID AND FLUID MEDIA

As sound waves, ultrasound is transmitted through any substances, solid, liquid or gas, which possesses elastic properties. The movement of the vibrating body (i.e. sound source) is communicated to the molecules of the medium, each of which transmits the motion to an adjoining molecule before returning to its approximately original position. For liquids and gases, particle oscillation takes place in the direction of the wave and produces *longitudinal waves*. Solids, however, since they also possess shear elasticity, can also support tangential stress giving rise to *transverses waves*, in which particle movement takes place perpendicular to the direction of the wave.

As the case in the air, the molecules of the liquid, under the action of the applied acoustic field, will vibrate about their mean position and an acoustic pressure ($P_a = P_A \sin 2\pi ft$) will be superimposed upon the already ambient pressure (usually hydrostatic, P_h) present in the liquid. The total pressure, P, in the liquid at any time is $P = P_h + P_a$, where P_A is the pressure amplitude, and f is the applied ultrasound frequency (Masion and Lorimer, 1988).

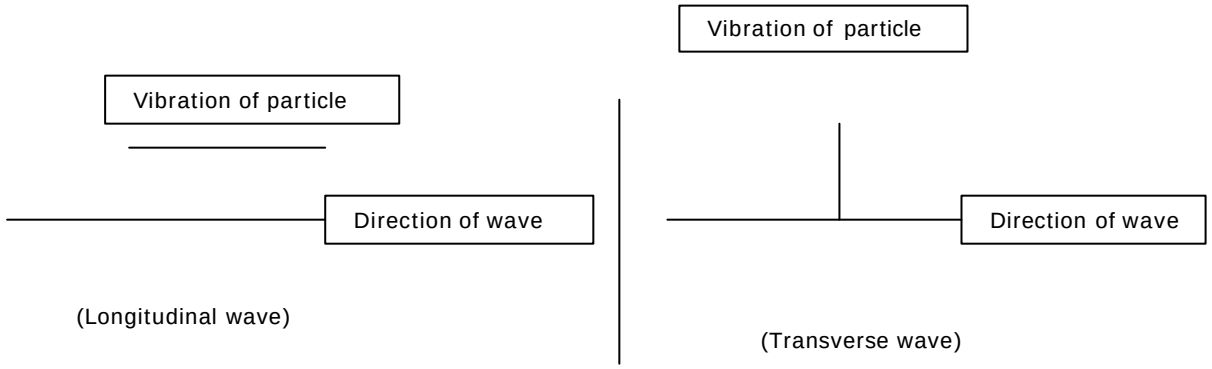

Figure A.1. Propagation of sound waves.

Attenuation of ultrasound wave in liquid phase

During propagation of a plane sound wave through a medium, the intensity of the wave decreases as the distance from the radiation source increases. The intensity, I, at some distance, d, from the source is given by:

$$I = I_0 \exp(-\alpha_I d) \qquad \text{(A-1)}$$

where α_I is the attenuation coefficient describing the decrease in intensity over distance d in nepers per meter (Np/m). When a logarithmic base, instead of a Naperian base is used, the units are expressed as dB/m. Also note that in the literature, the attenuation coefficient sometimes refers to the intensity, and not the sound pressure. Since the intensity is proportional to the square of the sound pressure, the attenuation coefficient associated with intensity can be related to the attenuation coefficient associated with pressure as follows

$$\exp(-\alpha_I d) = \exp(-2\alpha d) \text{ or } \alpha_I = 2\alpha \qquad \text{(A-4)}$$

This attenuation may arise as a result of reflection, refraction, diffraction or scattering of the wave or it may be the result of converting some of the mechanical (kinetic) energy of the wave into heat. For the sound wave propagating in liquid phase, it is the latter process which is most important. As the molecules of the medium vibrate under the action of sound wave, they experience viscous interactions which degrade ultrasound energy into heat, and it is the absorption of this degraded acoustic energy by the medium which gives rise to the small observed bulk heating effect during the application of high power ultrasound (Masion and Lorimer, 1988).

Kirchhoff (1868) also suggested that energy losses due to heat (thermal) conduction in the medium must also be considered. At any instant, the high pressure region will have a temperature above the average while the temperature of the low pressure region will be below average, heat will thus be conducted from the high to low temperature regions and a compressed region will return less work on expansion than was required to compress it. As a rough guide, Krautkrämer and Krautkrämer (1969) report values of 1-4 dB/m for water.

Attenuation of ultrasound waves in solid phases

The attenuation of ultrasound in a solid phase generally results from two causes, scattering and true absorption (Krautkrämer and Krautkrämer, 1969). The scattering results from the fact that the solid material is not strictly homogeneous. It contains boundaries, pores and crystal grains of various sizes and directions. As the ultrafiltration membrane is concerned, the pores and grains of the membrane fibre (10-100 nm) are normally far smaller than the wave length of the applied ultrasound (for 20 kHz ultrasound, it is about 75 mm), scattering can be negligible. Then the main cause of attenuation of ultrasound in membrane fibres is also absorption (Mason, 1958), which is a direct conversion of sound energy into heat.

If the decrease of the sound pressure is only as a result of attenuation, the total attenuation coefficient, α, of ultrasound over distance, d, can be expressed in decibel (dB)[c] as (Krautkrämer and Krautkrämer, 1969):

$$\alpha d = 20\log_{10}(p_0/p) \text{ [dB]} \qquad \text{(A-3)}$$

P_0 and P are the sound pressures at the beginning and the end, respectively, of a section of length d and with the attenuation coefficient of α.

Reflection and refraction of ultrasound wave at a liquid-solid interface

It is known that liquid can only transmit *longtitudinal waves,* solid can transmit both *longtitudinal waves* and *transverses waves.* When a ultrasound wave enters from the liquid phase to the solid phase, a reflected *longtitudinal wave* in liquid phase, a refracted *longtitudinal wave* and a *transverses wave* in solid phase will be developed. If the incident angle of the longitude wave from the liquid phase is vertical to the solid phase,

[c]For sound pressure p, we use the relationship: Sound pressure level $L_p = 10*\log(p^2/p_{ref}^2) = 20*\log(p/p_{ref})$ [dB] (relative to p_{ref}), where p = RMS sound pressure in Pa, and $p_{ref} = 2 \times 10^{-5}$ Pa in air, (sometimes written as 20 mPa = 20×10^{-6} Pa, which is the sound pressure at the threshold of hearing at 1000 Hz). The sound pressure level at the threshold of hearing is thus: $L_p = 20 \log(2x10^{-5}/2x10^{-5}) = 20 \log 1 = 0$ dB.

the reflection coefficient R_r and the refraction coefficient T_t can be given by (Kraut krämer and Krautkrämer, 1969):

$$R_r = \frac{\rho_2 c_2 - \rho_1 c_1}{\rho_2 c_2 + \rho_1 c_1} \qquad \text{(A-5)}$$

$$T_t = \frac{-2\rho_1 c_1}{\rho_2 c_2 + \rho_1 c_1} \qquad \text{(A-6)}$$

Where ρ_1 and ρ_2 are the liquid phase density and solid phase density respectively; C_1 and C_2 are the ultrasound transmitting velocities in the liquid and solid phase respectively. The value of ρc is refereed to as the specific acoustic impedance of the medium.

APPENDIX B:

CALIBRATION OF HYDROPHONE USED IN THE MEASUREMENT OF ULTRASOUND

Ultrasound pressure level measurements were performed using a hydrophone, calibrated as indicated in Appendix B. (Reson TC4013, with sensitivity of –211.4 dB relative to 1 V per μPa). A Tektronix TDS 3014 digital oscilloscope, Hewlett Packard 35760A dynamic signal analyzer, and a Stanford Research System SR560 differential preamplifier were included to perform the measurements as indicated in Figure B.1. The needle hydrophone was located at different positions inside the membrane filtration system, i.e. at measured distances from the source of the ultrasound.

The ultrasound source was generated from a horn ultrasonic processor (Ultrasonics Inc., USA, Model W-375). The sonic source was set at a 50% duty cycle at an output power setting of 8, under a constant frequency of 20.208 kHz. The voltages measured were root mean square (RMS) values averaged over 25 samples, which were converted to dB from the calibration curve of the hydrophone:

$$SL = 205.4 + 20*\log(V) \qquad \text{(B-1)}$$

where SL is the source level of the ultrasound energy in dB, and V is measured voltage.

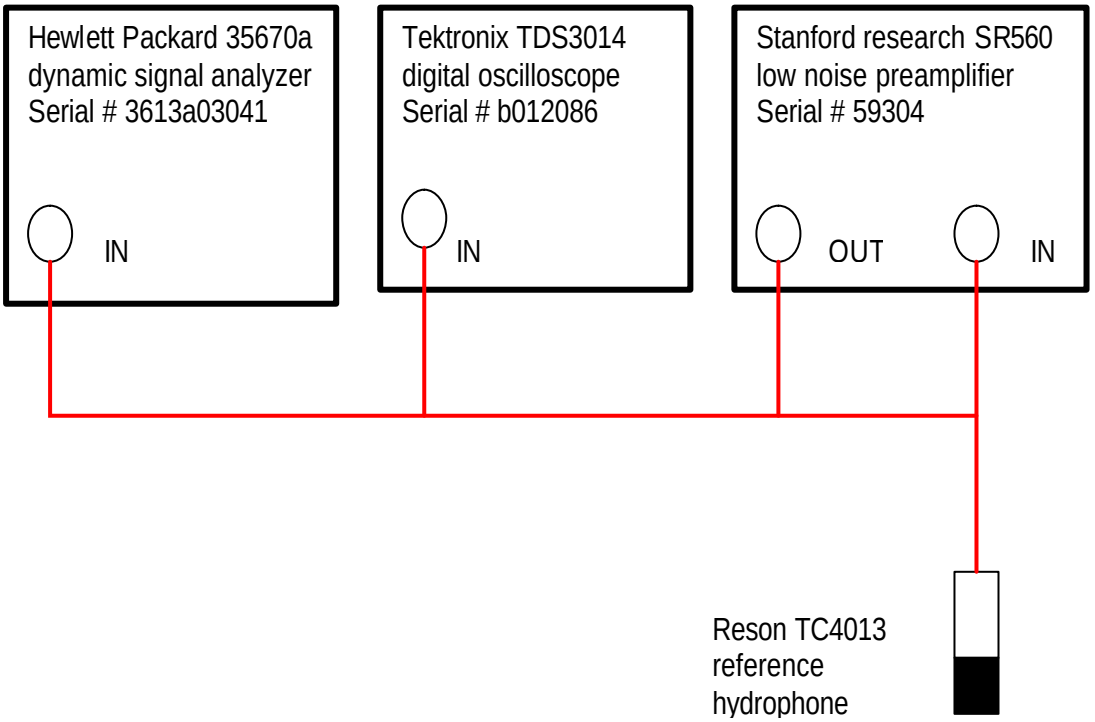

Figure B.1. Instrumental setup for real-time measurement of ultrasound energy distribution in the membrane filtration system using hydrophone.